

Thermodynamic insight in the high-pressure behavior of UiO–66: Effect of linker defects and linker expansion

Sven M. J. Rogge,[†] Jelle Wieme,[†] Louis Vanduyfhuys,[†] Steven Vandenbrande,[†]
Guillaume Maurin,[‡] Toon Verstraelen,[†] Michel Waroquier,[†]
and Veronique Van Speybroeck^{*,†}

*Center for Molecular Modeling (CMM), Ghent University, Technologiepark 903, 9052 Zwijnaarde, Belgium, and
Institut Charles Gerhardt Montpellier, Université Montpellier 2, Place E. Bataillon, 34095 Montpellier cedex 05,
France*

E-mail: Veronique.VanSpeybroeck@UGent.be

Supporting Information

1 Linker vacancies in UiO–66-type materials	S2	2.3.11 Type 7	S49
2 Force-field generation and validation	S5	2.4 Validation with respect to DFT results	S50
2.1 Different contributions to the force field	S5	3 Structural properties of the UiO–66 family	S53
2.2 Definition of the atom types	S7	3.1 Unit cell parameters	S53
2.3 Force field parameters	S11	3.2 Types of pores for pristine and defect structures	S53
2.3.1 UiO–66	S11	3.3 Pore size distribution of the UiO–66 family	S55
2.3.2 UiO–67	S12	4 Pressure and free energy profiles	S57
2.3.3 UiO–68	S15	4.1 Coefficients of the polynomial fit	S57
2.3.4 Type 0	S18	4.2 Free energy profiles	S58
2.3.5 Type 1	S23	4.3 Identification of the soft mode	S60
2.3.6 Type 2	S30	5 Study of finite-size effects	S62
2.3.7 Type 3	S34		
2.3.8 Type 4	S38		
2.3.9 Type 5	S46		
2.3.10 Type 6	S46		

[†]Ghent University

[‡]Université Montpellier

1 Linker vacancies in UiO–66-type materials

The crystal structure of pristine UiO–66-type materials corresponds to the **fcu** topology.¹ When considering the conventional unit cell of these materials, the four inorganic $\text{Zr}_6(\mu_3\text{-O})_4(\mu_3\text{-OH})_4$ bricks occupy the fcc positions, as shown in Figure S1. Each of the six inorganic bricks on the surface of the unit cell, **1** to **3**, is shared with one adjacent cell, while the eight inorganic bricks on the corner of the cell, **4**, are each shared with seven adjacent cells. In the pristine material, these four inorganic bricks are twelvefold coordinated, giving rise to 24 ligands (excluding periodic images), their midpoints occupying the 24d Wyckoff positions. In Figure S1, the twelve ligands **a** to **l**, as well as their periodic images **a'** to **l'**, lie on one of the surfaces of the unit cell, and are hence shared with an adjacent cell. These ligands are indicated in green. In contrast, the twelve blue ligands, **m** to **x**, lie completely inside the unit cell, and comprise one of the four octahedral cages present in the conventional unit cell. Note that this conventional unit cell has the advantage that every linker direction is equivalent, in contrast to the smaller unit cell containing only two inorganic bricks.

In general, d linker defects in this conventional unit cell can be introduced in (24 choose d) ways. However, some linker defects are equivalent due to the highly symmetric **fcu** topology and the choice of the conventional unit cell. For instance, consider removing one arbitrary ligand, obtaining a unit cell with an average coordination number of 11.5. By rotating the unit cell, and possibly translating its boundaries, all other unit cells with one missing ligand can be obtained. Hence, all 11.5 coordinated unit cells are equivalent. By removing this first linker and neglecting relaxation effects, the $Fm\bar{3}m$ space group of the pristine material is reduced to its $Cmmm$ subgroup.

To remove a second linker, obtaining an average coordination number of 11, 23 possibilities arise. However, some of these structures are equivalent. In Table S1, a classification of these 23 possibilities into seven distinct categories is proposed. This topology-based classification considers both the distance between the midpoints of the two removed linkers and the coordination number of the four inorganic bricks. Note that the set of coordination numbers alone is insufficient to fully categorize the structures with two linker defects. However, when adding the distance between each pair of linkers (in Table S1 this distance is normalized to the unit cell

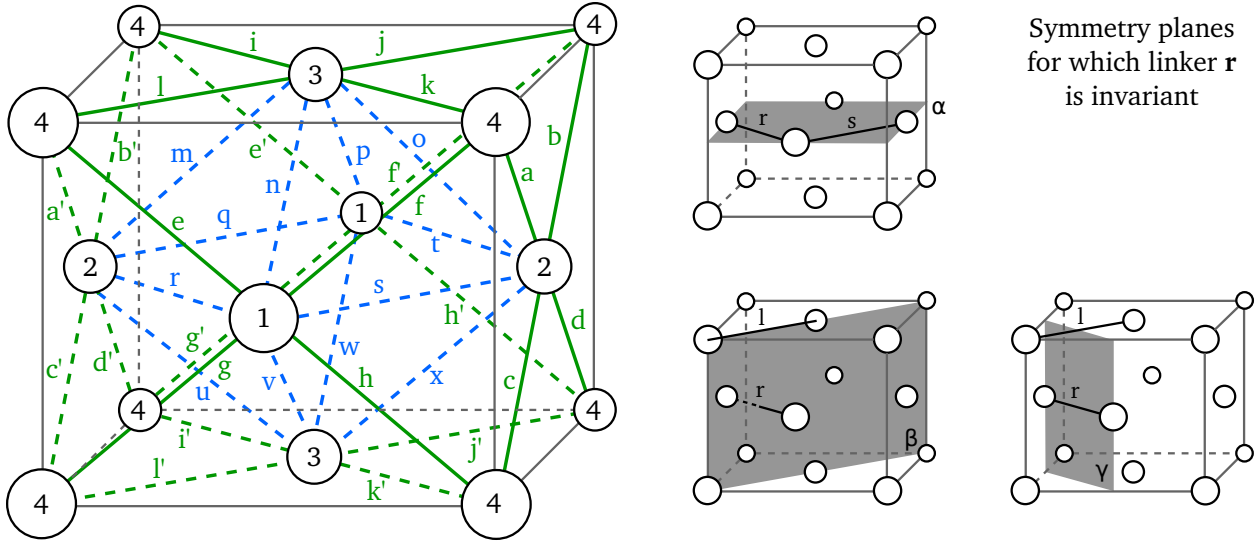


Figure S1: **Left:** Fcc unit cell of pristine UiO-66-type materials (**fcu** topology), with indication of the inorganic Zr₆O₄(OH)₄ bricks as black spheres and ligands as blue or green lines. The blue ligands are completely comprised in the unit cell and define an octahedral cage; the green ligands lie on the surfaces of the unit cell and are shared with adjacent unit cells. **Right:** The three mirror planes α , β and γ for which both the **fcu** topology and the ligand **r** are invariant.

parameter for transferability), a unique classification is obtained. For each category, one representative structure can be chosen to study the behavior of the whole category, as shown in Figure 2 of the main text. In Table S1, it is assumed that the first linker vacancy is created at **r**, which is possible due to the equivalence of all 11.5 coordinated structures. Once this ligand is fixed, we can define three symmetry planes which mirror both the **fcu** topology as well as the ligand **r** on themselves: (i) the plane α , which is spanned by the linkers **r** and **s**; (ii) the plane β , containing linker **1** and perpendicular to linker **r**; and (iii) the plane γ , containing linker **r** and perpendicular to linker **1**. When removing a second linker from this 11.5 coordinated structure, equivalent structures can be obtained by removing the linkers symmetric with respect to any of the three symmetry planes or a combination hereof. This yields, in general, eight equivalent second linkers, since linker **r** is transformed into itself by construction of the symmetry planes. This general case is fulfilled for any pair of **type 1** or **type 4** linkers (see Table S1). However, some exceptions from this general case emerge. When choosing linker **q** as the second linker, it can be verified that only the β and γ symmetry planes yield a different linker after mirroring, which is in both cases linker **s** (**type 2**). Likewise, linkers **i** and **k** form a pair (**type 5**). Hence,

only two equivalent linker defects are found for these categories. The three remaining linkers transform into themselves or their periodic image by mirroring with respect to any of the three abovementioned symmetry planes, and hence form categories of their own (**type 3**, **type 6** and **type 7**).

By removing two linkers, also the number of symmetry operators of the material is reduced. When simply removing the two linkers, and not taking into account possible relaxation effects, the space groups as obtained in the right column of Table S1 are obtained, corresponding to subgroups of the $Fm\bar{3}m$ space group of the pristine material.

Table S1: The seven types of UiO–66-type materials with an average coordination number of 11. Also indicated are the coordination numbers (CNs) of the four inequivalent inorganic bricks as shown in Figure S1, the normalized distance (LD) between the two linker vacancies, calculated between the midpoints of the removed linkers, and normalized on the unit cell parameter, and the $Fm\bar{3}m$ subgroup to which the defect structures can be classified.

ID	Equivalent structures	linker 1	linker 2	LD	CN ₁	CN ₂	CN ₃	CN ₄	Space group
type 1	8	r	a, a'	0.354	11	10	12	11	<i>Cm</i> (no. 8)
			c, c'		11	10	12	11	
			e, e'		10	11	12	11	
			g, g'		10	11	12	11	
			m		11	10	11	12	
			n		10	11	11	12	
			u		11	10	11	12	
			v		10	11	11	12	
type 2	2	r	q	0.500	10	10	12	12	<i>Pmma</i> (no. 51)
			s		10	10	12	12	
type 3	1	r	l, l'	0.500	11	11	11	11	<i>P4₂/mcm</i> (no. 132)
type 4	8	r	b, b'	0.612	11	10	12	11	<i>C2</i> (no. 5)
			d, d'		11	10	12	11	
			f, f'		10	11	12	11	
			h, h'		10	11	12	11	
			o		11	10	11	12	
			p		10	11	11	12	
			w		10	11	11	12	
			x		11	10	11	12	
			i, i'	0.707	11	11	11	11	<i>C2/m</i> (no. 12)
			k, k'		11	11	11	11	
type 6	1	r	t	0.707	10	10	12	12	<i>Pmmm</i> (no. 47)
type 7	1	r	j, j'	0.866	11	11	11	11	<i>P4₂/nnm</i> (no. 136)

2 Force-field generation and validation

As discussed in the main manuscript, all force fields considered in this work are of the form

$$\mathcal{V}^{\text{FF}} = \underbrace{\mathcal{V}_{\text{bond}} + \mathcal{V}_{\text{bend}} + \mathcal{V}_{\text{oopd}} + \mathcal{V}_{\text{torsion}}}_{\mathcal{V}_{\text{cov}}^{\text{FF}}} + \underbrace{\mathcal{V}_{\text{EI}} + \mathcal{V}_{\text{vdW}}}_{\mathcal{V}_{\text{noncov}}^{\text{FF}}}, \quad (\text{S2.1})$$

indicating a clear separation between the covalent (cov) and noncovalent contributions (noncov) to the force field. In the following subsections, the different contributions to the force field will be discussed thoroughly. Second, the different atom types for all model clusters are defined. Third, a complete overview of the force field parameters for both the covalent and noncovalent contributions to the potential energy of all eleven materials is given. Finally, the force fields are validated by comparing the optimized force field structures with our DFT results.

2.1 Different contributions to the force field

Electrostatic interactions The electrostatic interactions are described by the Coulomb interaction between spherical Gaussian densities with radii d_i and d_j containing charges q_i and q_j , respectively. By defining $d_{ij} = \sqrt{d_i^2 + d_j^2}$, the potential energy term for Gaussian charges separated by an internuclear distance r_{ij} reads

$$\mathcal{V}_{\text{EI}} = \frac{1}{2} \sum_{\substack{i,j=1 \\ (i \neq j)}} \frac{q_i q_j}{4\pi\epsilon_0 r_{ij}} \operatorname{erf}\left(\frac{r_{ij}}{d_{ij}}\right). \quad (\text{S2.2})$$

The charges q_i are derived from the DFT electron density of each model system, generated using the Minimal Basis Iterative Stockholder (MBIS) procedure,² while the charge radii d_i are obtained based on the fitting procedure of Chen and Martinéz.³ These parameters are provided to the QuickFF procedure *a priori*, as the corresponding electrostatic interactions are subtracted before fitting the covalent parameters to the first-principles Hessian. Since the electrostatic interactions between all pairs of atoms are included, there are no exclusion rules. The charges from the cluster calculations are transferred to the periodic structure via bond charge increments, similar to the approach in Ref. 4. These bond charge increments, associated with a pair of covalently bonded atoms, indicate the incremental charge that is added to the first atom and subtracted from the

second atom in the pair.⁵ This approach is chosen since bond charge increments, unlike atomic charges, are chemically transferable parameters.⁶

van der Waals interactions The van der Waals interaction $\mathcal{V}_{\text{vdW},ij}$ between two atoms i and j separated by a distance r_{ij} is modelled based on the two-parameter MM3 Buckingham potential⁷

$$\mathcal{V}_{\text{vdW},ij}(r_{ij}) = \varepsilon_{ij} \left[1.84 \times 10^5 \exp\left(-12 \frac{r_{ij}}{\sigma_{ij}}\right) - 2.25 \left(\frac{\sigma_{ij}}{r_{ij}}\right)^6 \right]. \quad (\text{S2.3})$$

The two parameters, σ_{ij} and ε_{ij} , are the equilibrium distance, respectively the well depth of the potential (corresponding to the sum of the van der Waals radii) and are determined via empirical mixing rules for the interaction between atom i and atom j :

$$\sigma_{ij} = \sigma_i + \sigma_j \text{ and } \varepsilon_{ij} = \sqrt{\varepsilon_i \varepsilon_j}. \quad (\text{S2.4})$$

The atomic parameters ε_i and σ_i are taken from Refs. 7 and 8, adopting the 1–2 and 1–3 exclusion rules for bonded pairs from the MM3 rules. Hence, for any pair of atoms which are either bonded or part of a valence angle, the van der Waals interaction is not taken into account. If these exclusion rules were to be omitted, the repulsion terms would be strongly overestimated, distorting bond lengths and valence angles. Since it is assumed that only the Pauli contributions are present in the DFT calculations on the isolated model systems, while the long-range dispersion interactions are missing, the van der Waals part of the force field is added *a posteriori*.

To limit the computational effort in the calculation of the long-range interactions, a cutoff radius $r_{\text{cut}} = 15 \text{ \AA}$ has been used throughout the manuscript. To suppress noise at this cutoff radius, a smoothing function with a width $w = 4 \text{ \AA}$ is used. The rescaled potential energy \mathcal{V}^{sc} of two interacting sites separated by a distance r is then calculated by multiplying the unscaled potential energy \mathcal{V} by a factor depending on the distance between the interacting sites:⁹

$$\mathcal{V}^{\text{sc}}(r) = \begin{cases} \mathcal{V}(r), & r \leq r_{\text{cut}} - w; \\ \left(3 - \frac{2(r_{\text{cut}} - r)}{w}\right) \frac{(r_{\text{cut}} - r)^2}{w^2} \mathcal{V}(r), & r_{\text{cut}} - w \leq r \leq r_{\text{cut}}; \\ 0, & r \geq r_{\text{cut}}, \end{cases} \quad (\text{S2.5})$$

The force acting between these two interacting sites is rescaled accordingly.

Covalent interactions The covalent parameters,

$$\mathcal{V}_{\text{bond}} = \sum_{n=1}^{N_{\text{bonds}}} \frac{K_{r,n}}{2} (r_n - r_{n,0})^2, \quad (\text{S2.6})$$

$$\mathcal{V}_{\text{bend}} = \sum_{n=1}^{N_{\text{bends}}} \frac{K_{\theta,n}}{2} (\theta_n - \theta_{n,0})^2, \quad (\text{S2.7})$$

$$\mathcal{V}_{\text{oopd}} = \sum_{n=1}^{N_{\text{oopd}}} \frac{K_{d,n}}{2} (d_n - d_{n,0})^2, \quad (\text{S2.8})$$

$$\mathcal{V}_{\text{torsion}} = \sum_{n=1}^{N_{\text{dih}}} \frac{K_{\phi,n}}{2} (1 - \cos(m_{\phi,n}(\phi - \phi_0))), \quad (\text{S2.9})$$

are determined using the in-house program QuickFF.⁴ Unless stated otherwise, $m_{\phi,n} = 2$ for all dihedral terms. As outlined in Section S2.3, some specific covalent force field terms are added to describe the correct linker behavior in UiO–67 and UiO–68.

2.2 Definition of the atom types

As shown in Figure 1 of the main text, six inorganic bricks and three different linkers are considered. Figure S2 reveals the atom types of the carboxylate oxygens, while the atom types for all other atoms present in the inorganic brick are labelled in Figure S3. Note that, to obtain the cluster models corresponding to the inorganic clusters, a phenyl ring should be added to each of the terminating CO₂ groups in the inorganic bricks of Figure S3.

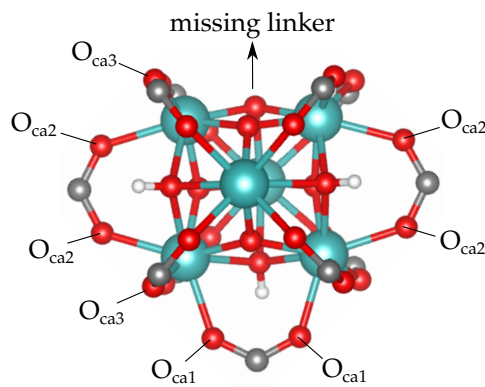
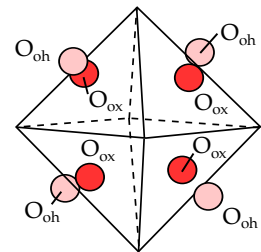
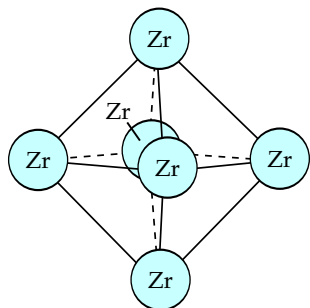
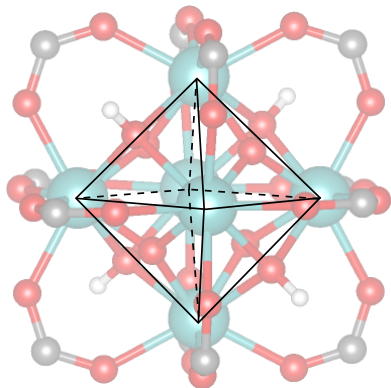
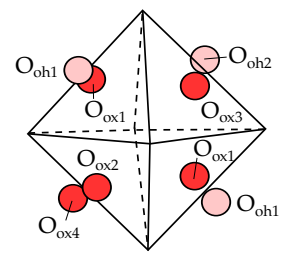
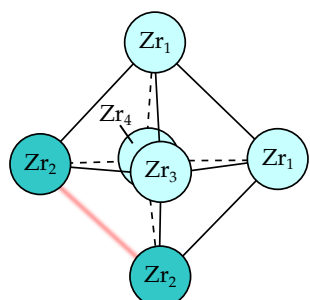
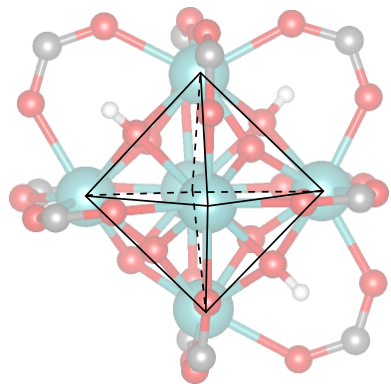


Figure S2: Overview of the different O_{ca} atom types. The carboxylate oxygens belonging to the organic linker in the opposite direction of a linker vacancy are labelled O_{ca1}. For the carboxylate oxygens belonging to organic linkers in the same plane of a removed linker, but not in the opposite direction, the atom type is O_{ca2}. Finally, carboxylate oxygens belonging to linkers which lie in defect-free planes are labelled O_{ca3}.

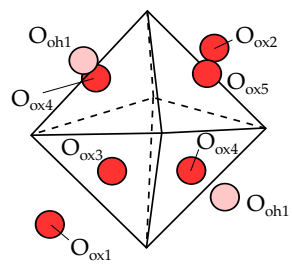
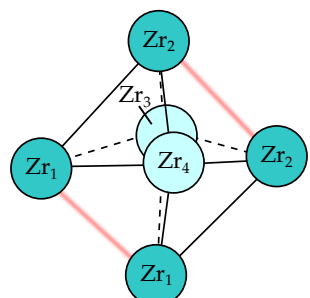
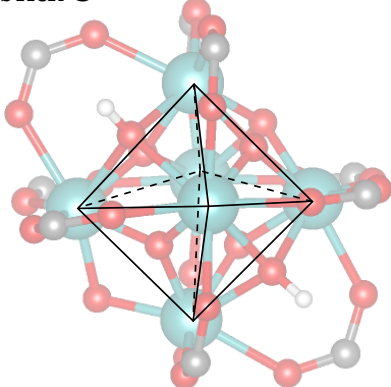
brick A



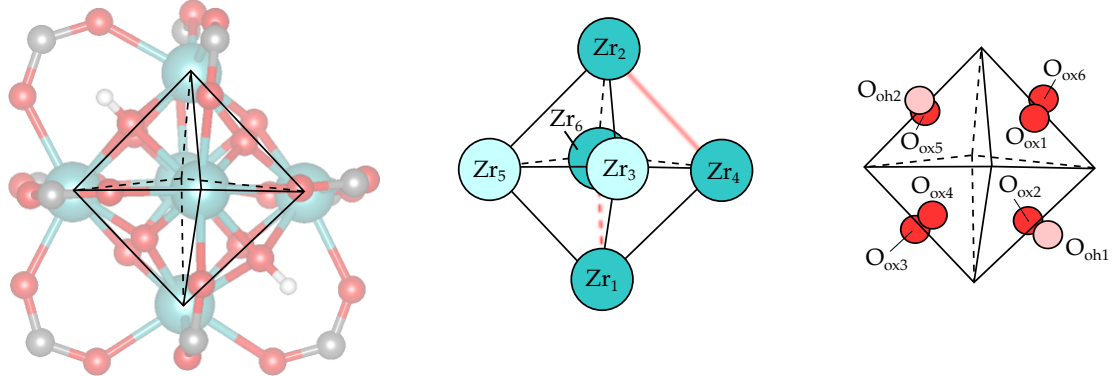
brick B



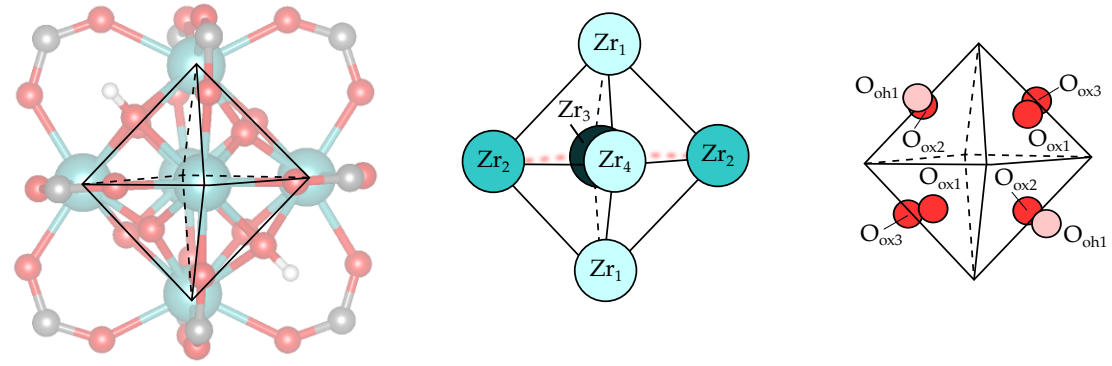
brick C



brick D



brick E



brick F

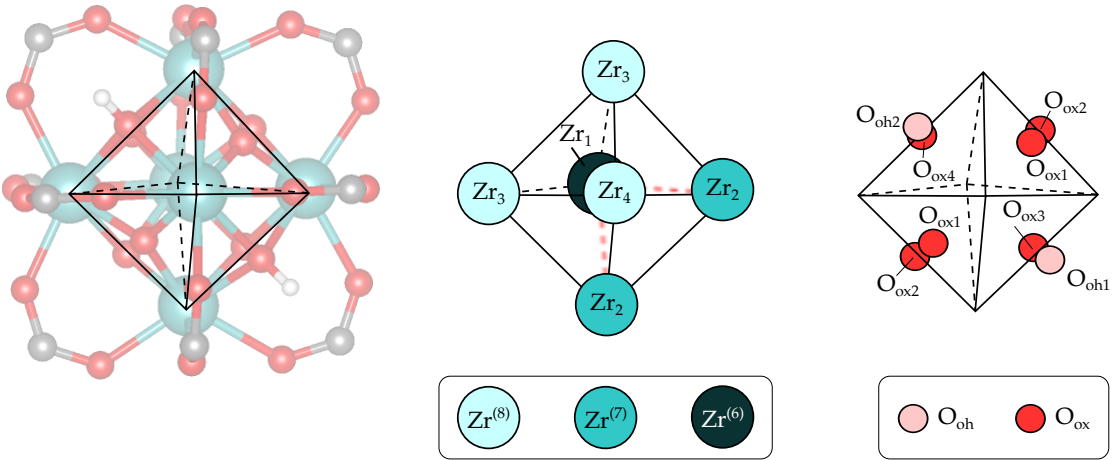


Figure S3: **Left:** Simplified inorganic cluster models, where the terminating phenyl rings are omitted. Also indicated are the distorted octahedra formed by connecting the zirconium atoms. **Middle:** Atom types for the zirconium atoms. The zirconiums are color coded according to their coordination numbers, from fully, eightfold coordinated to only sixfold coordinated. Missing linkers are indicated in red. **Right:** Atom types for the oxygen atoms of the inorganic bricks. The oxygen atoms are color coded according to whether they are bound to a hydrogen ($\mu_3\text{-OH}$) or not ($\mu_3\text{-O}$). Hydrogen atoms are omitted for clarity, their atom types correspond to the atom types of the oxygen atoms they are bounded to (i.e., $\text{H}_{\text{oh}1}$ is bound to $\text{O}_{\text{oh}1}$).

In Figure S4, the atom types present in the three linkers are indicated. Atoms which are equivalent through symmetry share the same atom type. The shaded inorganic bricks were present during the DFT calculations to take the local environment of the linkers correctly into account, but no force field parameters were derived from those bricks.

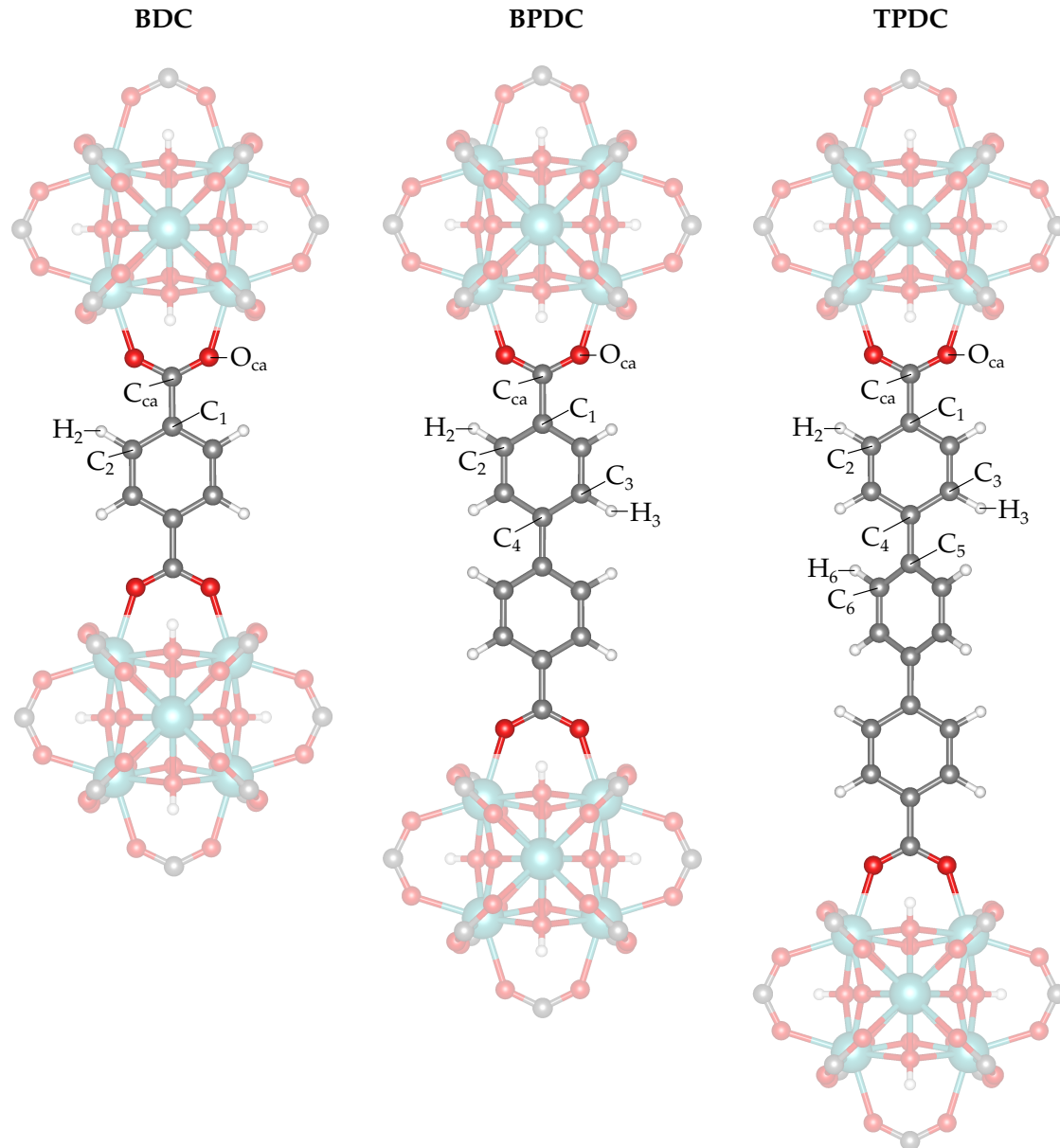


Figure S4: The atom types for the three organic ligands discussed in this work. From left to right: benzene-1,4-dicarboxylate (BDC), biphenyl-4,4'-dicarboxylate (BPDC), and p-terphenyl-4,4''-dicarboxylate (TPDC).

2.3 Force field parameters

2.3.1 UiO–66

Table S2: Parameters of the covalent contributions to the defect-free UiO–66 force field.

bonds	K [kJ/(mol·Å ²)]	r_0 [Å]
C _{ca} – C ₁	2087	1.499
C _{ca} – O _{ca} ^(A)	4414	1.274
C ₁ – C ₂	3140	1.400
C ₂ – C ₂	3382	1.388
C ₂ – H ₂	3376	1.083
H _{oh} ^(A) – O _{oh} ^(A)	4957	0.997
O _{ca} ^(A) – Zr ^(A)	522	2.212
O _{oh} ^(A) – Zr ^(A)	403	2.258
O _{ox} ^(A) – Zr ^(A)	819	2.070
bends	K [kJ/(mol·rad ²)]	θ_0 [deg]
C _{ca} – C ₁ – C ₂	617	120.1
C _{ca} – O _{ca} ^(A) – Zr ^(A)	298	134.9
C ₁ – C _{ca} – O _{ca} ^(A)	165	118.2
C ₁ – C ₂ – C ₂	464	120.1
C ₁ – C ₂ – H ₂	280	119.4
C ₂ – C ₁ – C ₂	449	119.9
C ₂ – C ₂ – H ₂	345	120.2
H _{oh} ^(A) – O _{oh} ^(A) – Zr ^(A)	161	114.9
O _{ca} ^(A) – C _{ca} – O _{ca} ^(A)	648	123.3
Zr ^(A) – O _{oh} ^(A) – Zr ^(A)	738	105.2
Zr ^(A) – O _{ox} ^(A) – Zr ^(A)	556	118.9
O _{ox} ^(A) – Zr ^(A) – O _{oh} ^(A)	174	67.2
dihedrals	K [kJ/mol]	ϕ_0 [deg]
C _{ca} – C ₁ – C ₂ – C ₂	34.8	0.000
C _{ca} – C ₁ – C ₂ – H ₂	16.0	0.000
C ₁ – C _{ca} – O _{ca} ^(A) – Zr ^(A)	49.4	0.000
C ₁ – C ₂ – C ₂ – C ₁	30.7	0.000
C ₁ – C ₂ – C ₂ – H ₂	36.2	0.000
C ₂ – C ₁ – C _{ca} – O _{ca} ^(A)	16.6	0.000
C ₂ – C ₁ – C ₂ – C ₂	31.7	0.000
C ₂ – C ₁ – C ₂ – H ₂	25.9	0.000
H ₂ – C ₂ – C ₂ – H ₂	16.6	0.000
O _{ca} ^(A) – C _{ca} – O _{ca} ^(A) – Zr ^(A)	4.4	0.000
out-of-plane-distance	K [kJ/(mol·Å ⁴)]	d_0 [Å]
C _{ca} – C ₂ – C ₂ – C ₁	44	0.000
C ₁ – C ₂ – H ₂ – C ₂	259	0.000
C ₁ – O _{ca} ^(A) – O _{ca} ^(A) – C _{ca}	1494	0.000
Zr ^(A) – Zr ^(A) – Zr ^(A) – O _{ox} ^(A)	343	0.145

Table S3: Parameters of the noncovalent contributions to the defect-free UiO–66 force field.

Atom type	q [e]	d [\AA]	ϵ [kcal/mol]	σ [\AA]
Zr ^(A)	2.370	2.367	0.300	2.540
O _{ox} ^(A)	-1.083	1.118	0.059	1.820
O _{oh} ^(A)	-1.037	1.118	0.059	1.820
O _{ca} ^(A)	-0.683	1.118	0.059	1.820
C _{ca}	0.764	1.163	0.056	1.940
C ₁	-0.135	1.163	0.056	1.960
C ₂	-0.106	1.163	0.056	1.960
H _{oh} ^(A)	0.497	0.724	0.016	1.600
H ₂	0.152	0.724	0.020	1.620

2.3.2 UiO–67

In addition to the generic force field terms expressed in Eqs. (S2.6–S2.9), a more specific dihedral term is added to adequately describe the C₃–C₄–C₄–C₃ dihedral angle in UiO–67:

$$\mathcal{V}_{\text{BPDC}}(\phi) = \frac{K_\phi}{2} [\cos(2\phi) - \cos(2\phi_0)]^2. \quad (\text{S2.10})$$

Indeed, as observed in Figure 3 of the main text, the planes determined by the two phenyl rings are not parallel ($\phi_0 \neq 0$), so that distinct minima are expected at $\pm\phi_0$ and $\pm(\pi - \phi_0)$. This cannot be captured by the generic dihedral term of Eq. (S2.9), but is incorporated in the dihedral term of Eq. (S2.10).

Table S4: Parameters of the covalent contributions to the defect-free UiO–67 force field (continued on the next page).

bonds	K [kJ/(mol·Å ²)]	r_0 [Å]
C ₁ – C ₂	3139	1.401
C ₁ – C _{ca}	2058	1.499
C ₂ – C ₃	3361	1.389
C ₂ – H ₂	3365	1.084
C ₃ – C ₄	2924	1.405
C ₃ – H ₃	3325	1.086
C ₄ – C ₄	2300	1.487
C _{ca} – O _{ca} ^(A)	4373	1.275
H _{oh} ^(A) – O _{oh} ^(A)	4957	0.997
O _{ca} ^(A) – Zr ^(A)	522	2.212
O _{oh} ^(A) – Zr ^(A)	403	2.258
O _{ox} ^(A) – Zr ^(A)	819	2.070
bends	K [kJ/(mol·rad ²)]	θ_0 [deg]
C ₁ – C ₂ – C ₃	441	120.4
C ₁ – C ₂ – H ₂	281	119.7
C ₁ – C _{ca} – O _{ca} ^(A)	171	118.3
C ₂ – C ₁ – C ₂	452	118.6
C ₂ – C ₁ – C _{ca}	598	120.7
C ₂ – C ₃ – C ₄	501	121.5
C ₂ – C ₃ – H ₃	353	118.8
C ₃ – C ₂ – H ₂	344	119.9
C ₃ – C ₄ – C ₃	408	117.6
C ₃ – C ₄ – C ₄	506	121.2
C ₄ – C ₃ – H ₃	305	119.6
C _{ca} – O _{ca} ^(A) – Zr ^(A)	298	134.9
H _{oh} ^(A) – O _{oh} ^(A) – Zr ^(A)	161	114.9
O _{ca} ^(A) – C _{ca} – O _{ca} ^(A)	644	123.0
Zr ^(A) – O _{oh} ^(A) – Zr ^(A)	738	105.2
Zr ^(A) – O _{ox} ^(A) – Zr ^(A)	556	118.9
O _{ox} ^(A) – Zr ^(A) – O _{oh} ^(A)	174	67.2

dihedrals	K [kJ/mol]	ϕ_0 [deg]
$C_1 - C_{\text{ca}} - O_{\text{ca}}^{(\text{A})} - \text{Zr}^{(\text{A})}$	49.4	0.000
$O_{\text{ca}}^{(\text{A})} - C_{\text{ca}} - O_{\text{ca}}^{(\text{A})} - \text{Zr}^{(\text{A})}$	4.4	0.000
$C_1 - C_2 - C_3 - C_4$	27.8	0.000
$C_1 - C_2 - C_3 - H_3$	33.4	0.000
$C_2 - C_1 - C_2 - C_3$	33.6	0.000
$C_2 - C_1 - C_2 - H_2$	26.5	0.000
$C_2 - C_1 - C_{\text{ca}} - O_{\text{ca}}^{(\text{A})}$	13.9	0.000
$C_2 - C_3 - C_4 - C_3$	30.6	0.000
$C_2 - C_3 - C_4 - C_4$	35.0	0.000
$C_3 - C_2 - C_1 - C_{\text{ca}}$	42.6	0.000
$C_3 - C_4 - C_3 - H_3$	33.6	0.000
$C_4 - C_3 - C_2 - H_2$	36.3	0.000
$C_4 - C_4 - C_3 - H_3$	14.6	0.000
$C_{\text{ca}} - C_1 - C_2 - H_2$	15.8	0.000
$H_2 - C_2 - C_3 - H_3$	15.9	0.000
dihedrals – type 2 (Eq. S2.10)	K [kJ/mol]	$\cos \phi_0$ [-]
$C_3 - C_4 - C_4 - C_3$	5.5	0.879
out-of-plane-distance	K [kJ/(mol·Å ⁴)]	d_0 [Å]
$C_1 - C_3 - H_2 - C_2$	274	0.000
$C_1 - O_{\text{ca}}^{(\text{A})} - O_{\text{ca}}^{(\text{A})} - C_{\text{ca}}$	1465	0.000
$C_2 - C_2 - C_{\text{ca}} - C_1$	83	0.000
$C_2 - C_4 - H_3 - C_3$	205	0.000
$C_3 - C_3 - C_4 - C_4$	441	0.000
$Zr^{(\text{A})} - Zr^{(\text{A})} - Zr^{(\text{A})} - O_{\text{ox}}^{(\text{A})}$	343	0.145

Table S5: Parameters of the noncovalent contributions to the defect-free UiO–67 force field.

Atom type	q [e]	d [Å]	ε [kcal/mol]	σ [Å]
$Zr^{(\text{A})}$	2.370	2.367	0.300	2.540
$O_{\text{ox}}^{(\text{A})}$	-1.083	1.118	0.059	1.820
$O_{\text{oh}}^{(\text{A})}$	-1.037	1.118	0.059	1.820
$O_{\text{ca}}^{(\text{A})}$	-0.686	1.118	0.059	1.820
C_{ca}	0.761	1.163	0.056	1.940
C_1	-0.157	1.163	0.056	1.960
C_2	-0.088	1.163	0.056	1.960
C_3	-1.740	1.163	0.056	1.960
C_4	0.070	1.163	0.056	1.960
$H_{\text{oh}}^{(\text{A})}$	0.497	0.724	0.016	1.600
H_2	0.148	0.724	0.020	1.620
H_3	0.141	0.724	0.020	1.620

2.3.3 UiO-68

In addition to the force field terms expressed in Eqs. (S2.6–S2.9), a more specific term is added to adequately describe the C₃–C₄–C₅–C₆ dihedral angles in the TPDC ligand (see Figure 3 of the main text):

$$\mathcal{V}_{\text{TPDC}}(\phi) = \sum_{i=1}^3 \left[\frac{K_{\phi,i}^{(1)}}{2} [1 - \cos(2i(\phi - \phi_0^{(1)}))] + \frac{K_{\phi,i}^{(2)}}{2} [1 - \cos(2i(\phi - \phi_0^{(2)}))] \right]. \quad (\text{S2.11})$$

This term can be seen as the sum of six ‘ordinary’ dihedral terms, expressed in Eq. (S2.9), where the multiplicity $m_{\phi,n}$ is either 2, 4 or 6 and where ϕ_0 can take on two different values. The six terms contributing to the expression in Eq. (S2.11) are indicated in Table S6. As shown in Figure S5, this improved force field term is able to correctly reproduce the dihedral pattern in the TPDC ligand.

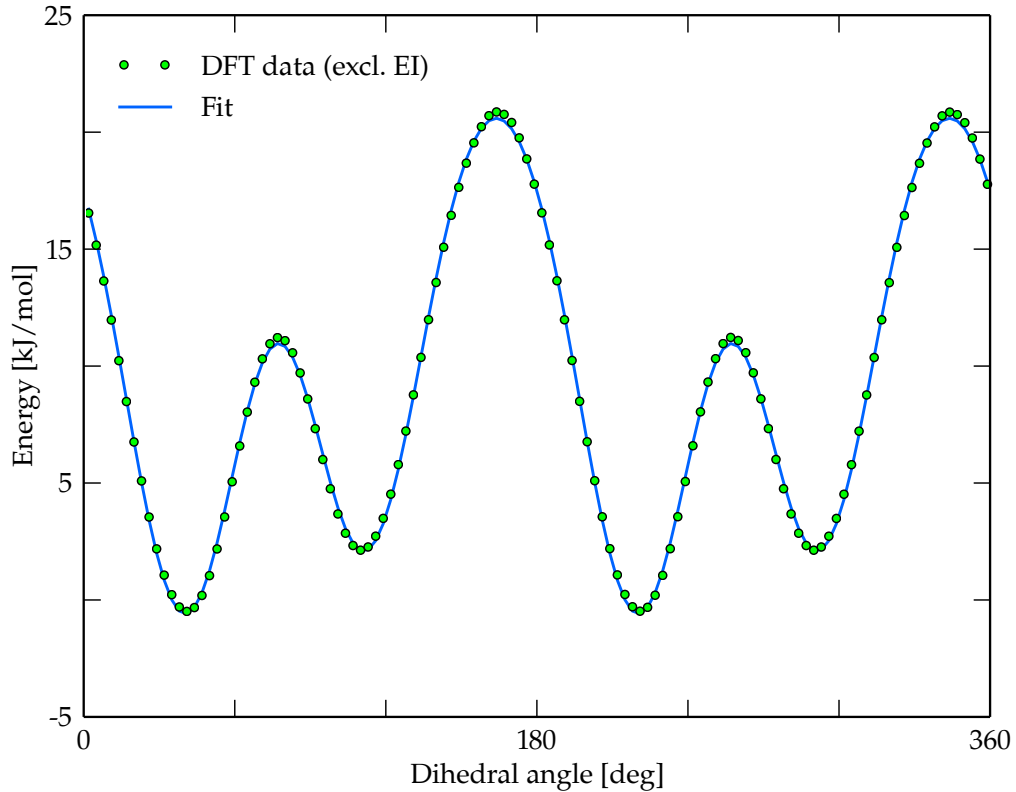


Figure S5: Comparison between the DFT pattern (excluding electrostatic interactions) and the force field pattern for the C₃–C₄–C₅–C₆ dihedral in UiO-68.

Table S6: Parameters of the covalent contributions to the defect-free UiO–68 force field (continued on the next page). ^aThe six terms contributing to the dihedral force field term in Eq. (S2.11).

bonds	K [kJ/(mol·Å ²)]	r_0 [Å]
$C_1 - C_2$	3115	1.402
$C_1 - C_{\text{ca}}$	1993	1.502
$C_2 - C_3$	3324	1.390
$C_2 - H_2$	3365	1.084
$C_3 - C_4$	2920	1.405
$C_3 - H_3$	3313	1.087
$C_4 - C_5$	2302	1.489
$C_5 - C_6$	2955	1.404
$C_6 - C_6$	3311	1.391
$C_6 - H_6$	3311	1.087
$C_{\text{ca}} - O_{\text{ca}}^{(\text{A})}$	4355	1.276
$H_{\text{oh}}^{(\text{A})} - O_{\text{oh}}^{(\text{A})}$	4957	0.997
$O_{\text{ca}}^{(\text{A})} - \text{Zr}^{(\text{A})}$	522	2.212
$O_{\text{oh}}^{(\text{A})} - \text{Zr}^{(\text{A})}$	403	2.258
$O_{\text{ox}}^{(\text{A})} - \text{Zr}^{(\text{A})}$	819	2.070
bends	K [kJ/(mol·rad ²)]	θ_0 [deg]
$C_1 - C_2 - C_3$	441	120.6
$C_1 - C_2 - H_2$	279	119.7
$C_1 - C_{\text{ca}} - O_{\text{ca}}^{(\text{A})}$	166	118.3
$C_2 - C_1 - C_2$	444	118.3
$C_2 - C_1 - C_{\text{ca}}$	615	120.9
$C_2 - C_3 - C_4$	500	121.5
$C_2 - C_3 - H_3$	353	119.0
$C_3 - C_2 - H_2$	347	119.8
$C_3 - C_4 - C_3$	405	117.5
$C_3 - C_4 - C_4$	506	121.2
$C_3 - C_4 - C_5$	512	121.3
$C_4 - C_3 - H_3$	302	119.3
$C_4 - C_5 - C_6$	506	121.5
$C_5 - C_6 - C_6$	475	121.5
$C_5 - C_6 - H_6$	305	119.5
$C_6 - C_5 - C_6$	417	117.0
$C_6 - C_6 - H_6$	352	118.9
$C_{\text{ca}} - O_{\text{ca}}^{(\text{A})} - \text{Zr}^{(\text{A})}$	298	134.9
$H_{\text{oh}}^{(\text{A})} - O_{\text{oh}}^{(\text{A})} - \text{Zr}^{(\text{A})}$	161	114.9
$O_{\text{ca}}^{(\text{A})} - C_{\text{ca}} - O_{\text{ca}}^{(\text{A})}$	641	122.9
$\text{Zr}^{(\text{A})} - O_{\text{oh}}^{(\text{A})} - \text{Zr}^{(\text{A})}$	738	105.2
$\text{Zr}^{(\text{A})} - O_{\text{ox}}^{(\text{A})} - \text{Zr}^{(\text{A})}$	556	118.9
$O_{\text{ox}}^{(\text{A})} - \text{Zr}^{(\text{A})} - O_{\text{oh}}^{(\text{A})}$	174	67.2

dihedrals	K [kJ/mol]	ϕ_0 [deg]
C ₁ - C _{ca} - O _{ca} ^(A) - Zr ^(A)	49.4	0.000
O _{ca} ^(A) - C _{ca} - O _{ca} ^(A) - Zr ^(A)	4.4	0.000
C ₁ - C ₂ - C ₃ - C ₄	27.1	0.000
C ₁ - C ₂ - C ₃ - H ₃	36.9	0.000
C ₂ - C ₁ - C ₂ - C ₃	35.2	0.000
C ₂ - C ₁ - C ₂ - H ₂	25.5	0.000
C ₂ - C ₁ - C _{ca} - O _{ca} ^(A)	16.7	0.000
C ₂ - C ₃ - C ₄ - C ₃	29.7	0.000
C ₂ - C ₃ - C ₄ - C ₅	31.6	0.000
C ₃ - C ₂ - C ₁ - C _{ca}	36.3	0.000
C ₃ - C ₄ - C ₃ - H ₃	31.8	0.000
C ₄ - C ₃ - C ₂ - H ₂	37.3	0.000
C _{ca} - C ₁ - C ₂ - H ₂	12.9	0.000
H ₂ - C ₂ - C ₃ - H ₃	16.1	0.000
C ₄ - C ₅ - C ₆ - C ₆	33.8	0.000
C ₄ - C ₅ - C ₆ - H ₆	11.3	0.000
C ₅ - C ₄ - C ₃ - H ₃	11.3	0.000
C ₅ - C ₆ - C ₆ - C ₅	24.0	0.000
C ₅ - C ₆ - C ₆ - H ₆	35.2	0.000
C ₆ - C ₅ - C ₆ - C ₆	33.6	0.000
C ₆ - C ₅ - C ₆ - H ₆	32.5	0.000
H ₆ - C ₆ - C ₆ - H ₆	15.0	0.000
C ₃ - C ₄ - C ₅ - C ₆ [†] ($m_\phi = 2$)	2.5	40.000
C ₃ - C ₄ - C ₅ - C ₆ [†] ($m_\phi = 4$)	1.1	40.000
C ₃ - C ₄ - C ₅ - C ₆ [†] ($m_\phi = 6$)	0.2	40.000
C ₃ - C ₄ - C ₅ - C ₆ [†] ($m_\phi = 2$)	2.1	110.000
C ₃ - C ₄ - C ₅ - C ₆ [†] ($m_\phi = 4$)	1.1	110.000
C ₃ - C ₄ - C ₅ - C ₆ [†] ($m_\phi = 6$)	0.2	110.000
out-of-plane-distance	K [kJ/(mol·Å ⁴)]	d_0 [Å]
C ₁ - C ₃ - H ₂ - C ₂	305	0.000
C ₁ - O _{ca} ^(A) - O _{ca} ^(A) - C _{ca}	1486	0.000
C ₂ - C ₄ - H ₃ - C ₃	234	0.000
C ₃ - C ₃ - C ₅ - C ₄	480	0.000
C ₄ - C ₆ - C ₆ - C ₅	402	0.000
C ₅ - C ₆ - H ₆ - C ₆	265	0.000
Zr ^(A) - Zr ^(A) - Zr ^(A) - O _{ox} ^(A)	343	0.145

Table S7: Parameters of the noncovalent contributions to the defect-free UiO–68 force field.

Atom type	q [e]	d [\AA]	ϵ [kcal/mol]	σ [\AA]
Zr ^(A)	2.370	2.367	0.300	2.540
O _{ox} ^(A)	-1.083	1.118	0.059	1.820
O _{oh} ^(A)	-1.037	1.118	0.059	1.820
O _{ca} ^(A)	-0.686	1.118	0.059	1.820
C _{ca}	0.759	1.163	0.056	1.940
C ₁	-0.164	1.163	0.056	1.960
C ₂	-0.084	1.163	0.056	1.960
C ₃	-0.183	1.163	0.056	1.960
C ₄	0.080	1.163	0.056	1.960
C ₅	0.048	1.163	0.056	1.960
C ₆	-0.159	1.163	0.056	1.960
H _{oh} ^(A)	0.497	0.724	0.016	1.600
H ₂	0.147	0.724	0.020	1.620
H ₃	0.142	0.724	0.020	1.620
H ₆	0.140	0.724	0.020	1.620

2.3.4 Type 0

Table S8: Parameters of the covalent contributions to the UiO–66 force field for the **type 0** structure, having an average coordination number of 11.5 (continued on the next pages).

bonds	K [kJ/(mol· \AA^2)]	r_0 [\AA]
C _{ca} – C ₁	2087	1.499
C _{ca} – O _{ca} ^(A)	4414	1.274
C _{ca} – O _{ca1} ^(B)	4419	1.274
C _{ca} – O _{ca2} ^(B)	4403	1.275
C _{ca} – O _{ca3} ^(B)	4381	1.274
C ₁ – C ₂	3140	1.400
C ₂ – C ₂	3382	1.388
C ₂ – H ₂	3376	1.083
H _{oh} ^(A) – O _{oh} ^(A)	4957	0.997
O _{ca} ^(A) – Zr ^(A)	522	2.212
O _{oh} ^(A) – Zr ^(A)	403	2.258
O _{ox} ^(A) – Zr ^(A)	819	2.070

bonds	K [kJ/(mol·Å ²)]	r_0 [Å]
H _{oh1} ^(B) - O _{oh1} ^(B)	4954	0.997
H _{oh2} ^(B) - O _{oh2} ^(B)	4967	0.996
O _{ca1} ^(B) - Zr ₁ ^(B)	597	2.182
O _{ca2} ^(B) - Zr ₁ ^(B)	490	2.201
O _{ca2} ^(B) - Zr ₂ ^(B)	403	2.240
O _{ca3} ^(B) - Zr ₁ ^(B)	535	2.194
O _{ca3} ^(B) - Zr ₂ ^(B)	518	2.193
O _{ca3} ^(B) - Zr ₃ ^(B)	522	2.207
O _{ca3} ^(B) - Zr ₄ ^(B)	507	2.208
O _{oh1} ^(B) - Zr ₁ ^(B)	354	2.281
O _{oh1} ^(B) - Zr ₂ ^(B)	464	2.251
O _{oh1} ^(B) - Zr ₃ ^(B)	387	2.263
O _{oh2} ^(B) - Zr ₁ ^(B)	410	2.262
O _{oh2} ^(B) - Zr ₄ ^(B)	225	2.323
O _{ox1} ^(B) - Zr ₁ ^(B)	856	2.071
O _{ox1} ^(B) - Zr ₂ ^(B)	1237	2.009
O _{ox1} ^(B) - Zr ₄ ^(B)	851	2.063
O _{ox2} ^(B) - Zr ₂ ^(B)	882	2.072
O _{ox2} ^(B) - Zr ₃ ^(B)	968	2.035
O _{ox3} ^(B) - Zr ₁ ^(B)	783	2.077
O _{ox3} ^(B) - Zr ₃ ^(B)	778	2.072
O _{ox4} ^(B) - Zr ₂ ^(B)	692	2.087
O _{ox4} ^(B) - Zr ₄ ^(B)	37	2.258
bends	K [kJ/(mol·rad ²)]	θ_0 [deg]
C _{ca} - C ₁ - C ₂	617	120.1
C _{ca} - O _{ca} ^(A) - Zr ^(A)	298	134.9
C _{ca} - O _{ca1} ^(B) - Zr ₁ ^(B)	286	136.0
C _{ca} - O _{ca2} ^(B) - Zr ₁ ^(B)	317	135.1
C _{ca} - O _{ca2} ^(B) - Zr ₂ ^(B)	313	134.9
C _{ca} - O _{ca3} ^(B) - Zr ₁ ^(B)	302	136.4
C _{ca} - O _{ca3} ^(B) - Zr ₂ ^(B)	283	131.1
C _{ca} - O _{ca3} ^(B) - Zr ₃ ^(B)	300	136.1
C _{ca} - O _{ca3} ^(B) - Zr ₄ ^(B)	299	136.7
C ₁ - C _{ca} - O _{ca1} ^(B)	173	118.4
C ₁ - C _{ca} - O _{ca2} ^(B)	166	118.5
C ₁ - C _{ca} - O _{ca3} ^(B)	171	118.2
C ₁ - C _{ca} - O _{ca} ^(A)	165	118.2
C ₁ - C ₂ - C ₂	464	120.1
C ₁ - C ₂ - H ₂	280	119.4

bends	K [kJ/(mol·rad ²)]	θ_0 [deg]
$C_2 - C_1 - C_2$	449	119.9
$C_2 - C_2 - H_2$	345	120.2
$H_{\text{oh}}^{(\text{A})} - O_{\text{oh}}^{(\text{A})} - \text{Zr}^{(\text{A})}$	161	114.9
$O_{\text{ca}}^{(\text{A})} - C_{\text{ca}} - O_{\text{ca}}^{(\text{A})}$	644	123.1
$\text{Zr}^{(\text{A})} - O_{\text{oh}}^{(\text{A})} - \text{Zr}^{(\text{A})}$	738	105.2
$\text{Zr}^{(\text{A})} - O_{\text{ox}}^{(\text{A})} - \text{Zr}^{(\text{A})}$	556	118.9
$O_{\text{ox}}^{(\text{A})} - \text{Zr}^{(\text{A})} - O_{\text{oh}}^{(\text{A})}$	174	67.2
$H_{\text{oh1}}^{(\text{B})} - O_{\text{oh1}}^{(\text{B})} - \text{Zr}_1^{(\text{B})}$	154	115.6
$H_{\text{oh1}}^{(\text{B})} - O_{\text{oh1}}^{(\text{B})} - \text{Zr}_2^{(\text{B})}$	154	116.5
$H_{\text{oh1}}^{(\text{B})} - O_{\text{oh1}}^{(\text{B})} - \text{Zr}_3^{(\text{B})}$	156	115.9
$H_{\text{oh2}}^{(\text{B})} - O_{\text{oh2}}^{(\text{B})} - \text{Zr}_1^{(\text{B})}$	165	114.5
$H_{\text{oh2}}^{(\text{B})} - O_{\text{oh2}}^{(\text{B})} - \text{Zr}_4^{(\text{B})}$	151	114.5
$O_{\text{ca1}}^{(\text{B})} - C_{\text{ca}} - O_{\text{ca1}}^{(\text{B})}$	652	123.0
$O_{\text{ca2}}^{(\text{B})} - C_{\text{ca}} - O_{\text{ca2}}^{(\text{B})}$	638	123.0
$O_{\text{ca3}}^{(\text{B})} - C_{\text{ca}} - O_{\text{ca3}}^{(\text{B})}$	642	123.0
$\text{Zr}_1^{(\text{B})} - O_{\text{oh1}}^{(\text{B})} - \text{Zr}_2^{(\text{B})}$	719	101.8
$\text{Zr}_1^{(\text{B})} - O_{\text{oh1}}^{(\text{B})} - \text{Zr}_3^{(\text{B})}$	672	104.1
$\text{Zr}_1^{(\text{B})} - O_{\text{oh2}}^{(\text{B})} - \text{Zr}_1^{(\text{B})}$	713	104.5
$\text{Zr}_1^{(\text{B})} - O_{\text{oh2}}^{(\text{B})} - \text{Zr}_4^{(\text{B})}$	715	104.0
$\text{Zr}_1^{(\text{B})} - O_{\text{ox1}}^{(\text{B})} - \text{Zr}_2^{(\text{B})}$	443	118.3
$\text{Zr}_1^{(\text{B})} - O_{\text{ox1}}^{(\text{B})} - \text{Zr}_4^{(\text{B})}$	429	120.8
$\text{Zr}_1^{(\text{B})} - O_{\text{ox3}}^{(\text{B})} - \text{Zr}_1^{(\text{B})}$	532	117.8
$\text{Zr}_1^{(\text{B})} - O_{\text{ox3}}^{(\text{B})} - \text{Zr}_3^{(\text{B})}$	540	118.8
$\text{Zr}_2^{(\text{B})} - O_{\text{oh1}}^{(\text{B})} - \text{Zr}_3^{(\text{B})}$	711	102.7
$\text{Zr}_2^{(\text{B})} - O_{\text{ox1}}^{(\text{B})} - \text{Zr}_4^{(\text{B})}$	584	111.3
$\text{Zr}_2^{(\text{B})} - O_{\text{ox2}}^{(\text{B})} - \text{Zr}_2^{(\text{B})}$	595	110.9
$\text{Zr}_2^{(\text{B})} - O_{\text{ox2}}^{(\text{B})} - \text{Zr}_3^{(\text{B})}$	443	118.3
$\text{Zr}_2^{(\text{B})} - O_{\text{ox4}}^{(\text{B})} - \text{Zr}_2^{(\text{B})}$	827	110.5
$\text{Zr}_2^{(\text{B})} - O_{\text{ox4}}^{(\text{B})} - \text{Zr}_4^{(\text{B})}$	851	103.0
$O_{\text{oh1}}^{(\text{B})} - \text{Zr}_1^{(\text{B})} - O_{\text{ox1}}^{(\text{B})}$	223	69.0
$O_{\text{oh1}}^{(\text{B})} - \text{Zr}_1^{(\text{B})} - O_{\text{ox3}}^{(\text{B})}$	212	67.9
$O_{\text{oh1}}^{(\text{B})} - \text{Zr}_2^{(\text{B})} - O_{\text{ox1}}^{(\text{B})}$	258	70.8
$O_{\text{oh1}}^{(\text{B})} - \text{Zr}_2^{(\text{B})} - O_{\text{ox2}}^{(\text{B})}$	318	69.5
$O_{\text{oh1}}^{(\text{B})} - \text{Zr}_3^{(\text{B})} - O_{\text{ox2}}^{(\text{B})}$	239	69.5
$O_{\text{oh1}}^{(\text{B})} - \text{Zr}_3^{(\text{B})} - O_{\text{ox3}}^{(\text{B})}$	170	68.1
$O_{\text{oh2}}^{(\text{B})} - \text{Zr}_1^{(\text{B})} - O_{\text{ox1}}^{(\text{B})}$	259	67.9
$O_{\text{oh2}}^{(\text{B})} - \text{Zr}_1^{(\text{B})} - O_{\text{ox3}}^{(\text{B})}$	220	68.2
$O_{\text{oh2}}^{(\text{B})} - \text{Zr}_4^{(\text{B})} - O_{\text{ox1}}^{(\text{B})}$	320	67.2
$O_{\text{ox1}}^{(\text{B})} - \text{Zr}_2^{(\text{B})} - O_{\text{ox4}}^{(\text{B})}$	182	74.5
$O_{\text{ox1}}^{(\text{B})} - \text{Zr}_4^{(\text{B})} - O_{\text{ox4}}^{(\text{B})}$	387	70.6
$O_{\text{ox2}}^{(\text{B})} - \text{Zr}_2^{(\text{B})} - O_{\text{ox4}}^{(\text{B})}$	453	69.6

dihedrals	K [kJ/mol]	ϕ_0 [deg]
C _{ca} - C ₁ - C ₂ - C ₂	34.8	0.000
C _{ca} - C ₁ - C ₂ - H ₂	16.0	0.000
C ₁ - C _{ca} - O _{ca} ^(A) - Zr ^(A)	49.4	0.000
C ₁ - C ₂ - C ₂ - C ₁	30.7	0.000
C ₁ - C ₂ - C ₂ - H ₂	36.2	0.000
C ₂ - C ₁ - C _{ca} - O _{ca} ^(A)	16.6	0.000
C ₂ - C ₁ - C ₂ - C ₂	31.7	0.000
C ₂ - C ₁ - C ₂ - H ₂	25.9	0.000
H ₂ - C ₂ - C ₂ - H ₂	16.6	0.000
O _{ca} ^(A) - C _{ca} - O _{ca} ^(A) - Zr ^(A)	4.4	0.000
O _{ca1} ^(B) - C _{ca} - O _{ca1} ^(B) - Zr ₁ ^(B)	3.7	0.000
O _{ca2} ^(B) - C _{ca} - O _{ca2} ^(B) - Zr ₁ ^(B)	3.3	0.000
O _{ca2} ^(B) - C _{ca} - O _{ca2} ^(B) - Zr ₂ ^(B)	7.6	0.000
O _{ca3} ^(B) - C _{ca} - O _{ca3} ^(B) - Zr ₁ ^(B)	4.2	0.000
O _{ca3} ^(B) - C _{ca} - O _{ca3} ^(B) - Zr ₂ ^(B)	5.9	0.000
O _{ca3} ^(B) - C _{ca} - O _{ca3} ^(B) - Zr ₃ ^(B)	5.7	0.000
O _{ca3} ^(B) - C _{ca} - O _{ca3} ^(B) - Zr ₄ ^(B)	4.9	0.000
C ₂ - C ₁ - C _{ca} - O _{ca1} ^(B)	16.6	0.000
C ₂ - C ₁ - C _{ca} - O _{ca2} ^(B)	16.6	0.000
C ₂ - C ₁ - C _{ca} - O _{ca3} ^(B)	16.6	0.000
C ₁ - C _{ca} - O _{ca1} ^(B) - Zr ₁ ^(B)	42.0	0.000
C ₁ - C _{ca} - O _{ca2} ^(B) - Zr ₁ ^(B)	48.7	0.000
C ₁ - C _{ca} - O _{ca2} ^(B) - Zr ₂ ^(B)	44.7	0.000
C ₁ - C _{ca} - O _{ca3} ^(B) - Zr ₁ ^(B)	44.1	0.000
C ₁ - C _{ca} - O _{ca3} ^(B) - Zr ₂ ^(B)	39.5	0.000
C ₁ - C _{ca} - O _{ca3} ^(B) - Zr ₃ ^(B)	43.3	0.000
C ₁ - C _{ca} - O _{ca3} ^(B) - Zr ₄ ^(B)	38.2	0.000
out-of-plane-distance	K [kJ/(mol·Å ⁴)]	d_0 [Å]
C _{ca} - C ₂ - C ₂ - C ₁	44	0.000
C ₁ - C ₂ - H ₂ - C ₂	259	0.000
C ₁ - O _{ca} ^(A) - O _{ca} ^(A) - C _{ca}	1494	0.000
Zr ^(A) - Zr ^(A) - Zr ^(A) - O _{ox} ^(A)	343	0.145
C ₁ - O _{ca1} ^(B) - O _{ca1} ^(B) - C _{ca}	1463	0.000
C ₁ - O _{ca2} ^(B) - O _{ca2} ^(B) - C _{ca}	1428	0.000
C ₁ - O _{ca3} ^(B) - O _{ca3} ^(B) - C _{ca}	1424	0.000
Zr ₁ ^(B) - Zr ₁ ^(B) - Zr ₃ ^(B) - O _{ox3} ^(B)	193	0.221
Zr ₁ ^(B) - Zr ₂ ^(B) - Zr ₄ ^(B) - O _{ox1} ^(B)	421	0.356
Zr ₂ ^(B) - Zr ₂ ^(B) - Zr ₃ ^(B) - O _{ox2} ^(B)	180	0.400
Zr ₂ ^(B) - Zr ₂ ^(B) - Zr ₄ ^(B) - O _{ox4} ^(B)	8	0.860

Table S9: Parameters of the noncovalent contributions to the UiO–66 force field for the **type 0** structure, having an average coordination number of 11.5.

Atom type	q [e]	d [\AA]	ϵ [kcal/mol]	σ [\AA]
Zr ^(A)	2.370	2.367	0.300	2.540
Zr ₁ ^(B)	2.374	2.367	0.300	2.540
Zr ₂ ^(B)	2.336	2.367	0.300	2.540
Zr ₃ ^(B)	2.375	2.367	0.300	2.540
Zr ₄ ^(B)	2.363	2.367	0.300	2.540
O _{ox} ^(A)	-1.083	1.118	0.059	1.820
O _{ox1} ^(B)	-1.074	1.118	0.059	1.820
O _{ox2} ^(B)	-1.104	1.118	0.059	1.820
O _{ox3} ^(B)	-1.091	1.118	0.059	1.820
O _{ox4} ^(B)	-1.109	1.118	0.059	1.820
O _{oh} ^(A)	-1.037	1.118	0.059	1.820
O _{oh1} ^(B)	-1.039	1.118	0.059	1.820
O _{oh2} ^(B)	-1.026	1.118	0.059	1.820
O _{ca} ^(A)	-0.682	1.118	0.059	1.820
O _{ca1} ^(B)	-0.682	1.118	0.059	1.820
O _{ca2} ^(B)	-0.683	1.118	0.059	1.820
O _{ca3} ^(B)	-0.685	1.118	0.059	1.820
C _{ca}	0.764	1.163	0.056	1.940
C ₁	-0.135	1.163	0.056	1.960
C ₂	-0.106	1.163	0.056	1.960
H _{oh} ^(A)	0.497	0.724	0.016	1.600
H _{oh1} ^(B)	0.496	0.724	0.016	1.600
H _{oh2} ^(B)	0.490	0.724	0.016	1.600
H ₂	0.152	0.724	0.020	1.620

2.3.5 Type 1

Table S10: Parameters of the covalent contributions to the UiO–66 force field for the **type 1** structure, having an average coordination number of 11 (continued on the next pages).

bonds	K [kJ/(mol·Å ²)]	r_0 [Å]
C _{ca} – C ₁	2087	1.499
C _{ca} – O _{ca} ^(A)	4414	1.274
C _{ca} – O _{ca1} ^(B)	4419	1.274
C _{ca} – O _{ca2} ^(B)	4403	1.275
C _{ca} – O _{ca3} ^(B)	4381	1.274
C ₁ – C ₂	3140	1.400
C ₂ – C ₂	3382	1.388
C ₂ – H ₂	3376	1.083
H _{oh} ^(A) – O _{oh} ^(A)	4957	0.997
O _{ca} ^(A) – Zr ^(A)	522	2.212
O _{oh} ^(A) – Zr ^(A)	403	2.258
O _{ox} ^(A) – Zr ^(A)	819	2.070
H _{oh1} ^(B) – O _{oh1} ^(B)	4954	0.997
H _{oh2} ^(B) – O _{oh2} ^(B)	4967	0.996
O _{ca1} ^(B) – Zr ₁ ^(B)	597	2.182
O _{ca2} ^(B) – Zr ₁ ^(B)	490	2.201
O _{ca2} ^(B) – Zr ₂ ^(B)	403	2.240
O _{ca3} ^(B) – Zr ₁ ^(B)	535	2.194
O _{ca3} ^(B) – Zr ₂ ^(B)	518	2.193
O _{ca3} ^(B) – Zr ₃ ^(B)	522	2.207
O _{ca3} ^(B) – Zr ₄ ^(B)	507	2.208
O _{oh1} ^(B) – Zr ₁ ^(B)	354	2.281
O _{oh1} ^(B) – Zr ₂ ^(B)	464	2.251
O _{oh1} ^(B) – Zr ₃ ^(B)	387	2.263
O _{oh2} ^(B) – Zr ₁ ^(B)	410	2.262
O _{oh2} ^(B) – Zr ₄ ^(B)	225	2.323
O _{ox1} ^(B) – Zr ₁ ^(B)	856	2.071
O _{ox1} ^(B) – Zr ₂ ^(B)	1237	2.009
O _{ox1} ^(B) – Zr ₄ ^(B)	851	2.063
O _{ox2} ^(B) – Zr ₂ ^(B)	882	2.072
O _{ox2} ^(B) – Zr ₃ ^(B)	968	2.035
O _{ox3} ^(B) – Zr ₁ ^(B)	783	2.077
O _{ox3} ^(B) – Zr ₃ ^(B)	778	2.072
O _{ox4} ^(B) – Zr ₂ ^(B)	692	2.087
O _{ox4} ^(B) – Zr ₄ ^(B)	37	2.258

bonds	K [kJ/(mol·Å ²)]	r_0 [Å]
C _{ca} - O _{ca1} ^(F)	4382	1.276
C _{ca} - O _{ca2} ^(F)	4390	1.274
C _{ca} - O _{ca3} ^(F)	4350	1.276
H _{oh1} ^(F) - O _{oh1} ^(F)	4937	0.997
H _{oh2} ^(F) - O _{oh2} ^(F)	4969	0.996
O _{ca1} ^(F) - Zr ₃ ^(F)	517	2.204
O _{ca1} ^(F) - Zr ₄ ^(F)	567	2.181
O _{ca2} ^(F) - Zr ₁ ^(F)	495	2.210
O _{ca2} ^(F) - Zr ₂ ^(F)	395	2.249
O _{ca2} ^(F) - Zr ₃ ^(F)	544	2.181
O _{ca2} ^(F) - Zr ₄ ^(F)	564	2.178
O _{ca3} ^(F) - Zr ₂ ^(F)	466	2.214
O _{ca3} ^(F) - Zr ₃ ^(F)	504	2.207
O _{oh1} ^(F) - Zr ₂ ^(F)	551	2.217
O _{oh1} ^(F) - Zr ₄ ^(F)	243	2.329
O _{oh2} ^(F) - Zr ₃ ^(F)	243	2.316
O _{oh2} ^(F) - Zr ₄ ^(F)	439	2.255
O _{ox1} ^(F) - Zr ₂ ^(F)	1109	2.026
O _{ox1} ^(F) - Zr ₃ ^(F)	772	2.082
O _{ox1} ^(F) - Zr ₄ ^(F)	859	2.073
O _{ox2} ^(F) - Zr ₁ ^(F)	771	2.074
O _{ox2} ^(F) - Zr ₂ ^(F)	780	2.069
O _{ox2} ^(F) - Zr ₃ ^(F)	162	2.233
O _{ox3} ^(F) - Zr ₁ ^(F)	893	2.079
O _{ox3} ^(F) - Zr ₂ ^(F)	561	2.121
O _{ox4} ^(F) - Zr ₁ ^(F)	1585	1.962
O _{ox4} ^(F) - Zr ₃ ^(F)	840	2.077
bends	K [kJ/(mol·rad ²)]	θ_0 [deg]
C _{ca} - C ₁ - C ₂	617	120.1
C _{ca} - O _{ca} ^(A) - Zr ^(A)	298	134.9
C _{ca} - O _{ca1} ^(B) - Zr ₁ ^(B)	286	136.0
C _{ca} - O _{ca2} ^(B) - Zr ₁ ^(B)	317	135.1
C _{ca} - O _{ca2} ^(B) - Zr ₂ ^(B)	313	134.9
C _{ca} - O _{ca3} ^(B) - Zr ₁ ^(B)	302	136.4
C _{ca} - O _{ca3} ^(B) - Zr ₂ ^(B)	283	131.1
C _{ca} - O _{ca3} ^(B) - Zr ₃ ^(B)	300	136.1
C _{ca} - O _{ca3} ^(B) - Zr ₄ ^(B)	299	136.7
C ₁ - C _{ca} - O _{ca1} ^(B)	173	118.4
C ₁ - C _{ca} - O _{ca2} ^(B)	166	118.5
C ₁ - C _{ca} - O _{ca3} ^(B)	171	118.2
C ₁ - C _{ca} - O _{ca} ^(A)	165	118.2

bends	K [kJ/(mol·rad ²)]	θ_0 [deg]
C ₁ - C ₂ - C ₂	464	120.1
C ₁ - C ₂ - H ₂	280	119.4
C ₂ - C ₁ - C ₂	449	119.9
C ₂ - C ₂ - H ₂	345	120.2
H _{oh} ^(A) - O _{oh} ^(A) - Zr ^(A)	161	114.9
O _{ca} ^(A) - C _{ca} - O _{ca} ^(A)	644	123.1
Zr ^(A) - O _{oh} ^(A) - Zr ^(A)	738	105.2
Zr ^(A) - O _{ox} ^(A) - Zr ^(A)	556	118.9
O _{ox} ^(A) - Zr ^(A) - O _{oh} ^(A)	174	67.2
H _{oh1} ^(B) - O _{oh1} ^(B) - Zr ₁ ^(B)	154	115.6
H _{oh1} ^(B) - O _{oh1} ^(B) - Zr ₂ ^(B)	154	116.5
H _{oh1} ^(B) - O _{oh1} ^(B) - Zr ₃ ^(B)	156	115.9
H _{oh2} ^(B) - O _{oh2} ^(B) - Zr ₁ ^(B)	165	114.5
H _{oh2} ^(B) - O _{oh2} ^(B) - Zr ₄ ^(B)	151	114.5
O _{ca1} ^(B) - C _{ca} - O _{ca1} ^(B)	652	123.0
O _{ca2} ^(B) - C _{ca} - O _{ca2} ^(B)	638	123.0
O _{ca3} ^(B) - C _{ca} - O _{ca3} ^(B)	642	123.0
Zr ₁ ^(B) - O _{oh1} ^(B) - Zr ₂ ^(B)	719	101.8
Zr ₁ ^(B) - O _{oh1} ^(B) - Zr ₃ ^(B)	672	104.1
Zr ₁ ^(B) - O _{oh2} ^(B) - Zr ₁ ^(B)	713	104.5
Zr ₁ ^(B) - O _{oh2} ^(B) - Zr ₄ ^(B)	715	104.0
Zr ₁ ^(B) - O _{ox1} ^(B) - Zr ₂ ^(B)	443	118.3
Zr ₁ ^(B) - O _{ox1} ^(B) - Zr ₄ ^(B)	429	120.8
Zr ₁ ^(B) - O _{ox3} ^(B) - Zr ₁ ^(B)	532	117.8
Zr ₁ ^(B) - O _{ox3} ^(B) - Zr ₃ ^(B)	540	118.8
Zr ₂ ^(B) - O _{oh1} ^(B) - Zr ₃ ^(B)	711	102.7
Zr ₂ ^(B) - O _{ox1} ^(B) - Zr ₄ ^(B)	584	111.3
Zr ₂ ^(B) - O _{ox2} ^(B) - Zr ₂ ^(B)	595	110.9
Zr ₂ ^(B) - O _{ox2} ^(B) - Zr ₃ ^(B)	443	118.3
Zr ₂ ^(B) - O _{ox4} ^{(B) - Zr₂^(B)}	827	110.5
Zr ₂ ^(B) - O _{ox4} ^(B) - Zr ₄ ^(B)	851	103.0
O _{oh1} ^(B) - Zr ₁ ^(B) - O _{ox1} ^(B)	223	69.0
O _{oh1} ^(B) - Zr ₁ ^(B) - O _{ox3} ^(B)	212	67.9
O _{oh1} ^(B) - Zr ₂ ^(B) - O _{ox1} ^(B)	258	70.8
O _{oh1} ^(B) - Zr ₂ ^(B) - O _{ox2} ^(B)	318	69.5
O _{oh1} ^(B) - Zr ₃ ^(B) - O _{ox2} ^(B)	239	69.5
O _{oh1} ^(B) - Zr ₃ ^(B) - O _{ox3} ^(B)	170	68.1
O _{oh2} ^(B) - Zr ₁ ^(B) - O _{ox1} ^(B)	259	67.9
O _{oh2} ^(B) - Zr ₁ ^(B) - O _{ox3} ^(B)	220	68.2
O _{oh2} ^(B) - Zr ₄ ^(B) - O _{ox1} ^(B)	320	67.2
O _{ox1} ^(B) - Zr ₂ ^(B) - O _{ox4} ^(B)	182	74.5
O _{ox1} ^(B) - Zr ₄ ^(B) - O _{ox4} ^(B)	387	70.6
O _{ox2} ^(B) - Zr ₂ ^(B) - O _{ox4} ^(B)	453	69.6

bends	K [kJ/(mol·rad ²)]	θ_0 [deg]
C _{ca} - O _{ca1} ^(F) - Zr ₃ ^(F)	283	136.6
C _{ca} - O _{ca1} ^(F) - Zr ₄ ^(F)	295	136.4
C _{ca} - O _{ca2} ^(F) - Zr ₁ ^(F)	263	129.9
C _{ca} - O _{ca2} ^(F) - Zr ₂ ^(F)	299	134.6
C _{ca} - O _{ca2} ^(F) - Zr ₃ ^(F)	298	136.8
C _{ca} - O _{ca2} ^(F) - Zr ₄ ^(F)	297	136.8
C _{ca} - O _{ca3} ^(F) - Zr ₂ ^(F)	293	131.7
C _{ca} - O _{ca3} ^(F) - Zr ₃ ^(F)	305	137.4
C ₁ - C _{ca} - O _{ca1} ^(F)	179	118.4
C ₁ - C _{ca} - O _{ca2} ^(F)	173	118.2
C ₁ - C _{ca} - O _{ca3} ^(F)	170	118.2
H _{oh1} ^(F) - O _{oh1} ^(F) - Zr ₂ ^(F)	148	115.1
H _{oh1} ^(F) - O _{oh1} ^(F) - Zr ₄ ^(F)	134	117.4
H _{oh2} ^(F) - O _{oh2} ^(F) - Zr ₃ ^(F)	156	114.1
H _{oh2} ^(F) - O _{oh2} ^(F) - Zr ₄ ^(F)	163	116.0
O _{ca1} ^(F) - C _{ca} - O _{ca1} ^(F)	656	123.5
O _{ca1} ^(F) - C _{ca} - O _{ca3} ^(F)	656	123.6
O _{ca2} ^(F) - C _{ca} - O _{ca2} ^(F)	650	123.1
O _{ca3} ^(F) - C _{ca} - O _{ca3} ^(F)	638	123.2
O _{oh1} ^(F) - Zr ₂ ^(F) - O _{ox1} ^(F)	322	69.9
O _{oh1} ^(F) - Zr ₂ ^(F) - O _{ox3} ^(F)	307	73.5
O _{oh1} ^(F) - Zr ₄ ^(F) - O _{ox1} ^(F)	251	66.7
O _{oh2} ^(F) - Zr ₃ ^(F) - O _{ox1} ^(F)	312	66.9
O _{oh2} ^(F) - Zr ₃ ^(F) - O _{ox4} ^(F)	381	66.9
O _{oh2} ^(F) - Zr ₄ ^(F) - O _{ox1} ^(F)	275	67.8
O _{ox1} ^(F) - Zr ₂ ^(F) - O _{ox2} ^(F)	255	72.8
O _{ox1} ^(F) - Zr ₃ ^(F) - O _{ox2} ^(F)	426	68.8
O _{ox2} ^(F) - Zr ₁ ^(F) - O _{ox2} ^(F)	106	122.3
O _{ox2} ^(F) - Zr ₁ ^(F) - O _{ox3} ^(F)	418	71.5
O _{ox2} ^(F) - Zr ₁ ^(F) - O _{ox4} ^(F)	344	75.6
O _{ox2} ^(F) - Zr ₂ ^(F) - O _{ox3} ^(F)	470	70.8
O _{ox2} ^(F) - Zr ₃ ^(F) - O _{ox4} ^(F)	538	70.8
O _{ox3} ^(F) - Zr ₁ ^(F) - O _{ox4} ^(F)	41	108.8
Zr ₁ ^(F) - O _{ox2} ^(F) - Zr ₂ ^(F)	754	109.3
Zr ₁ ^(F) - O _{ox2} ^(F) - Zr ₃ ^(F)	628	102.1
Zr ₁ ^(F) - O _{ox3} ^(F) - Zr ₂ ^(F)	622	107.8
Zr ₁ ^(F) - O _{ox4} ^(F) - Zr ₃ ^(F)	443	111.2
Zr ₂ ^(F) - O _{oh1} ^(F) - Zr ₂ ^(F)	681	102.9
Zr ₂ ^(F) - O _{oh1} ^(F) - Zr ₄ ^(F)	610	103.5
Zr ₂ ^(F) - O _{ox1} ^(F) - Zr ₃ ^(F)	599	111.9
Zr ₂ ^(F) - O _{ox1} ^(F) - Zr ₄ ^(F)	437	119.8
Zr ₂ ^(F) - O _{ox2} ^(F) - Zr ₃ ^(F)	725	105.4
Zr ₂ ^(F) - O _{ox3} ^(F) - Zr ₂ ^(F)	456	109.9

bends	K [kJ/(mol·rad ²)]	θ_0 [deg]
Zr ₃ ^(F) - O _{oh2} ^(F) - Zr ₃ ^(F)	705	104.1
Zr ₃ ^(F) - O _{oh2} ^(F) - Zr ₄ ^(F)	671	104.5
Zr ₃ ^(F) - O _{ox1} ^(F) - Zr ₄ ^(F)	433	120.2
Zr ₃ ^(F) - O _{ox4} ^(F) - Zr ₃ ^(F)	304	122.4
dihedrals	K [kJ/mol]	ϕ_0 [deg]
C _{ca} - C ₁ - C ₂ - C ₂	34.8	0.000
C _{ca} - C ₁ - C ₂ - H ₂	16.0	0.000
C ₁ - C _{ca} - O _{ca} ^(A) - Zr ^(A)	49.4	0.000
C ₁ - C ₂ - C ₂ - C ₁	30.7	0.000
C ₁ - C ₂ - C ₂ - H ₂	36.2	0.000
C ₂ - C ₁ - C _{ca} - O _{ca} ^(A)	16.6	0.000
C ₂ - C ₁ - C ₂ - C ₂	31.7	0.000
C ₂ - C ₁ - C ₂ - H ₂	25.9	0.000
H ₂ - C ₂ - C ₂ - H ₂	16.6	0.000
O _{ca} ^(A) - C _{ca} - O _{ca} ^(A) - Zr ^(A)	4.4	0.000
O _{ca1} ^(B) - C _{ca} - O _{ca1} ^(B) - Zr ₁ ^(B)	3.7	0.000
O _{ca2} ^(B) - C _{ca} - O _{ca2} ^(B) - Zr ₁ ^(B)	3.3	0.000
O _{ca2} ^(B) - C _{ca} - O _{ca2} ^(B) - Zr ₂ ^(B)	7.6	0.000
O _{ca3} ^(B) - C _{ca} - O _{ca3} ^(B) - Zr ₁ ^(B)	4.2	0.000
O _{ca3} ^(B) - C _{ca} - O _{ca3} ^(B) - Zr ₂ ^(B)	5.9	0.000
O _{ca3} ^(B) - C _{ca} - O _{ca3} ^(B) - Zr ₃ ^(B)	5.7	0.000
O _{ca3} ^(B) - C _{ca} - O _{ca3} ^(B) - Zr ₄ ^(B)	4.9	0.000
C ₂ - C ₁ - C _{ca} - O _{ca1} ^(B)	16.6	0.000
C ₂ - C ₁ - C _{ca} - O _{ca2} ^(B)	16.6	0.000
C ₂ - C ₁ - C _{ca} - O _{ca3} ^(B)	16.6	0.000
C ₁ - C _{ca} - O _{ca1} ^(B) - Zr ₁ ^(B)	42.0	0.000
C ₁ - C _{ca} - O _{ca2} ^(B) - Zr ₁ ^(B)	48.7	0.000
C ₁ - C _{ca} - O _{ca2} ^(B) - Zr ₂ ^(B)	44.7	0.000
C ₁ - C _{ca} - O _{ca3} ^(B) - Zr ₁ ^(B)	44.1	0.000
C ₁ - C _{ca} - O _{ca3} ^(B) - Zr ₂ ^(B)	39.5	0.000
C ₁ - C _{ca} - O _{ca3} ^(B) - Zr ₃ ^(B)	43.3	0.000
C ₁ - C _{ca} - O _{ca3} ^(B) - Zr ₄ ^(B)	38.2	0.000
C ₂ - C ₁ - C _{ca} - O _{ca1} ^(F)	16.6	0.000
C ₂ - C ₁ - C _{ca} - O _{ca2} ^(F)	16.6	0.000
C ₂ - C ₁ - C _{ca} - O _{ca3} ^(F)	16.6	0.000
C ₁ - C _{ca} - O _{ca1} ^(F) - Zr ₃ ^(F)	41.2	0.000
C ₁ - C _{ca} - O _{ca1} ^(F) - Zr ₄ ^(F)	46.2	0.000
C ₁ - C _{ca} - O _{ca2} ^(F) - Zr ₁ ^(F)	43.1	0.000
C ₁ - C _{ca} - O _{ca2} ^(F) - Zr ₂ ^(F)	48.3	0.000
C ₁ - C _{ca} - O _{ca2} ^(F) - Zr ₃ ^(F)	37.2	0.000
C ₁ - C _{ca} - O _{ca2} ^(F) - Zr ₄ ^(F)	45.6	0.000
C ₁ - C _{ca} - O _{ca3} ^(F) - Zr ₂ ^(F)	47.4	0.000
C ₁ - C _{ca} - O _{ca3} ^(F) - Zr ₃ ^(F)	39.8	0.000

dihedrals	K [kJ/mol]	ϕ_0 [deg]
$O_{ca1}^{(F)} - C_{ca} - O_{ca1}^{(F)} - Zr_3^{(F)}$	3.9	0.000
$O_{ca1}^{(F)} - C_{ca} - O_{ca1}^{(F)} - Zr_4^{(F)}$	3.3	0.000
$O_{ca1}^{(F)} - C_{ca} - O_{ca3}^{(F)} - Zr_3^{(F)}$	2.9	0.000
$O_{ca2}^{(F)} - C_{ca} - O_{ca2}^{(F)} - Zr_1^{(F)}$	9.4	0.000
$O_{ca2}^{(F)} - C_{ca} - O_{ca2}^{(F)} - Zr_2^{(F)}$	9.2	0.000
$O_{ca2}^{(F)} - C_{ca} - O_{ca2}^{(F)} - Zr_3^{(F)}$	2.6	0.000
$O_{ca2}^{(F)} - C_{ca} - O_{ca2}^{(F)} - Zr_4^{(F)}$	1.8	0.000
$O_{ca3}^{(F)} - C_{ca} - O_{ca1}^{(F)} - Zr_4^{(F)}$	3.7	0.000
$O_{ca3}^{(F)} - C_{ca} - O_{ca3}^{(F)} - Zr_2^{(F)}$	7.5	0.000
$O_{ca3}^{(F)} - C_{ca} - O_{ca3}^{(F)} - Zr_3^{(F)}$	5.5	0.000
out-of-plane-distance	K [kJ/(mol·Å ⁴)]	d_0 [Å]
$C_{ca} - C_2 - C_2 - C_1$	44	0.000
$C_1 - C_2 - H_2 - C_2$	259	0.000
$C_1 - O_{ca}^{(A)} - O_{ca}^{(A)} - C_{ca}$	1494	0.000
$Zr^{(A)} - Zr^{(A)} - Zr^{(A)} - O_{ox}^{(A)}$	343	0.145
$C_1 - O_{ca1}^{(B)} - O_{ca1}^{(B)} - C_{ca}$	1463	0.000
$C_1 - O_{ca2}^{(B)} - O_{ca2}^{(B)} - C_{ca}$	1428	0.000
$C_1 - O_{ca3}^{(B)} - O_{ca3}^{(B)} - C_{ca}$	1424	0.000
$Zr_1^{(B)} - Zr_1^{(B)} - Zr_3^{(B)} - O_{ox3}^{(B)}$	193	0.221
$Zr_1^{(B)} - Zr_2^{(B)} - Zr_4^{(B)} - O_{ox1}^{(B)}$	421	0.356
$Zr_2^{(B)} - Zr_2^{(B)} - Zr_3^{(B)} - O_{ox2}^{(B)}$	180	0.400
$Zr_2^{(B)} - Zr_2^{(B)} - Zr_4^{(B)} - O_{ox4}^{(B)}$	8	0.860
$C_1 - O_{ca1}^{(F)} - O_{ca1}^{(F)} - C_{ca}$	1510	0.000
$C_1 - O_{ca1}^{(F)} - O_{ca3}^{(F)} - C_{ca}$	1509	0.000
$C_1 - O_{ca2}^{(F)} - O_{ca2}^{(F)} - C_{ca}$	1481	0.000
$C_1 - O_{ca3}^{(F)} - O_{ca3}^{(F)} - C_{ca}$	1472	0.000
$Zr_1^{(F)} - Zr_2^{(F)} - Zr_2^{(F)} - O_{ox3}^{(F)}$	4	0.731
$Zr_1^{(F)} - Zr_2^{(F)} - Zr_3^{(F)} - O_{ox2}^{(F)}$	47	0.840
$Zr_1^{(F)} - Zr_3^{(F)} - Zr_3^{(F)} - O_{ox4}^{(F)}$	225	0.444
$Zr_2^{(F)} - Zr_3^{(F)} - Zr_4^{(F)} - O_{ox1}^{(F)}$	293	0.331

Table S11: Parameters of the noncovalent contributions to the UiO–66 force field for the **type 1** structure, having an average coordination number of 11.

Atom type	q [e]	d [\AA]	ε [kcal/mol]	σ [\AA]
Zr ^(A)	2.370	2.367	0.300	2.540
Zr ₁ ^(B)	2.374	2.367	0.300	2.540
Zr ₂ ^(B)	2.336	2.367	0.300	2.540
Zr ₃ ^(B)	2.375	2.367	0.300	2.540
Zr ₄ ^(B)	2.363	2.367	0.300	2.540
Zr ₁ ^(F)	2.272	2.367	0.300	2.540
Zr ₂ ^(F)	2.338	2.367	0.300	2.540
Zr ₃ ^(F)	2.375	2.367	0.300	2.540
Zr ₄ ^(F)	2.363	2.367	0.300	2.540
O _{ox} ^(A)	-1.083	1.118	0.059	1.820
O _{ox1} ^(B)	-1.074	1.118	0.059	1.820
O _{ox2} ^(B)	-1.104	1.118	0.059	1.820
O _{ox3} ^(B)	-1.091	1.118	0.059	1.820
O _{ox4} ^(B)	-1.109	1.118	0.059	1.820
O _{ox1} ^(F)	-1.081	1.118	0.059	1.820
O _{ox2} ^(F)	-1.103	1.118	0.059	1.820
O _{ox3} ^(F)	-1.161	1.118	0.059	1.820
O _{ox4} ^(F)	-1.051	1.118	0.059	1.820
O _{oh} ^(A)	-1.037	1.118	0.059	1.820
O _{oh1} ^(B)	-1.039	1.118	0.059	1.820
O _{oh2} ^(B)	-1.026	1.118	0.059	1.820
O _{oh1} ^(F)	-1.044	1.118	0.059	1.820
O _{oh2} ^(F)	-1.025	1.118	0.059	1.820
O _{ca} ^(A)	-0.682	1.118	0.059	1.820
O _{ca1} ^(B)	-0.682	1.118	0.059	1.820
O _{ca2} ^(B)	-0.683	1.118	0.059	1.820
O _{ca3} ^(B)	-0.685	1.118	0.059	1.820
O _{ca1} ^(F)	-0.682	1.118	0.059	1.820
O _{ca2} ^(F)	-0.685	1.118	0.059	1.820
O _{ca3} ^(F)	-0.686	1.118	0.059	1.820
C _{ca}	0.768	1.163	0.056	1.940
C ₁	-0.135	1.163	0.056	1.960
C ₂	-0.106	1.163	0.056	1.960
H _{oh} ^(A)	0.497	0.724	0.016	1.600
H _{oh1} ^(B)	0.496	0.724	0.016	1.600
H _{oh2} ^(B)	0.490	0.724	0.016	1.600
H _{oh1} ^(F)	0.504	0.724	0.016	1.600
H _{oh2} ^(F)	0.488	0.724	0.016	1.600
H ₂	0.152	0.724	0.020	1.620

2.3.6 Type 2

Table S12: Parameters of the covalent contributions to the UiO–66 force field for the **type 2** structure, having an average coordination number of 11 (continued on the next pages).

bonds	K [kJ/(mol·Å ²)]	r_0 [Å]
C _{ca} – C ₁	2087	1.499
C _{ca} – O _{ca} ^(A)	4414	1.274
C _{ca} – O _{ca1} ^(E)	4359	1.275
C _{ca} – O _{ca2} ^(E)	4408	1.274
C ₁ – C ₂	3140	1.400
C ₂ – C ₂	3382	1.388
C ₂ – C ₂	3376	1.083
H _{oh} ^(A) – O _{oh} ^(A)	4957	0.997
O _{ca} ^(A) – Zr ^(A)	522	2.212
O _{oh} ^(A) – Zr ^(A)	403	2.258
O _{ox} ^(A) – Zr ^(A)	819	2.070
H _{oh1} ^(E) – O _{oh1} ^(E)	4960	0.996
O _{ca1} ^(E) – Zr ₁ ^(E)	520	2.214
O _{ca1} ^(E) – Zr ₂ ^(E)	546	2.183
O _{ca1} ^(E) – Zr ₃ ^(E)	441	2.207
O _{ca1} ^(E) – Zr ₄ ^(E)	627	2.167
O _{ca2} ^(E) – Zr ₂ ^(E)	447	2.227
O _{ca2} ^(E) – Zr ₄ ^(E)	551	2.186
O _{oh1} ^(E) – Zr ₁ ^(E)	238	2.318
O _{oh1} ^(E) – Zr ₂ ^(E)	546	2.227
O _{oh1} ^(E) – Zr ₄ ^(E)	342	2.286
O _{ox1} ^(E) – Zr ₁ ^(E)	757	2.079
O _{ox1} ^(E) – Zr ₂ ^(E)	1199	2.013
O _{ox1} ^(E) – Zr ₄ ^(E)	853	2.074
O _{ox2} ^(E) – Zr ₁ ^(E)	920	2.043
O _{ox2} ^(E) – Zr ₂ ^(E)	848	2.087
O _{ox2} ^(E) – Zr ₃ ^(E)	1148	2.032
O _{ox3} ^(E) – Zr ₁ ^(E)	83	2.242
O _{ox3} ^(E) – Zr ₂ ^(E)	622	2.110
O _{ox3} ^(E) – Zr ₃ ^(E)	861	2.062
bends	K [kJ/(mol·rad ²)]	θ_0 [deg]
C _{ca} – C ₁ – C ₂	617	120.1
C _{ca} – O _{ca} ^(A) – Zr ^(A)	298	134.9
C _{ca} – O _{ca1} ^(E) – Zr ₁ ^(E)	292	136.5
C _{ca} – O _{ca1} ^(E) – Zr ₂ ^(E)	285	131.7
C _{ca} – O _{ca1} ^(E) – Zr ₃ ^(E)	263	128.6

bends	K [kJ/(mol·rad ²)]	θ_0 [deg]
C _{ca} - O _{ca1} ^(E) - Zr ₄ ^(E)	301	137.7
C _{ca} - O _{ca2} ^(E) - Zr ₂ ^(E)	300	135.3
C _{ca} - O _{ca2} ^(E) - Zr ₄ ^(E)	300	135.1
C ₁ - C _{ca} - O _{ca} ^(A)	165	118.2
C ₁ - C _{ca} - O _{ca1} ^(E)	175	118.4
C ₁ - C _{ca} - O _{ca2} ^(E)	169	118.5
C ₁ - C ₂ - C ₂	464	120.1
C ₁ - C ₂ - C ₂	280	119.4
C ₂ - C ₁ - C ₂	449	119.9
C ₂ - C ₂ - C ₂	345	120.2
H _{oh} ^(A) - O _{oh} ^(A) - Zr ^(A)	161	114.9
H _{oh1} ^(E) - O _{oh1} ^(E) - Zr ₁ ^(E)	143	114.4
H _{oh1} ^(E) - O _{oh1} ^(E) - Zr ₂ ^(E)	156	116.4
H _{oh1} ^(E) - O _{oh1} ^(E) - Zr ₄ ^(E)	151	116.6
O _{ca} ^(A) - C _{ca} - O _{ca} ^(A)	644	123.1
O _{ca1} ^(E) - C _{ca} - O _{ca1} ^(E)	642	123.0
O _{ca2} ^(E) - C _{ca} - O _{ca2} ^(E)	641	122.9
Zr ^(A) - O _{oh} ^(A) - Zr ^(A)	738	105.2
Zr ^(A) - O _{ox} ^(A) - Zr ^(A)	556	118.9
O _{ox} ^(A) - Zr ^(A) - O _{oh} ^(A)	174	67.2
O _{oh1} ^(E) - Zr ₁ ^(E) - O _{ox1} ^(E)	329	66.9
O _{oh1} ^(E) - Zr ₁ ^(E) - O _{ox2} ^(E)	330	69.5
O _{oh1} ^(E) - Zr ₂ ^(E) - O _{ox1} ^(E)	281	70.6
O _{oh1} ^(E) - Zr ₂ ^(E) - O _{ox2} ^(E)	334	70.3
O _{oh1} ^(E) - Zr ₄ ^(E) - O _{ox1} ^(E)	275	67.6
O _{ox1} ^(E) - Zr ₁ ^(E) - O _{ox3} ^(E)	395	69.9
O _{ox1} ^(E) - Zr ₂ ^(E) - O _{ox3} ^(E)	209	73.5
O _{ox3} ^(E) - Zr ₁ ^(E) - O _{ox3} ^(E)	431	72.4
O _{ox3} ^(E) - Zr ₂ ^(E) - O _{ox3} ^(E)	529	69.5
O _{ox2} ^(E) - Zr ₃ ^(E) - O _{ox3} ^(E)	416	73.7
O _{ox3} ^(E) - Zr ₃ ^(E) - O _{ox3} ^(E)	150	124.8
Zr ₁ ^(E) - O _{oh1} ^(E) - Zr ₂ ^(E)	713	102.3
Zr ₁ ^(E) - O _{oh1} ^(E) - Zr ₄ ^(E)	623	104.1
Zr ₁ ^(E) - O _{ox1} ^(E) - Zr ₂ ^(E)	568	112.3
Zr ₁ ^(E) - O _{ox1} ^(E) - Zr ₄ ^(E)	423	121.5
Zr ₁ ^(E) - O _{ox2} ^(E) - Zr ₂ ^(E)	376	118.0
Zr ₁ ^(E) - O _{ox2} ^(E) - Zr ₃ ^(E)	505	110.1
Zr ₁ ^(E) - O _{ox3} ^(E) - Zr ₂ ^(E)	756	103.6
Zr ₁ ^(E) - O _{ox3} ^(E) - Zr ₃ ^(E)	769	101.9
Zr ₂ ^(E) - O _{oh1} ^(E) - Zr ₄ ^(E)	678	102.5
Zr ₂ ^(E) - O _{ox1} ^(E) - Zr ₄ ^(E)	436	118.2
Zr ₂ ^(E) - O _{ox2} ^(E) - Zr ₃ ^(E)	560	110.1
Zr ₂ ^(E) - O _{ox3} ^(E) - Zr ₃ ^(E)	738	108.7

dihedrals	K [kJ/mol]	ϕ_0 [deg]
$C_{ca} - C_1 - C_2 - C_2$	34.8	0.000
$C_{ca} - C_1 - C_2 - C_2$	16.0	0.000
$C_1 - C_{ca} - O_{ca}^{(A)} - Zr^{(A)}$	49.4	0.000
$C_1 - C_{ca} - O_{ca1}^{(E)} - Zr_1^{(E)}$	36.8	0.000
$C_1 - C_{ca} - O_{ca1}^{(E)} - Zr_2^{(E)}$	43.9	0.000
$C_1 - C_{ca} - O_{ca1}^{(E)} - Zr_3^{(E)}$	39.7	0.000
$C_1 - C_{ca} - O_{ca1}^{(E)} - Zr_4^{(E)}$	42.7	0.000
$C_1 - C_{ca} - O_{ca2}^{(E)} - Zr_2^{(E)}$	44.6	0.000
$C_1 - C_{ca} - O_{ca2}^{(E)} - Zr_4^{(E)}$	47.7	0.000
$C_1 - C_2 - C_2 - C_1$	30.7	0.000
$C_1 - C_2 - C_2 - C_2$	36.2	0.000
$C_2 - C_1 - C_{ca} - O_{ca}^{(A)}$	16.6	0.000
$C_2 - C_1 - C_{ca} - O_{ca1}^{(E)}$	16.6	0.000
$C_2 - C_1 - C_{ca} - O_{ca2}^{(E)}$	16.6	0.000
$C_2 - C_1 - C_2 - C_2$	31.7	0.000
$C_2 - C_1 - C_2 - C_2$	25.9	0.000
$C_2 - C_2 - C_2 - C_2$	16.6	0.000
$O_{ca}^{(A)} - C_{ca} - O_{ca}^{(A)} - Zr^{(A)}$	4.4	0.000
$O_{ca1}^{(E)} - C_{ca} - O_{ca1}^{(E)} - Zr_1^{(E)}$	6.8	0.000
$O_{ca1}^{(E)} - C_{ca} - O_{ca1}^{(E)} - Zr_2^{(E)}$	5.1	0.000
$O_{ca1}^{(E)} - C_{ca} - O_{ca1}^{(E)} - Zr_3^{(E)}$	5.7	0.000
$O_{ca1}^{(E)} - C_{ca} - O_{ca1}^{(E)} - Zr_4^{(E)}$	3.4	0.000
$O_{ca2}^{(E)} - C_{ca} - O_{ca2}^{(E)} - Zr_2^{(E)}$	6.7	0.000
$O_{ca2}^{(E)} - C_{ca} - O_{ca2}^{(E)} - Zr_4^{(E)}$	3.2	0.000
out-of-plane-distance	K [kJ/(mol·Å ⁴)]	d_0 [Å]
$C_{ca} - C_2 - C_2 - C_1$	44	0.000
$C_1 - C_2 - C_2 - C_2$	259	0.000
$C_1 - O_{ca}^{(A)} - O_{ca}^{(A)} - C_{ca}$	1494	0.000
$C_1 - O_{ca1}^{(E)} - O_{ca1}^{(E)} - C_{ca}$	1479	0.000
$C_1 - O_{ca2}^{(E)} - O_{ca2}^{(E)} - C_{ca}$	1491	0.000
$Zr^{(A)} - Zr^{(A)} - Zr^{(A)} - O_{ox}^{(A)}$	343	0.145
$Zr_1^{(E)} - Zr_2^{(E)} - Zr_3^{(E)} - O_{ox2}^{(E)}$	124	0.557
$Zr_1^{(E)} - Zr_2^{(E)} - Zr_3^{(E)} - O_{ox3}^{(E)}$	34	0.875
$Zr_1^{(E)} - Zr_2^{(E)} - Zr_4^{(E)} - O_{ox1}^{(E)}$	294	0.324

Table S13: Parameters of the noncovalent contributions to the UiO–66 force field for the **type 2** structure, having an average coordination number of 11.

Atom type	q [e]	d [\AA]	ε [kcal/mol]	σ [\AA]
Zr ^(A)	2.370	2.367	0.300	2.540
Zr ₁ ^(E)	2.367	2.367	0.300	2.540
Zr ₂ ^(E)	2.344	2.367	0.300	2.540
Zr ₃ ^(E)	2.286	2.367	0.300	2.540
Zr ₄ ^(E)	2.384	2.367	0.300	2.540
O _{ox} ^(A)	-1.083	1.118	0.059	1.820
O _{ox1} ^(E)	-1.085	1.118	0.059	1.820
O _{ox2} ^(E)	-1.099	1.118	0.059	1.820
O _{ox3} ^(E)	-1.107	1.118	0.059	1.820
O _{oh} ^(A)	-1.037	1.118	0.059	1.820
O _{oh1} ^(E)	-1.034	1.118	0.059	1.820
O _{ca} ^(A)	-0.682	1.118	0.059	1.820
O _{ca1} ^(E)	-0.687	1.118	0.059	1.820
O _{ca2} ^(E)	-0.684	1.118	0.059	1.820
C _{ca}	0.773	1.163	0.056	1.940
C ₁	-0.135	1.163	0.056	1.960
C ₂	-0.106	1.163	0.056	1.960
H _{oh} ^(A)	0.497	0.724	0.016	1.600
H _{oh1} ^(E)	0.493	0.724	0.016	1.600
H ₂	0.152	0.724	0.020	1.620

2.3.7 Type 3

Table S14: Parameters of the covalent contributions to the UiO–66 force field for the **type 3** structure, having an average coordination number of 11 (continued on the next pages).

bonds	K [kJ/(mol·Å ²)]	r_0 [Å]
C _{ca} – C ₁	2087	1.499
C _{ca} – O _{ca1} ^(B)	4419	1.274
C _{ca} – O _{ca2} ^(B)	4403	1.275
C _{ca} – O _{ca3} ^(B)	4381	1.274
C ₁ – C ₂	3140	1.400
C ₂ – C ₂	3382	1.388
C ₂ – H ₂	3376	1.083
H _{oh1} ^(B) – O _{oh1} ^(B)	4954	0.997
H _{oh2} ^(B) – O _{oh2} ^(B)	4967	0.996
O _{ca1} ^(B) – Zr ₁ ^(B)	597	2.182
O _{ca2} ^(B) – Zr ₁ ^(B)	490	2.201
O _{ca2} ^(B) – Zr ₂ ^(B)	403	2.240
O _{ca3} ^(B) – Zr ₁ ^(B)	535	2.194
O _{ca3} ^(B) – Zr ₂ ^(B)	518	2.193
O _{ca3} ^(B) – Zr ₃ ^(B)	522	2.207
O _{ca3} ^(B) – Zr ₄ ^(B)	507	2.208
O _{oh1} ^(B) – Zr ₁ ^(B)	354	2.281
O _{oh1} ^(B) – Zr ₂ ^(B)	464	2.251
O _{oh1} ^(B) – Zr ₃ ^(B)	387	2.263
O _{oh2} ^(B) – Zr ₁ ^(B)	410	2.262
O _{oh2} ^(B) – Zr ₄ ^(B)	225	2.323
O _{ox1} ^(B) – Zr ₁ ^(B)	856	2.071
O _{ox1} ^(B) – Zr ₂ ^(B)	1237	2.009
O _{ox1} ^(B) – Zr ₄ ^(B)	851	2.063
O _{ox2} ^(B) – Zr ₂ ^(B)	882	2.072
O _{ox2} ^(B) – Zr ₃ ^(B)	968	2.035
O _{ox3} ^(B) – Zr ₁ ^(B)	783	2.077
O _{ox3} ^(B) – Zr ₃ ^(B)	778	2.072
O _{ox4} ^(B) – Zr ₂ ^(B)	692	2.087
O _{ox4} ^(B) – Zr ₄ ^(B)	37	2.258
bends	K [kJ/(mol·rad ²)]	θ_0 [deg]
C _{ca} – C ₁ – C ₂	617	120.1
C _{ca} – O _{ca1} ^(B) – Zr ₁ ^(B)	286	136.0
C _{ca} – O _{ca2} ^(B) – Zr ₁ ^(B)	317	135.1
C _{ca} – O _{ca2} ^(B) – Zr ₂ ^(B)	313	134.9
C _{ca} – O _{ca3} ^(B) – Zr ₁ ^(B)	302	136.4
C _{ca} – O _{ca3} ^(B) – Zr ₂ ^(B)	283	131.1

bends	K [kJ/(mol·rad ²)]	θ_0 [deg]
C _{ca} - O _{ca3} ^(B) - Zr ₃ ^(B)	300	136.1
C _{ca} - O _{ca3} ^(B) - Zr ₄ ^(B)	299	136.7
C ₁ - C _{ca} - O _{ca1} ^(B)	173	118.4
C ₁ - C _{ca} - O _{ca2} ^(B)	166	118.5
C ₁ - C _{ca} - O _{ca3} ^(B)	171	118.2
C ₁ - C ₂ - C ₂	464	120.1
C ₁ - C ₂ - H ₂	280	119.4
C ₂ - C ₁ - C ₂	449	119.9
C ₂ - C ₂ - H ₂	345	120.2
H _{oh1} ^(B) - O _{oh1} ^(B) - Zr ₁ ^(B)	154	115.6
H _{oh1} ^(B) - O _{oh1} ^(B) - Zr ₂ ^(B)	154	116.5
H _{oh1} ^(B) - O _{oh1} ^(B) - Zr ₃ ^(B)	156	115.9
H _{oh2} ^(B) - O _{oh2} ^(B) - Zr ₁ ^(B)	165	114.5
H _{oh2} ^(B) - O _{oh2} ^(B) - Zr ₄ ^(B)	151	114.5
O _{ca1} ^(B) - C _{ca} - O _{ca1} ^(B)	652	123.0
O _{ca2} ^(B) - C _{ca} - O _{ca2} ^(B)	638	123.0
O _{ca3} ^(B) - C _{ca} - O _{ca3} ^(B)	642	123.0
Zr ₁ ^(B) - O _{oh1} ^(B) - Zr ₂ ^(B)	719	101.8
Zr ₁ ^(B) - O _{oh1} ^(B) - Zr ₃ ^(B)	672	104.1
Zr ₁ ^(B) - O _{oh2} ^(B) - Zr ₁ ^(B)	713	104.5
Zr ₁ ^(B) - O _{oh2} ^(B) - Zr ₄ ^(B)	715	104.0
Zr ₁ ^(B) - O _{ox1} ^(B) - Zr ₂ ^(B)	443	118.3
Zr ₁ ^(B) - O _{ox1} ^(B) - Zr ₄ ^(B)	429	120.8
Zr ₁ ^(B) - O _{ox3} ^(B) - Zr ₁ ^(B)	532	117.8
Zr ₁ ^(B) - O _{ox3} ^(B) - Zr ₃ ^(B)	540	118.8
Zr ₂ ^(B) - O _{oh1} ^(B) - Zr ₃ ^(B)	711	102.7
Zr ₂ ^(B) - O _{ox1} ^(B) - Zr ₄ ^(B)	584	111.3
Zr ₂ ^(B) - O _{ox2} ^(B) - Zr ₂ ^(B)	595	110.9
Zr ₂ ^(B) - O _{ox2} ^(B) - Zr ₃ ^(B)	443	118.3
Zr ₂ ^(B) - O _{ox4} ^(B) - Zr ₂ ^(B)	827	110.5
Zr ₂ ^(B) - O _{ox4} ^(B) - Zr ₄ ^(B)	851	103.0
O _{oh1} ^(B) - Zr ₁ ^(B) - O _{ox1} ^(B)	223	69.0
O _{oh1} ^(B) - Zr ₁ ^(B) - O _{ox3} ^(B)	212	67.9
O _{oh1} ^(B) - Zr ₂ ^(B) - O _{ox1} ^(B)	258	70.8
O _{oh1} ^(B) - Zr ₂ ^(B) - O _{ox2} ^(B)	318	69.5
O _{oh1} ^(B) - Zr ₃ ^(B) - O _{ox2} ^(B)	239	69.5
O _{oh1} ^(B) - Zr ₃ ^(B) - O _{ox3} ^(B)	170	68.1
O _{oh2} ^(B) - Zr ₁ ^(B) - O _{ox1} ^(B)	259	67.9
O _{oh2} ^(B) - Zr ₁ ^(B) - O _{ox3} ^(B)	220	68.2
O _{oh2} ^(B) - Zr ₄ ^(B) - O _{ox1} ^(B)	320	67.2
O _{ox1} ^(B) - Zr ₂ ^(B) - O _{ox4} ^(B)	182	74.5
O _{ox1} ^(B) - Zr ₄ ^(B) - O _{ox4} ^(B)	387	70.6
O _{ox2} ^(B) - Zr ₂ ^(B) - O _{ox4} ^(B)	453	69.6

dihedrals	K [kJ/mol]	ϕ_0 [deg]
$C_{ca} - C_1 - C_2 - C_2$	34.8	0.000
$C_{ca} - C_1 - C_2 - H_2$	16.0	0.000
$C_1 - C_{ca} - O_{ca1}^{(B)} - Zr_1^{(B)}$	42.0	0.000
$C_1 - C_{ca} - O_{ca2}^{(B)} - Zr_1^{(B)}$	48.7	0.000
$C_1 - C_{ca} - O_{ca2}^{(B)} - Zr_2^{(B)}$	44.7	0.000
$C_1 - C_{ca} - O_{ca3}^{(B)} - Zr_1^{(B)}$	44.1	0.000
$C_1 - C_{ca} - O_{ca3}^{(B)} - Zr_2^{(B)}$	39.5	0.000
$C_1 - C_{ca} - O_{ca3}^{(B)} - Zr_3^{(B)}$	43.3	0.000
$C_1 - C_{ca} - O_{ca3}^{(B)} - Zr_4^{(B)}$	38.2	0.000
$C_1 - C_2 - C_2 - C_1$	30.7	0.000
$C_1 - C_2 - C_2 - H_2$	36.2	0.000
$C_2 - C_1 - C_{ca} - O_{ca1}^{(B)}$	16.6	0.000
$C_2 - C_1 - C_{ca} - O_{ca2}^{(B)}$	16.6	0.000
$C_2 - C_1 - C_{ca} - O_{ca3}^{(B)}$	16.6	0.000
$C_2 - C_1 - C_2 - C_2$	31.7	0.000
$C_2 - C_1 - C_2 - H_2$	25.9	0.000
$H_2 - C_2 - C_2 - H_2$	16.6	0.000
$O_{ca1}^{(B)} - C_{ca} - O_{ca1}^{(B)} - Zr_1^{(B)}$	3.7	0.000
$O_{ca2}^{(B)} - C_{ca} - O_{ca2}^{(B)} - Zr_1^{(B)}$	3.3	0.000
$O_{ca2}^{(B)} - C_{ca} - O_{ca2}^{(B)} - Zr_2^{(B)}$	7.6	0.000
$O_{ca3}^{(B)} - C_{ca} - O_{ca3}^{(B)} - Zr_1^{(B)}$	4.2	0.000
$O_{ca3}^{(B)} - C_{ca} - O_{ca3}^{(B)} - Zr_2^{(B)}$	5.9	0.000
$O_{ca3}^{(B)} - C_{ca} - O_{ca3}^{(B)} - Zr_3^{(B)}$	5.7	0.000
$O_{ca3}^{(B)} - C_{ca} - O_{ca3}^{(B)} - Zr_4^{(B)}$	4.9	0.000
out-of-plane-distance	K [kJ/(mol·Å ⁴)]	d_0 [Å]
$C_{ca} - C_2 - C_2 - C_1$	44	0.000
$C_1 - C_2 - H_2 - C_2$	259	0.000
$C_1 - O_{ca1}^{(B)} - O_{ca1}^{(B)} - C_{ca}$	1463	0.000
$C_1 - O_{ca2}^{(B)} - O_{ca2}^{(B)} - C_{ca}$	1428	0.000
$C_1 - O_{ca3}^{(B)} - O_{ca3}^{(B)} - C_{ca}$	1424	0.000
$Zr_1^{(B)} - Zr_1^{(B)} - Zr_3^{(B)} - O_{ox3}^{(B)}$	193	0.221
$Zr_1^{(B)} - Zr_2^{(B)} - Zr_4^{(B)} - O_{ox1}^{(B)}$	421	0.356
$Zr_2^{(B)} - Zr_2^{(B)} - Zr_3^{(B)} - O_{ox2}^{(B)}$	180	0.400
$Zr_2^{(B)} - Zr_2^{(B)} - Zr_4^{(B)} - O_{ox4}^{(B)}$	8	0.860

Table S15: Parameters of the noncovalent contributions to the UiO–66 force field for the **type 3** structure, having an average coordination number of 11.

Atom type	q [e]	d [\AA]	ϵ [kcal/mol]	σ [\AA]
Zr ₁ ^(B)	2.374	2.367	0.300	2.540
Zr ₂ ^(B)	2.336	2.367	0.300	2.540
Zr ₃ ^(B)	2.375	2.367	0.300	2.540
Zr ₄ ^(B)	2.363	2.367	0.300	2.540
O _{ox1} ^(B)	-1.074	1.118	0.059	1.820
O _{ox2} ^(B)	-1.104	1.118	0.059	1.820
O _{ox3} ^(B)	-1.091	1.118	0.059	1.820
O _{ox4} ^(B)	-1.109	1.118	0.059	1.820
O _{oh1} ^(B)	-1.039	1.118	0.059	1.820
O _{oh2} ^(B)	-1.026	1.118	0.059	1.820
O _{ca1} ^(B)	-0.682	1.118	0.059	1.820
O _{ca2} ^(B)	-0.683	1.118	0.059	1.820
O _{ca3} ^(B)	-0.685	1.118	0.059	1.820
C _{ca}	0.768	1.163	0.056	1.940
C ₁	-0.135	1.163	0.056	1.960
C ₂	-0.106	1.163	0.056	1.960
H _{oh1} ^(B)	0.496	0.724	0.016	1.600
H _{oh2} ^(B)	0.490	0.724	0.016	1.600
H ₂	0.152	0.724	0.020	1.620

2.3.8 Type 4

Table S16: Parameters of the covalent contributions to the UiO–66 force field for the **type 4** structure, having an average coordination number of 11 (continued on the next pages).

bonds	K [kJ/(mol·Å ²)]	r_0 [Å]
C _{ca} – C ₁	2087	1.499
C _{ca} – O _{ca} ^(A)	4414	1.274
C _{ca} – O _{ca1} ^(B)	4419	1.274
C _{ca} – O _{ca2} ^(B)	4403	1.275
C _{ca} – O _{ca3} ^(B)	4381	1.274
C ₁ – C ₂	3140	1.400
C ₂ – C ₂	3382	1.388
C ₂ – H ₂	3376	1.083
H _{oh} ^(A) – O _{oh} ^(A)	4957	0.997
O _{ca} ^(A) – Zr ^(A)	522	2.212
O _{oh} ^(A) – Zr ^(A)	403	2.258
O _{ox} ^(A) – Zr ^(A)	819	2.070
H _{oh1} ^(B) – O _{oh1} ^(B)	4954	0.997
H _{oh2} ^(B) – O _{oh2} ^(B)	4967	0.996
O _{ca1} ^(B) – Zr ₁ ^(B)	597	2.182
O _{ca2} ^(B) – Zr ₁ ^(B)	490	2.201
O _{ca2} ^(B) – Zr ₂ ^(B)	403	2.240
O _{ca3} ^(B) – Zr ₁ ^(B)	535	2.194
O _{ca3} ^(B) – Zr ₂ ^(B)	518	2.193
O _{ca3} ^(B) – Zr ₃ ^(B)	522	2.207
O _{ca3} ^(B) – Zr ₄ ^(B)	507	2.208
O _{oh1} ^(B) – Zr ₁ ^(B)	354	2.281
O _{oh1} ^(B) – Zr ₂ ^(B)	464	2.251
O _{oh1} ^(B) – Zr ₃ ^(B)	387	2.263
O _{oh2} ^(B) – Zr ₁ ^(B)	410	2.262
O _{oh2} ^(B) – Zr ₄ ^(B)	225	2.323
O _{ox1} ^(B) – Zr ₁ ^(B)	856	2.071
O _{ox1} ^(B) – Zr ₂ ^(B)	1237	2.009
O _{ox1} ^(B) – Zr ₄ ^(B)	851	2.063
O _{ox2} ^(B) – Zr ₂ ^(B)	882	2.072
O _{ox2} ^(B) – Zr ₃ ^(B)	968	2.035
O _{ox3} ^(B) – Zr ₁ ^(B)	783	2.077
O _{ox3} ^(B) – Zr ₃ ^(B)	778	2.072
O _{ox4} ^(B) – Zr ₂ ^(B)	692	2.087
O _{ox4} ^(B) – Zr ₄ ^(B)	37	2.258
C _{ca} – O _{ca1} ^(D)	4362	1.276
C _{ca} – O _{ca2} ^(D)	4375	1.276

bonds	K [kJ/(mol·Å ²)]	r_0 [Å]
C _{ca} – O _{ca3} ^(D)	4364	1.275
H _{oh1} ^(D) – O _{oh1} ^(D)	4966	0.996
H _{oh2} ^(D) – O _{oh2} ^(D)	4950	0.997
O _{ca1} ^(D) – Zr ₁ ^(D)	509	2.184
O _{ca1} ^(D) – Zr ₂ ^(D)	579	2.178
O _{ca1} ^(D) – Zr ₃ ^(D)	593	2.190
O _{ca1} ^(D) – Zr ₄ ^(D)	585	2.179
O _{ca2} ^(D) – Zr ₁ ^(D)	495	2.189
O _{ca2} ^(D) – Zr ₂ ^(D)	426	2.216
O _{ca2} ^(D) – Zr ₃ ^(D)	506	2.193
O _{ca2} ^(D) – Zr ₄ ^(D)	390	2.240
O _{ca2} ^(D) – Zr ₅ ^(D)	432	2.235
O _{ca2} ^(D) – Zr ₆ ^(D)	514	2.205
O _{ca3} ^(D) – Zr ₃ ^(D)	549	2.194
O _{ca3} ^(D) – Zr ₄ ^(D)	576	2.185
O _{ca3} ^(D) – Zr ₅ ^(D)	576	2.178
O _{ca3} ^(D) – Zr ₆ ^(D)	567	2.179
O _{oh1} ^(D) – Zr ₁ ^(D)	507	2.237
O _{oh1} ^(D) – Zr ₃ ^(D)	420	2.256
O _{oh1} ^(D) – Zr ₄ ^(D)	138	2.358
O _{oh2} ^(D) – Zr ₂ ^(D)	399	2.262
O _{oh2} ^(D) – Zr ₃ ^(D)	331	2.287
O _{oh2} ^(D) – Zr ₅ ^(D)	474	2.239
O _{ox1} ^(D) – Zr ₂ ^(D)	1200	2.016
O _{ox1} ^(D) – Zr ₃ ^(D)	828	2.071
O _{ox1} ^(D) – Zr ₄ ^(D)	835	2.071
O _{ox2} ^(D) – Zr ₁ ^(D)	1257	2.008
O _{ox2} ^(D) – Zr ₄ ^(D)	849	2.063
O _{ox2} ^(D) – Zr ₆ ^(D)	1142	2.021
O _{ox3} ^(D) – Zr ₁ ^(D)	544	2.126
O _{ox3} ^(D) – Zr ₅ ^(D)	684	2.091
O _{ox3} ^(D) – Zr ₆ ^(D)	294	2.170
O _{ox4} ^(D) – Zr ₁ ^(D)	848	2.077
O _{ox4} ^(D) – Zr ₃ ^(D)	967	2.039
O _{ox4} ^(D) – Zr ₅ ^(D)	756	2.093
O _{ox5} ^(D) – Zr ₂ ^(D)	778	2.095
O _{ox5} ^(D) – Zr ₅ ^(D)	1284	1.992
O _{ox5} ^(D) – Zr ₆ ^(D)	859	2.075
O _{ox6} ^(D) – Zr ₂ ^(D)	818	2.061
O _{ox6} ^(D) – Zr ₄ ^(D)	174	2.210
O _{ox6} ^(D) – Zr ₆ ^(D)	343	2.164

bends	K [kJ/(mol·rad ²)]	θ_0 [deg]
C _{ca} - C ₁ - C ₂	617	120.1
C _{ca} - O _{ca} ^(A) - Zr ^(A)	298	134.9
C _{ca} - O _{ca1} ^(B) - Zr ₁ ^(B)	286	136.0
C _{ca} - O _{ca2} ^(B) - Zr ₁ ^(B)	317	135.1
C _{ca} - O _{ca2} ^(B) - Zr ₂ ^(B)	313	134.9
C _{ca} - O _{ca3} ^(B) - Zr ₁ ^(B)	302	136.4
C _{ca} - O _{ca3} ^(B) - Zr ₂ ^(B)	283	131.1
C _{ca} - O _{ca3} ^(B) - Zr ₃ ^(B)	300	136.1
C _{ca} - O _{ca3} ^(B) - Zr ₄ ^(B)	299	136.7
C ₁ - C _{ca} - O _{ca1} ^(B)	173	118.4
C ₁ - C _{ca} - O _{ca2} ^(B)	166	118.5
C ₁ - C _{ca} - O _{ca3} ^(B)	171	118.2
C ₁ - C _{ca} - O _{ca} ^(A)	165	118.2
C ₁ - C ₂ - C ₂	464	120.1
C ₁ - C ₂ - H ₂	280	119.4
C ₂ - C ₁ - C ₂	449	119.9
C ₂ - C ₂ - H ₂	345	120.2
H _{oh} ^(A) - O _{oh} ^(A) - Zr ^(A)	161	114.9
O _{ca} ^(A) - C _{ca} - O _{ca} ^(A)	644	123.1
Zr ^(A) - O _{oh} ^(A) - Zr ^(A)	738	105.2
Zr ^(A) - O _{ox} ^(A) - Zr ^(A)	556	118.9
O _{ox} ^(A) - Zr ^(A) - O _{oh} ^(A)	174	67.2
H _{oh1} ^(B) - O _{oh1} ^(B) - Zr ₁ ^(B)	154	115.6
H _{oh1} ^(B) - O _{oh1} ^(B) - Zr ₂ ^(B)	154	116.5
H _{oh1} ^(B) - O _{oh1} ^(B) - Zr ₃ ^(B)	156	115.9
H _{oh2} ^(B) - O _{oh2} ^(B) - Zr ₁ ^(B)	165	114.5
H _{oh2} ^(B) - O _{oh2} ^(B) - Zr ₄ ^(B)	151	114.5
O _{ca1} ^(B) - C _{ca} - O _{ca1} ^(B)	652	123.0
O _{ca2} ^(B) - C _{ca} - O _{ca2} ^(B)	638	123.0
O _{ca3} ^(B) - C _{ca} - O _{ca3} ^(B)	642	123.0
Zr ₁ ^(B) - O _{oh1} ^(B) - Zr ₂ ^(B)	719	101.8
Zr ₁ ^(B) - O _{oh1} ^(B) - Zr ₃ ^(B)	672	104.1
Zr ₁ ^(B) - O _{oh2} ^(B) - Zr ₁ ^(B)	713	104.5
Zr ₁ ^(B) - O _{oh2} ^(B) - Zr ₄ ^(B)	715	104.0
Zr ₁ ^(B) - O _{ox1} ^(B) - Zr ₂ ^(B)	443	118.3
Zr ₁ ^(B) - O _{ox1} ^(B) - Zr ₄ ^(B)	429	120.8
Zr ₁ ^(B) - O _{ox3} ^(B) - Zr ₁ ^(B)	532	117.8
Zr ₁ ^(B) - O _{ox3} ^(B) - Zr ₃ ^(B)	540	118.8
Zr ₂ ^(B) - O _{oh1} ^(B) - Zr ₃ ^(B)	711	102.7
Zr ₂ ^(B) - O _{ox1} ^(B) - Zr ₄ ^(B)	584	111.3
Zr ₂ ^(B) - O _{ox2} ^(B) - Zr ₂ ^(B)	595	110.9
Zr ₂ ^(B) - O _{ox2} ^(B) - Zr ₃ ^(B)	443	118.3

bends	K [kJ/(mol·rad ²)]	θ_0 [deg]
Zr ₂ ^(B) - O _{ox4} ^(B) - Zr ₂ ^(B)	827	110.5
Zr ₂ ^(B) - O _{ox4} ^(B) - Zr ₄ ^(B)	851	103.0
O _{oh1} ^(B) - Zr ₁ ^(B) - O _{ox1} ^(B)	223	69.0
O _{oh1} ^(B) - Zr ₁ ^(B) - O _{ox3} ^(B)	212	67.9
O _{oh1} ^(B) - Zr ₂ ^(B) - O _{ox1} ^(B)	258	70.8
O _{oh1} ^(B) - Zr ₂ ^(B) - O _{ox2} ^(B)	318	69.5
O _{oh1} ^(B) - Zr ₃ ^(B) - O _{ox2} ^(B)	239	69.5
O _{oh1} ^(B) - Zr ₃ ^(B) - O _{ox3} ^(B)	170	68.1
O _{oh2} ^(B) - Zr ₁ ^(B) - O _{ox1} ^(B)	259	67.9
O _{oh2} ^(B) - Zr ₁ ^(B) - O _{ox3} ^(B)	220	68.2
O _{oh2} ^(B) - Zr ₄ ^(B) - O _{ox1} ^(B)	320	67.2
O _{ox1} ^(B) - Zr ₂ ^(B) - O _{ox4} ^(B)	182	74.5
O _{ox1} ^(B) - Zr ₄ ^(B) - O _{ox4} ^(B)	387	70.6
O _{ox2} ^(B) - Zr ₂ ^(B) - O _{ox4} ^(B)	453	69.6
C _{ca} - O _{ca1} ^(D) - Zr ₁ ^(D)	279	133.6
C _{ca} - O _{ca1} ^(D) - Zr ₂ ^(D)	277	129.8
C _{ca} - O _{ca1} ^(D) - Zr ₃ ^(D)	297	137.4
C _{ca} - O _{ca1} ^(D) - Zr ₄ ^(D)	296	138.4
C _{ca} - O _{ca2} ^(D) - Zr ₁ ^(D)	302	132.8
C _{ca} - O _{ca2} ^(D) - Zr ₂ ^(D)	303	134.9
C _{ca} - O _{ca2} ^(D) - Zr ₃ ^(D)	314	134.8
C _{ca} - O _{ca2} ^(D) - Zr ₄ ^(D)	310	135.5
C _{ca} - O _{ca2} ^(D) - Zr ₅ ^(D)	314	135.4
C _{ca} - O _{ca2} ^(D) - Zr ₆ ^(D)	308	136.6
C _{ca} - O _{ca3} ^(D) - Zr ₃ ^(D)	285	136.8
C _{ca} - O _{ca3} ^(D) - Zr ₄ ^(D)	289	137.4
C _{ca} - O _{ca3} ^(D) - Zr ₅ ^(D)	265	132.5
C _{ca} - O _{ca3} ^(D) - Zr ₆ ^(D)	270	132.6
C ₁ - C _{ca} - O _{ca1} ^(D)	178	118.7
C ₁ - C _{ca} - O _{ca2} ^(D)	173	118.6
C ₁ - C _{ca} - O _{ca3} ^(D)	180	118.6
H _{oh1} ^(B) - O _{oh1} ^(D) - Zr ₁ ^(D)	157	116.8
H _{oh1} ^(B) - O _{oh1} ^(D) - Zr ₃ ^(D)	157	116.9
H _{oh1} ^(B) - O _{oh1} ^(D) - Zr ₄ ^(D)	142	114.1
H _{oh2} ^(B) - O _{oh2} ^(D) - Zr ₂ ^(D)	150	115.9
H _{oh2} ^(B) - O _{oh2} ^(D) - Zr ₃ ^(D)	145	116.7
H _{oh2} ^(B) - O _{oh2} ^(D) - Zr ₅ ^(D)	150	116.5
O _{ca1} ^(D) - C _{ca} - O _{ca1} ^(D)	636	122.5
O _{ca2} ^(D) - C _{ca} - O _{ca2} ^(D)	636	122.8
O _{ca3} ^(D) - C _{ca} - O _{ca3} ^(D)	646	122.8
O _{oh1} ^(D) - Zr ₁ ^(D) - O _{ox2} ^(D)	296	70.5
O _{oh1} ^(D) - Zr ₁ ^(D) - O _{ox4} ^(D)	315	68.9

bends	K [kJ/(mol·rad ²)]	θ_0 [deg]
O _{oh1} ^(D) - Zr ₃ ^(D) - O _{ox1} ^(D)	213	68.1
O _{oh1} ^(D) - Zr ₃ ^(D) - O _{ox4} ^(D)	274	69.1
O _{oh1} ^(D) - Zr ₄ ^(D) - O _{ox1} ^(D)	316	66.5
O _{oh1} ^(D) - Zr ₄ ^(D) - O _{ox2} ^(D)	295	67.5
O _{oh2} ^(D) - Zr ₂ ^(D) - O _{ox1} ^(D)	295	69.6
O _{oh2} ^(D) - Zr ₂ ^(D) - O _{ox5} ^(D)	281	70.5
O _{oh2} ^(D) - Zr ₃ ^(D) - O _{ox1} ^(D)	185	68.1
O _{oh2} ^(D) - Zr ₃ ^(D) - O _{ox4} ^(D)	266	68.5
O _{oh2} ^(D) - Zr ₅ ^(D) - O _{ox4} ^(D)	283	68.7
O _{oh2} ^(D) - Zr ₅ ^(D) - O _{ox5} ^(D)	260	72.9
O _{ox1} ^(D) - Zr ₂ ^(D) - O _{ox6} ^(D)	238	74.2
O _{ox1} ^(D) - Zr ₄ ^(D) - O _{ox6} ^(D)	452	70.6
O _{ox2} ^(D) - Zr ₁ ^(D) - O _{ox3} ^(D)	269	74.4
O _{ox2} ^(D) - Zr ₄ ^(D) - O _{ox6} ^(D)	436	70.8
O _{ox2} ^(D) - Zr ₆ ^(D) - O _{ox3} ^(D)	475	74.1
O _{ox2} ^(D) - Zr ₆ ^(D) - O _{ox6} ^(D)	335	72.5
O _{ox3} ^(D) - Zr ₁ ^(D) - O _{ox4} ^(D)	478	68.2
O _{ox3} ^(D) - Zr ₅ ^(D) - O _{ox4} ^(D)	462	68.5
O _{ox3} ^(D) - Zr ₅ ^(D) - O _{ox5} ^(D)	274	76.8
O _{ox3} ^(D) - Zr ₆ ^(D) - O _{ox5} ^(D)	473	74.1
O _{ox5} ^(D) - Zr ₂ ^(D) - O _{ox6} ^(D)	528	68.9
O _{ox5} ^(D) - Zr ₆ ^(D) - O _{ox6} ^(D)	564	67.7
Zr ₁ ^(D) - O _{oh1} ^(D) - Zr ₃ ^(D)	679	104.0
Zr ₁ ^(D) - O _{oh1} ^(D) - Zr ₄ ^(D)	736	101.2
Zr ₁ ^(D) - O _{ox2} ^(D) - Zr ₄ ^(D)	350	120.9
Zr ₁ ^(D) - O _{ox2} ^(D) - Zr ₆ ^(D)	551	110.0
Zr ₁ ^(D) - O _{ox3} ^(D) - Zr ₅ ^(D)	792	111.5
Zr ₁ ^(D) - O _{ox3} ^(D) - Zr ₆ ^(D)	790	101.4
Zr ₁ ^(D) - O _{ox4} ^(D) - Zr ₃ ^(D)	452	118.0
Zr ₁ ^(D) - O _{ox4} ^(D) - Zr ₅ ^(D)	603	112.4
Zr ₂ ^(D) - O _{oh2} ^(D) - Zr ₃ ^(D)	672	102.6
Zr ₂ ^(D) - O _{oh2} ^(D) - Zr ₅ ^(D)	752	100.9
Zr ₂ ^(D) - O _{ox1} ^(D) - Zr ₃ ^(D)	430	119.6
Zr ₂ ^(D) - O _{ox1} ^(D) - Zr ₄ ^(D)	607	109.8
Zr ₂ ^(D) - O _{ox5} ^(D) - Zr ₅ ^(D)	355	115.8
Zr ₂ ^(D) - O _{ox5} ^(D) - Zr ₆ ^(D)	544	112.6
Zr ₂ ^(D) - O _{ox6} ^(D) - Zr ₄ ^(D)	785	103.9
Zr ₂ ^(D) - O _{ox6} ^(D) - Zr ₆ ^(D)	784	110.6
Zr ₃ ^(D) - O _{oh1} ^(D) - Zr ₄ ^(D)	666	103.6
Zr ₃ ^(D) - O _{oh2} ^(D) - Zr ₅ ^(D)	630	104.1
Zr ₃ ^(D) - O _{ox1} ^(D) - Zr ₄ ^(D)	414	121.6
Zr ₃ ^(D) - O _{ox4} ^(D) - Zr ₅ ^(D)	436	118.8

bends	K [kJ/(mol·rad ²)]	θ_0 [deg]
Zr ₄ ^(D) - O _{ox2} ^(D) - Zr ₆ ^(D)	443	113.5
Zr ₄ ^(D) - O _{ox6} ^(D) - Zr ₆ ^(D)	772	103.3
Zr ₅ ^(D) - O _{ox3} ^(D) - Zr ₆ ^(D)	831	101.4
Zr ₅ ^(D) - O _{ox5} ^(D) - Zr ₆ ^(D)	595	107.9
dihedrals	K [kJ/mol]	ϕ_0 [deg]
C _{ca} - C ₁ - C ₂ - C ₂	34.8	0.000
C _{ca} - C ₁ - C ₂ - H ₂	16.0	0.000
C ₁ - C _{ca} - O _{ca} ^(A) - Zr ^(A)	49.4	0.000
C ₁ - C ₂ - C ₂ - C ₁	30.7	0.000
C ₁ - C ₂ - C ₂ - H ₂	36.2	0.000
C ₂ - C ₁ - C _{ca} - O _{ca} ^(A)	16.6	0.000
C ₂ - C ₁ - C ₂ - C ₂	31.7	0.000
C ₂ - C ₁ - C ₂ - H ₂	25.9	0.000
H ₂ - C ₂ - C ₂ - H ₂	16.6	0.000
O _{ca} ^(A) - C _{ca} - O _{ca} ^(A) - Zr ^(A)	4.4	0.000
O _{ca1} ^(B) - C _{ca} - O _{ca1} ^(B) - Zr ₁ ^(B)	3.7	0.000
O _{ca2} ^(B) - C _{ca} - O _{ca2} ^(B) - Zr ₁ ^(B)	3.3	0.000
O _{ca2} ^(B) - C _{ca} - O _{ca2} ^(B) - Zr ₂ ^(B)	7.6	0.000
O _{ca3} ^(B) - C _{ca} - O _{ca3} ^(B) - Zr ₁ ^(B)	4.2	0.000
O _{ca3} ^(B) - C _{ca} - O _{ca3} ^(B) - Zr ₂ ^(B)	5.9	0.000
O _{ca3} ^(B) - C _{ca} - O _{ca3} ^(B) - Zr ₃ ^(B)	5.7	0.000
O _{ca3} ^(B) - C _{ca} - O _{ca3} ^(B) - Zr ₄ ^(B)	4.9	0.000
O _{ca1} ^(D) - C _{ca} - O _{ca1} ^(D) - Zr ₁ ^(D)	5.1	0.000
O _{ca1} ^(D) - C _{ca} - O _{ca1} ^(D) - Zr ₂ ^(D)	8.2	0.000
O _{ca1} ^(D) - C _{ca} - O _{ca1} ^(D) - Zr ₃ ^(D)	7.8	0.000
O _{ca1} ^(D) - C _{ca} - O _{ca1} ^(D) - Zr ₄ ^(D)	3.9	0.000
O _{ca2} ^(D) - C _{ca} - O _{ca2} ^(D) - Zr ₁ ^(D)	6.3	0.000
O _{ca2} ^(D) - C _{ca} - O _{ca2} ^(D) - Zr ₂ ^(D)	5.6	0.000
O _{ca2} ^(D) - C _{ca} - O _{ca2} ^(D) - Zr ₃ ^(D)	7.3	0.000
O _{ca2} ^(D) - C _{ca} - O _{ca2} ^(D) - Zr ₄ ^(D)	7.7	0.000
O _{ca2} ^(D) - C _{ca} - O _{ca2} ^(D) - Zr ₅ ^(D)	9.0	0.000
O _{ca2} ^(D) - C _{ca} - O _{ca2} ^(D) - Zr ₆ ^(D)	6.3	0.000
O _{ca3} ^(D) - C _{ca} - O _{ca3} ^(D) - Zr ₃ ^(D)	5.8	0.000
O _{ca3} ^(D) - C _{ca} - O _{ca3} ^(D) - Zr ₄ ^(D)	4.3	0.000
O _{ca3} ^(D) - C _{ca} - O _{ca3} ^(D) - Zr ₅ ^(D)	5.2	0.000
O _{ca3} ^(D) - C _{ca} - O _{ca3} ^(D) - Zr ₆ ^(D)	6.8	0.000
C ₂ - C ₁ - C _{ca} - O _{ca1} ^(B)	16.6	0.000
C ₂ - C ₁ - C _{ca} - O _{ca2} ^(B)	16.6	0.000
C ₂ - C ₁ - C _{ca} - O _{ca3} ^(B)	16.6	0.000
C ₂ - C ₁ - C _{ca} - O _{ca1} ^(D)	16.6	0.000
C ₂ - C ₁ - C _{ca} - O _{ca2} ^(D)	16.6	0.000
C ₂ - C ₁ - C _{ca} - O _{ca3} ^(D)	16.6	0.000

dihedrals	K [kJ/mol]	ϕ_0 [deg]
$C_1 - C_{ca} - O_{ca1}^{(B)} - Zr_1^{(B)}$	42.0	0.000
$C_1 - C_{ca} - O_{ca2}^{(B)} - Zr_1^{(B)}$	48.7	0.000
$C_1 - C_{ca} - O_{ca2}^{(B)} - Zr_2^{(B)}$	44.7	0.000
$C_1 - C_{ca} - O_{ca3}^{(B)} - Zr_1^{(B)}$	44.1	0.000
$C_1 - C_{ca} - O_{ca3}^{(B)} - Zr_2^{(B)}$	39.5	0.000
$C_1 - C_{ca} - O_{ca3}^{(B)} - Zr_3^{(B)}$	43.3	0.000
$C_1 - C_{ca} - O_{ca3}^{(B)} - Zr_4^{(B)}$	38.2	0.000
$C_1 - C_{ca} - O_{ca1}^{(D)} - Zr_1^{(D)}$	32.2	0.000
$C_1 - C_{ca} - O_{ca1}^{(D)} - Zr_2^{(D)}$	46.3	0.000
$C_1 - C_{ca} - O_{ca1}^{(D)} - Zr_3^{(D)}$	37.1	0.000
$C_1 - C_{ca} - O_{ca1}^{(D)} - Zr_4^{(D)}$	29.3	0.000
$C_1 - C_{ca} - O_{ca2}^{(D)} - Zr_1^{(D)}$	51.9	0.000
$C_1 - C_{ca} - O_{ca2}^{(D)} - Zr_2^{(D)}$	42.8	0.000
$C_1 - C_{ca} - O_{ca2}^{(D)} - Zr_3^{(D)}$	48.4	0.000
$C_1 - C_{ca} - O_{ca2}^{(D)} - Zr_4^{(D)}$	44.1	0.000
$C_1 - C_{ca} - O_{ca2}^{(D)} - Zr_5^{(D)}$	47.6	0.000
$C_1 - C_{ca} - O_{ca2}^{(D)} - Zr_6^{(D)}$	33.5	0.000
$C_1 - C_{ca} - O_{ca3}^{(D)} - Zr_3^{(D)}$	43.8	0.000
$C_1 - C_{ca} - O_{ca3}^{(D)} - Zr_4^{(D)}$	36.9	0.000
$C_1 - C_{ca} - O_{ca3}^{(D)} - Zr_5^{(D)}$	34.3	0.000
$C_1 - C_{ca} - O_{ca3}^{(D)} - Zr_6^{(D)}$	36.1	0.000
out-of-plane-distance	K [kJ/(mol·Å ⁴)]	d_0 [Å]
$C_{ca} - C_2 - C_2 - C_1$	44	0.000
$C_1 - C_2 - H_2 - C_2$	259	0.000
$C_1 - O_{ca}^{(A)} - O_{ca}^{(A)} - C_{ca}$	1494	0.000
$Zr^{(A)} - Zr^{(A)} - Zr^{(A)} - O_{ox}^{(A)}$	343	0.145
$C_1 - O_{ca1}^{(B)} - O_{ca1}^{(B)} - C_{ca}$	1463	0.000
$C_1 - O_{ca2}^{(B)} - O_{ca2}^{(B)} - C_{ca}$	1428	0.000
$C_1 - O_{ca3}^{(B)} - O_{ca3}^{(B)} - C_{ca}$	1424	0.000
$C_1 - O_{ca1}^{(D)} - O_{ca1}^{(D)} - C_{ca}$	1476	0.000
$C_1 - O_{ca2}^{(D)} - O_{ca2}^{(D)} - C_{ca}$	1478	0.000
$C_1 - O_{ca3}^{(D)} - O_{ca3}^{(D)} - C_{ca}$	1488	0.000
$Zr_1^{(B)} - Zr_1^{(B)} - Zr_3^{(B)} - O_{ox3}^{(B)}$	193	0.221
$Zr_1^{(B)} - Zr_2^{(B)} - Zr_4^{(B)} - O_{ox1}^{(B)}$	421	0.356
$Zr_2^{(B)} - Zr_2^{(B)} - Zr_3^{(B)} - O_{ox2}^{(B)}$	180	0.400
$Zr_2^{(B)} - Zr_2^{(B)} - Zr_4^{(B)} - O_{ox4}^{(B)}$	8	0.860
$Zr_1^{(D)} - Zr_3^{(D)} - Zr_5^{(D)} - O_{ox4}^{(D)}$	216	0.374
$Zr_1^{(D)} - Zr_4^{(D)} - Zr_6^{(D)} - O_{ox2}^{(D)}$	220	0.457
$Zr_1^{(D)} - Zr_5^{(D)} - Zr_6^{(D)} - O_{ox3}^{(D)}$	19	0.868
$Zr_2^{(D)} - Zr_3^{(D)} - Zr_4^{(D)} - O_{ox1}^{(D)}$	276	0.342
$Zr_2^{(D)} - Zr_4^{(D)} - Zr_6^{(D)} - O_{ox6}^{(D)}$	47	0.837
$Zr_2^{(D)} - Zr_5^{(D)} - Zr_6^{(D)} - O_{ox5}^{(D)}$	115	0.582

Table S17: Parameters of the noncovalent contributions to the UiO–66 force field for the **type 4** structure, having an average coordination number of 11 (continued on the next page).

Atom type	q [e]	d [\AA]	ε [kcal/mol]	σ [\AA]
Zr ^(A)	2.370	2.367	0.300	2.540
Zr ₁ ^(B)	2.374	2.367	0.300	2.540
Zr ₂ ^(B)	2.336	2.367	0.300	2.540
Zr ₃ ^(B)	2.375	2.367	0.300	2.540
Zr ₄ ^(B)	2.363	2.367	0.300	2.540
Zr ₁ ^(D)	2.348	2.367	0.300	2.540
Zr ₂ ^(D)	2.339	2.367	0.300	2.540
Zr ₃ ^(D)	2.385	2.367	0.300	2.540
Zr ₄ ^(D)	2.371	2.367	0.300	2.540
Zr ₅ ^(D)	2.333	2.367	0.300	2.540
Zr ₆ ^(D)	2.331	2.367	0.300	2.540
O _{ox} ^(A)	-1.083	1.118	0.059	1.820
O _{ox1} ^(B)	-1.074	1.118	0.059	1.820
O _{ox2} ^(B)	-1.104	1.118	0.059	1.820
O _{ox3} ^(B)	-1.091	1.118	0.059	1.820
O _{ox4} ^(B)	-1.109	1.118	0.059	1.820
O _{ox1} ^(D)	-1.083	1.118	0.059	1.820
O _{ox2} ^(D)	-1.071	1.118	0.059	1.820
O _{ox3} ^(D)	-1.113	1.118	0.059	1.820
O _{ox4} ^(D)	-1.114	1.118	0.059	1.820
O _{ox5} ^(D)	-1.091	1.118	0.059	1.820
O _{ox6} ^(D)	-1.107	1.118	0.059	1.820
O _{oh} ^(A)	-1.037	1.118	0.059	1.820
O _{oh1} ^(B)	-1.039	1.118	0.059	1.820
O _{oh2} ^(B)	-1.026	1.118	0.059	1.820
O _{oh1} ^(D)	-0.540	1.118	0.059	1.820
O _{oh2} ^(D)	-0.544	1.118	0.059	1.820
O _{ca} ^(A)	-0.682	1.118	0.059	1.820
O _{ca1} ^(B)	-0.682	1.118	0.059	1.820
O _{ca2} ^(B)	-0.683	1.118	0.059	1.820
O _{ca3} ^(B)	-0.685	1.118	0.059	1.820
O _{ca1} ^(D)	-0.690	1.118	0.059	1.820
O _{ca2} ^(D)	-0.686	1.118	0.059	1.820
O _{ca3} ^(D)	-0.687	1.118	0.059	1.820
C _{ca}	0.773	1.163	0.056	1.940
C ₁	-0.135	1.163	0.056	1.960
C ₂	-0.106	1.163	0.056	1.960

Atom type	q [e]	d [\AA]	ε [kcal/mol]	σ [\AA]
$H_{\text{oh}}^{(\text{A})}$	0.497	0.724	0.016	1.600
$H_{\text{oh}1}^{(\text{B})}$	0.496	0.724	0.016	1.600
$H_{\text{oh}2}^{(\text{B})}$	0.490	0.724	0.016	1.600
$H_{\text{oh}1}^{(\text{D})}$	0.490	0.724	0.016	1.600
$H_{\text{oh}2}^{(\text{D})}$	0.496	0.724	0.016	1.600
H_2	0.152	0.724	0.020	1.620

2.3.9 Type 5

For the **type 5** defect structure, the same force field parameters as for the **type 3** defect structure apply.

2.3.10 Type 6

Table S18: Parameters of the covalent contributions to the UiO–66 force field for the **type 6** structure, having an average coordination number of 11 (continued on the next pages).

bonds	K [kJ/(mol· \AA^2)]	r_0 [\AA]
$C_{\text{ca}} - C_1$	2087	1.499
$C_{\text{ca}} - O_{\text{ca}}^{(\text{A})}$	4414	1.274
$C_{\text{ca}} - O_{\text{ca}1}^{(\text{C})}$	4414	1.274
$C_{\text{ca}} - O_{\text{ca}2}^{(\text{C})}$	4437	1.274
$C_1 - C_2$	3140	1.400
$C_2 - C_2$	3382	1.388
$C_2 - H_2$	3376	1.083
$H_{\text{oh}}^{(\text{A})} - O_{\text{oh}}^{(\text{A})}$	4957	0.997
$H_{\text{oh}1}^{(\text{C})} - O_{\text{oh}1}^{(\text{C})}$	4942	0.996
$O_{\text{ca}}^{(\text{A})} - \text{Zr}^{(\text{A})}$	522	2.212
$O_{\text{ca}1}^{(\text{C})} - \text{Zr}_1^{(\text{C})}$	435	2.247
$O_{\text{ca}1}^{(\text{C})} - \text{Zr}_2^{(\text{C})}$	427	2.217
$O_{\text{ca}2}^{(\text{C})} - \text{Zr}_1^{(\text{C})}$	663	2.162
$O_{\text{ca}2}^{(\text{C})} - \text{Zr}_2^{(\text{C})}$	539	2.194
$O_{\text{ca}2}^{(\text{C})} - \text{Zr}_3^{(\text{C})}$	566	2.177
$O_{\text{ca}2}^{(\text{C})} - \text{Zr}_4^{(\text{C})}$	499	2.218
$O_{\text{oh}}^{(\text{A})} - \text{Zr}^{(\text{A})}$	403	2.258
$O_{\text{oh}1}^{(\text{C})} - \text{Zr}_1^{(\text{C})}$	161	2.354
$O_{\text{oh}1}^{(\text{C})} - \text{Zr}_2^{(\text{C})}$	540	2.220
$O_{\text{oh}1}^{(\text{C})} - \text{Zr}_4^{(\text{C})}$	293	2.299

bonds	K [kJ/(mol·Å ²)]	r_0 [Å]
O _{ox} ^(A) - Zr ^(A)	819	2.070
O _{ox1} ^(C) - Zr ₁ ^(C)	1022	1.982
O _{ox2} ^(C) - Zr ₂ ^(C)	604	2.113
O _{ox2} ^(C) - Zr ₃ ^(C)	372	2.158
O _{ox3} ^(C) - Zr ₁ ^(C)	1023	2.048
O _{ox3} ^(C) - Zr ₄ ^(C)	1347	1.982
O _{ox4} ^(C) - Zr ₁ ^(C)	860	2.072
O _{ox4} ^(C) - Zr ₂ ^(C)	990	2.039
O _{ox4} ^(C) - Zr ₃ ^(C)	830	2.075
O _{ox5} ^(C) - Zr ₂ ^(C)	881	2.070
O _{ox5} ^(C) - Zr ₄ ^(C)	878	2.052
bends	K [kJ/(mol·rad ²)]	θ_0 [deg]
C _{ca} - C ₁ - C ₂	617	120.1
C _{ca} - O _{ca} ^(A) - Zr ^(A)	298	134.9
C _{ca} - O _{ca1} ^(C) - Zr ₁ ^(C)	276	133.4
C _{ca} - O _{ca1} ^(C) - Zr ₂ ^(C)	300	135.7
C _{ca} - O _{ca2} ^(C) - Zr ₁ ^(C)	283	136.6
C _{ca} - O _{ca2} ^(C) - Zr ₂ ^(C)	283	131.6
C _{ca} - O _{ca2} ^(C) - Zr ₃ ^(C)	296	138.3
C _{ca} - O _{ca2} ^(C) - Zr ₄ ^(C)	292	136.1
C ₁ - C _{ca} - O _{ca} ^(A)	165	118.2
C ₁ - C _{ca} - O _{ca1} ^(C)	172	118.4
C ₁ - C _{ca} - O _{ca2} ^(C)	174	118.5
C ₁ - C ₂ - C ₂	464	120.1
C ₁ - C ₂ - H ₂	280	119.4
C ₂ - C ₁ - C ₂	449	119.9
C ₂ - C ₂ - H ₂	345	120.2
H _{oh} ^(A) - O _{oh} ^(A) - Zr ^(A)	161	114.9
H _{oh1} ^(C) - O _{oh1} ^(C) - Zr ₁ ^(C)	144	118.8
H _{oh1} ^(C) - O _{oh1} ^(C) - Zr ₂ ^(C)	160	115.0
H _{oh1} ^(C) - O _{oh1} ^(C) - Zr ₄ ^(C)	157	118.1
O _{ca} ^(A) - C _{ca} - O _{ca} ^(A)	644	123.1
O _{ca1} ^(C) - C _{ca} - O _{ca1} ^(C)	638	122.8
O _{ca2} ^(C) - C _{ca} - O _{ca2} ^(C)	648	123.3
Zr ^(A) - O _{oh} ^(A) - Zr ^(A)	738	105.2
Zr ^(A) - O _{ox} ^(A) - Zr ^(A)	556	118.9
O _{ox} ^(A) - Zr ^(A) - O _{oh} ^(A)	174	67.2
O _{oh1} ^(C) - Zr ₁ ^(C) - O _{ox3} ^(C)	401	64.0
O _{oh1} ^(C) - Zr ₁ ^(C) - O _{ox4} ^(C)	109	70.0
O _{oh1} ^(C) - Zr ₂ ^(C) - O _{ox4} ^(C)	178	73.5
O _{oh1} ^(C) - Zr ₂ ^(C) - O _{ox5} ^(C)	316	71.6
O _{oh1} ^(C) - Zr ₄ ^(C) - O _{ox3} ^(C)	396	65.4
O _{oh1} ^(C) - Zr ₄ ^(C) - O _{ox5} ^(C)	188	70.1

bends	K [kJ/(mol·rad ²)]	θ_0 [deg]
O _{ox1} ^(C) - Zr ₁ ^(C) - O _{ox3} ^(C)	536	69.3
O _{ox1} ^(C) - Zr ₁ ^(C) - O _{ox4} ^(C)	164	95.5
O _{ox2} ^(C) - Zr ₂ ^(C) - O _{ox4} ^(C)	178	73.5
O _{ox2} ^(C) - Zr ₂ ^(C) - O _{ox5} ^(C)	450	69.9
O _{ox2} ^(C) - Zr ₃ ^(C) - O _{ox4} ^(C)	336	72.2
Zr ₁ ^(C) - O _{oh1} ^(C) - Zr ₂ ^(C)	756	99.9
Zr ₁ ^(C) - O _{oh1} ^(C) - Zr ₄ ^(C)	692	102.0
Zr ₂ ^(C) - O _{oh1} ^(C) - Zr ₄ ^(C)	688	104.8
Zr ₁ ^(C) - O _{ox1} ^(C) - Zr ₁ ^(C)	670	111.8
Zr ₁ ^(C) - O _{ox3} ^(C) - Zr ₁ ^(C)	683	104.8
Zr ₁ ^(C) - O _{ox3} ^(C) - Zr ₄ ^(C)	308	127.1
Zr ₁ ^(C) - O _{ox4} ^(C) - Zr ₂ ^(C)	424	116.3
Zr ₁ ^(C) - O _{ox4} ^(C) - Zr ₃ ^(C)	264	129.5
Zr ₂ ^(C) - O _{ox2} ^(C) - Zr ₂ ^(C)	863	108.4
Zr ₂ ^(C) - O _{ox2} ^(C) - Zr ₃ ^(C)	889	103.6
Zr ₂ ^(C) - O _{ox4} ^(C) - Zr ₃ ^(C)	707	108.0
Zr ₂ ^(C) - O _{ox5} ^(C) - Zr ₂ ^(C)	604	111.3
Zr ₂ ^(C) - O _{ox5} ^(C) - Zr ₄ ^(C)	467	116.4
dihedrals	K [kJ/mol]	ϕ_0 [deg]
C _{ca} - C ₁ - C ₂ - C ₂	34.8	0.000
C _{ca} - C ₁ - C ₂ - H ₂	16.0	0.000
C ₁ - C _{ca} - O _{ca1} ^(A) - Zr ^(A)	49.4	0.000
C ₁ - C _{ca} - O _{ca1} ^(C) - Zr ₁ ^(C)	42.0	0.000
C ₁ - C _{ca} - O _{ca1} ^(C) - Zr ₂ ^(C)	41.1	0.000
C ₁ - C _{ca} - O _{ca2} ^(C) - Zr ₁ ^(C)	30.3	0.000
C ₁ - C _{ca} - O _{ca2} ^(C) - Zr ₂ ^(C)	39.6	0.000
C ₁ - C _{ca} - O _{ca2} ^(C) - Zr ₃ ^(C)	30.6	0.000
C ₁ - C _{ca} - O _{ca2} ^(C) - Zr ₄ ^(C)	49.4	0.000
C ₁ - C ₂ - C ₂ - C ₁	30.7	0.000
C ₁ - C ₂ - C ₂ - H ₂	36.2	0.000
C ₂ - C ₁ - C _{ca} - O _{ca1} ^(A)	16.6	0.000
C ₂ - C ₁ - C _{ca} - O _{ca1} ^(C)	16.6	0.000
C ₂ - C ₁ - C _{ca} - O _{ca2} ^(C)	16.6	0.000
C ₂ - C ₁ - C ₂ - C ₂	31.7	0.000
C ₂ - C ₁ - C ₂ - H ₂	25.9	0.000
H ₂ - C ₂ - C ₂ - H ₂	16.6	0.000
O _{ca1} ^(A) - C _{ca} - O _{ca1} ^(A) - Zr ^(A)	4.4	0.000
O _{ca1} ^(C) - C _{ca} - O _{ca1} ^(C) - Zr ₁ ^(C)	7.3	0.000
O _{ca1} ^(C) - C _{ca} - O _{ca1} ^(C) - Zr ₂ ^(C)	4.1	0.000
O _{ca2} ^(C) - C _{ca} - O _{ca2} ^(C) - Zr ₁ ^(C)	5.2	0.000
O _{ca2} ^(C) - C _{ca} - O _{ca2} ^(C) - Zr ₂ ^(C)	6.2	0.000
O _{ca2} ^(C) - C _{ca} - O _{ca2} ^(C) - Zr ₃ ^(C)	3.2	0.000
O _{ca2} ^(C) - C _{ca} - O _{ca2} ^(C) - Zr ₄ ^(C)	6.4	0.000

out-of-plane-distance	K [kJ/(mol·Å ⁴)]	d_0 [Å]
C _{ca} - C ₂ - C ₂ - C ₁	44	0.000
C ₁ - C ₂ - H ₂ - C ₂	259	0.000
C ₁ - O _{ca} ^(A) - O _{ca} ^(A) - C _{ca}	1494	0.000
C ₁ - O _{ca1} ^(C) - O _{ca1} ^(C) - C _{ca}	1484	0.000
C ₁ - O _{ca2} ^(C) - O _{ca2} ^(C) - C _{ca}	1481	0.000
Zr ^(A) - Zr ^(A) - Zr ^(A) - O _{ox} ^(A)	343	0.145
Zr ₁ ^(C) - Zr ₁ ^(C) - Zr ₄ ^(C) - O _{ox3} ^(C)	349	0.037
Zr ₁ ^(C) - Zr ₂ ^(C) - Zr ₃ ^(C) - O _{ox4} ^(C)	389	0.278
Zr ₂ ^(C) - Zr ₂ ^(C) - Zr ₄ ^(C) - O _{ox5} ^(C)	191	0.466

Table S19: Parameters of the noncovalent contributions to the UiO–66 force field for the **type 6** structure, having an average coordination number of 11.

Atom type	q [e]	d [Å]	ϵ [kcal/mol]	σ [Å]
Zr ^(A)	2.370	2.367	0.300	2.540
Zr ₁ ^(C)	2.348	2.367	0.300	2.540
Zr ₂ ^(C)	2.339	2.367	0.300	2.540
Zr ₃ ^(C)	2.359	2.367	0.300	2.540
Zr ₄ ^(C)	2.371	2.367	0.300	2.540
O _{ox} ^(A)	-1.083	1.118	0.059	1.820
O _{ox1} ^(C)	-1.070	1.118	0.059	1.820
O _{ox2} ^(C)	-1.105	1.118	0.059	1.820
O _{ox3} ^(C)	-1.070	1.118	0.059	1.820
O _{ox4} ^(C)	-1.104	1.118	0.059	1.820
O _{ox5} ^(C)	-1.099	1.118	0.059	1.820
O _{oh} ^(A)	-1.037	1.118	0.059	1.820
O _{oh1} ^(C)	-1.031	1.118	0.059	1.820
O _{ca} ^(A)	-0.682	1.118	0.059	1.820
O _{ca1} ^(C)	-0.689	1.118	0.059	1.820
O _{ca2} ^(C)	-0.689	1.118	0.059	1.820
C _{ca}	0.764	1.163	0.056	1.940
C ₁	-0.135	1.163	0.056	1.960
C ₂	-0.106	1.163	0.056	1.960
H _{oh} ^(A)	0.497	0.724	0.016	1.600
H _{oh1} ^(C)	0.485	0.724	0.016	1.600
H ₂	0.152	0.724	0.020	1.620

2.3.11 Type 7

For the **type 7** defect structure, the same force field parameters as for the **type 3** defect structure apply.

2.4 Validation with respect to DFT results

To validate the accuracy of the newly derived force fields, they were used to optimize the different materials under study. When optimized without van der Waals contributions, the force field

Table S20: Comparison between a geometry optimization at 0 K using the newly derived force fields without the van der Waals contribution and DFT cluster data at the B3LYP level of theory.
 *Taken from the Zr brick model system. **Taken from the organic linker model system. ***Averaged over both model systems. [†]For UiO-66, the atom types C₂ and C₃ coincide. [‡]For UiO-67, the atom types C₄ and C₅ coincide.

interatomic distance [Å]		UiO-66		UiO-67		UiO-68	
		FF	DFT	FF	DFT	FF	DFT
Zr ··· Zr	*	3.500	3.568	3.501	3.568	3.500	3.568
Zr ··· O _{oh}	*	2.260	2.285	2.261	2.285	2.260	2.285
Zr ··· O _{ox}	*	2.084	2.087	2.081	2.087	2.083	2.087
Zr ··· O _{ca}	*	2.302	2.242	2.306	2.242	2.306	2.242
O _{ca} ··· C _{ca}	***	1.267	1.267	1.269	1.269	1.269	1.269
C _{ca} ··· C ₁	**	1.493	1.493	1.494	1.493	1.497	1.497
C ₁ ··· C ₂	**	1.399	1.399	1.399	1.399	1.400	1.400
C ₂ ··· C ₃ [†]	**	1.388	1.387	1.389	1.388	1.390	1.390
C ₃ ··· C ₄	**	—	—	1.406	1.406	1.406	1.406
C ₄ ··· C ₅ [‡]	**	—	—	1.488	1.486	1.488	1.488
C ₅ ··· C ₆	**	—	—	—	—	1.404	1.404
C ₆ ··· C ₆	**	—	—	—	—	1.391	1.391
interatomic angle [deg]							
		FF	DFT	FF	DFT	FF	DFT
Zr – O _{ox} – Zr	*	114.2	117.4	114.5	117.4	114.4	117.4
Zr – O _{oh} – Zr	*	101.5	102.6	101.5	102.6	101.5	102.6
Zr – O _{ca} – C _{ca}	*	132.3	134.5	132.2	134.5	132.3	134.5
O _{ca} – C _{ca} – O _{ca}	***	126.4	125.2	126.3	124.9	126.2	124.8
O _{ca} – C _{ca} – C ₁	**	116.8	117.4	116.8	117.7	116.8	117.8
C _{ca} – C ₁ – C ₂	**	119.9	119.9	120.5	120.5	120.6	120.6
C ₁ – C ₂ – C ₃ [†]	**	119.9	119.9	120.4	120.4	120.6	120.5
C ₂ – C ₃ – C ₄	**	—	—	121.3	121.3	121.2	121.3
C ₃ – C ₄ – C ₅ [‡]	**	—	—	121.2	121.2	121.2	121.2
C ₄ – C ₅ – C ₆	**	—	—	—	—	121.4	121.5
C ₅ – C ₆ – C ₆	**	—	—	—	—	121.4	121.5
dihedral angle [deg]							
		FF	DFT	FF	DFT	FF	DFT
Zr – O _{ca} – C _{ca} – C ₁	*	177.2	176.5	176.5	176.5	177.9	176.5
Zr – O _{ca} – C _{ca} – O _{ca}	*	6.1	2.0	5.7	2.0	5.3	2.0

results should mimic the DFT cluster results to which the force field parameters were fitted, since long-range dispersion is assumed to be absent in the DFT results. As shown in Table S20, the UiO–66 to –68 force fields are able to reproduce the DFT values relatively well.

Furthermore, after inclusion of the van der Waals parameters, it is possible to compare the

Table S21: Comparison between a geometry optimization at 0 K, carried out with our periodic force fields, and periodic DFT data at the PBE level.¹⁰ [†]For UiO–66, the atom types C₂ and C₃ coincide. [‡]For UiO–67, the atom types C₄ and C₅ coincide. *Not reported in Ref. 10.

interatomic distance [Å]	UiO–66		UiO–67		UiO–68	
	This work	DFT ¹⁰	This work	DFT ¹⁰	This work	DFT ¹⁰
Zr ··· Zr	3.509	3.558	3.512	—*	3.510	—*
Zr ··· O _{oh}	2.267	2.245	2.269	2.277	2.268	2.277
Zr ··· O _{ox}	2.085	2.086	2.083	2.087	2.084	2.085
Zr ··· O _{ca}	2.311	2.277	2.314	2.249	2.315	2.244
O _{ca} ··· C _{ca}	1.271	1.280	1.272	1.282	1.273	1.281
C _{ca} ··· C ₁	1.511	1.498	1.510	1.493	1.514	1.493
C ₁ ··· C ₂	1.409	1.404	1.409	1.401	1.412	1.402
C ₂ ··· C ₃ [†]	1.393	1.391	1.394	1.389	1.395	1.390
C ₃ ··· C ₄	—	—	1.416	1.411	1.412	1.411
C ₄ ··· C ₅ [‡]	—	—	1.505	1.486	1.495	1.482
C ₅ ··· C ₆	—	—	—	—	1.412	1.409
C ₆ ··· C ₆	—	—	—	—	1.396	1.390
interatomic angle [deg]						
Zr – O _{ox} – Zr	114.6	117.1	114.9	117.1	114.7	117.1
Zr – O _{oh} – Zr	101.4	102.8	101.4	103.2	101.4	102.8
Zr – O _{ca} – C _{ca}	132.9	133.8	132.7	133.6	132.9	133.8
O _{ca} – C _{ca} – O _{ca}	125.3	125.6	125.3	125.8	125.2	125.6
O _{ca} – C _{ca} – C ₁	117.2	117.2	117.2	117.1	117.3	117.2
C _{ca} – C ₁ – C ₂	120.5	120.1	121.0	120.7	121.1	120.7
C ₁ – C ₂ – C ₃ [†]	120.5	120.1	120.9	120.6	121.0	120.6
C ₂ – C ₃ – C ₄	—	—	121.8	121.7	121.4	121.7
C ₃ – C ₄ – C ₅ [‡]	—	—	121.7	121.6	121.3	121.5
C ₄ – C ₅ – C ₆	—	—	—	—	121.4	122.0
C ₅ – C ₆ – C ₆	—	—	—	—	121.4	122.0
dihedral angle [deg]						
Zr – O _{ca} – C _{ca} – C ₁	178.3	—*	175.8	—*	177.9	—*
Zr – O _{ca} – C _{ca} – O _{ca}	7.9	—*	8.3	—*	8.0	—*

optimizations with our periodic force fields to published DFT results which explicitly include dispersion interactions. In Table S21, a selected set of internal coordinates of UiO–66 to –68, calculated via optimizations using the newly derived force fields, is compared to periodic DFT results obtained by Yang *et al.*¹⁰ In Table S22, the same comparison is carried out for the unit cell parameters at 0 K. Again, a very good correspondence is found, with a maximal deviation of 1.5% in the bond length between the zirconium atoms and their neighboring carboxylate oxygens. The maximal deviation in interatomic angles, which amounts to 2.3%, is found for the angle between two neighbouring zirconium atoms and their intermediate oxo-oxygen.

Table S22: Unit cell properties for UiO–66 to –68 as calculated via a geometry optimization at 0 K, compared to periodic DFT data at the PBE level of theory.¹⁰

Material	Cell length [Å]		Cell volume [Å ³]		Space group	
	This work	DFT ¹⁰	This work	DFT ¹⁰	This work	DFT ¹⁰
UiO–66	21.16	20.96	9 478	9 210	$F\bar{4}3m$	$F\bar{4}3m$
UiO–67	27.40	27.13	20 567	19 991	$F\bar{4}3m$	$P\bar{4}3m$
UiO–68	33.56	33.31	37 797	36 647	$F\bar{4}3m$	$F\bar{4}3m$

3 Structural properties of the UiO–66 family

To validate the force fields with experiment, ($N, P, \sigma_a = 0, T$) MD simulations at 300 K and 100 kPa were carried out for each material. For each simulation, the first 50 ps were discarded as equilibration time, while results were calculated based on the remaining 500 ps. For a MOF force field to be reliable, both its highly-ordered structure as well as its nanoporosity need to be captured. In Table 1 and Table 2 of the main manuscript, the internal coordinates, unit cell parameters and space group were provided for those materials for which single-crystal X-ray diffraction (SCXRD) data are available, allowing comparison with the experimental, highly-ordered structure. Here, the unit cell parameters, space groups and pore size distributions are stated for all other materials, for which no comparison with experiment is possible due to the absence of reliable SCXRD data. Furthermore, the correct reproduction of the nanoporous structure in the UiO–66 family is validated. First, the effect of linker vacancies on the presence of pores inside UiO–66-type materials will be elucidated, followed by a determination of the pore size distribution of all materials under study using Zeo++.^{11–13}

3.1 Unit cell parameters

The unit cell parameters (cell lengths, cell angles, cell volume and space group) for the eleven materials are listed in Table S23. For the space group, determined via PLATON using the default error margin, the Hermann-Mauguin notation is listed.¹⁴ Table S23 is the extension of Table 2 in the main manuscript.

3.2 Types of pores for pristine and defect structures

The **fcu** topology in UiO–66 gives rise to two types of pores in the material. On the one hand, six inorganic $Zr_6O_4(OH)_4$ bricks and the twelve ligands connecting these bricks enclose an octahedral pore, of which an example is shown in blue in Figure S1. On the other hand, four inorganic bricks and the six ligands connecting these bricks enclose a tetrahedral pore—see for instance the pore enclosed by the linkers **s**, **h**, **c**, **k'**, **x** and **v** in Figure S1. The faces of both types of polyhedra form trigonal windows alternatingly connecting both types of cages. Moreover, each linker is shared by four pores: two octahedral and two tetrahedral pores. In Figure S6, two octahedral and two

Table S23: Unit cell parameters and space groups of the different materials in the UiO–66 family as calculated via ($N, P, \sigma_a = 0, T$) MD simulations at 300 K and 100 kPa.

Material	a [Å]	b [Å]	c [Å]	α [deg]	β [deg]	γ [deg]	Volume [Å ³]	Space group
UiO–66	21.117	21.116	21.116	89.99	90.00	90.00	9 416	$Fm\bar{3}m$ (no. 225)
UiO–67	27.330	27.325	27.326	90.00	90.00	90.00	20 407	$Fm\bar{3}m$ (no. 225)
UiO–68	33.438	33.434	33.430	89.99	89.99	89.99	37 374	$Fm\bar{3}m$ (no. 225)
type 0	21.128	21.025	21.129	90.18	90.00	89.84	9 386	Cm (no. 8)
type 1	21.043	21.050	21.122	89.84	90.15	90.04	9 356	Cm (no. 8)
type 2	21.163	20.912	21.140	90.00	90.00	90.00	9 356	$P222_1$ (no. 17)
type 3	21.155	21.155	20.966	90.00	90.00	90.00	9 383	$P\bar{4}2m$ (no. 111)
type 4	20.993	21.010	21.146	90.14	90.04	89.94	9 327	$P1$ (no. 1)
type 5	20.935	21.172	21.168	90.12	90.00	90.00	9 382	$C2$ (no. 5)
type 6	21.122	20.930	21.124	90.32	89.64	90.30	9 338	$P4/nmm$ (no. 129)
type 7	21.170	20.948	21.172	90.00	90.02	90.00	9 389	$P\bar{4}2_1m$ (no. 113)

tetrahedral pores are shown, where the inorganic bricks and organic ligands are replaced by points and lines, respectively. The linker shared between these four pores is indicated in red.

To determine the pore volume inside a nanoporous material, often the diameter of the largest included sphere is reported. For the UiO–66 family, the two types of cages will evidently give rise to two distinct spheres: small spheres filling the tetrahedral pores (green) on the one hand, and larger spheres filling the octahedral pores (yellow) on the other hand. When a linker vacancy is created in UiO–66, the two octahedral and two tetrahedral cages sharing this linker will merge. This creates a pore with a considerably larger volume. However, when determining the largest sphere included in this pore, the same sphere as found in a pristine octahedral cage is retrieved. Indeed, while creating a linker defect increases the pore size in one dimension, the other two dimensions remain unaltered, and will limit the size of this sphere. Hence, creating a linker vacancy will result in a pore size distribution for which the peaks of the tetrahedral and octahedral pores are decreased, since two tetrahedral and one octahedral cage are effectively removed. Also the creation of a second linker vacancy will not increase the size of the largest included sphere. Hence, for all defect materials studied here, only a difference in the peak height of the pore size distribution with respect to the defect-free UiO–66 is to be expected, where the largest difference is to be found in the tetrahedral peak.

3.3 Pore size distribution of the UiO–66 family

In Figure S7, the pore size distribution (PSD) calculated using Zeo++ is shown for the different investigated materials. As mentioned in the original Zeo++ article discussing similar pore landscapes, the derivative of the pore size distribution is plotted since this essentially provides a normalized representation of the bin count histogram. It states how many additional pores will be available if the probe radius is decreased.¹³

For all materials under study in this work, two peaks can be distinguished, corresponding to tetrahedral and octahedral cages. In the UiO–66 to –68 series, shown in the left pane of Figure

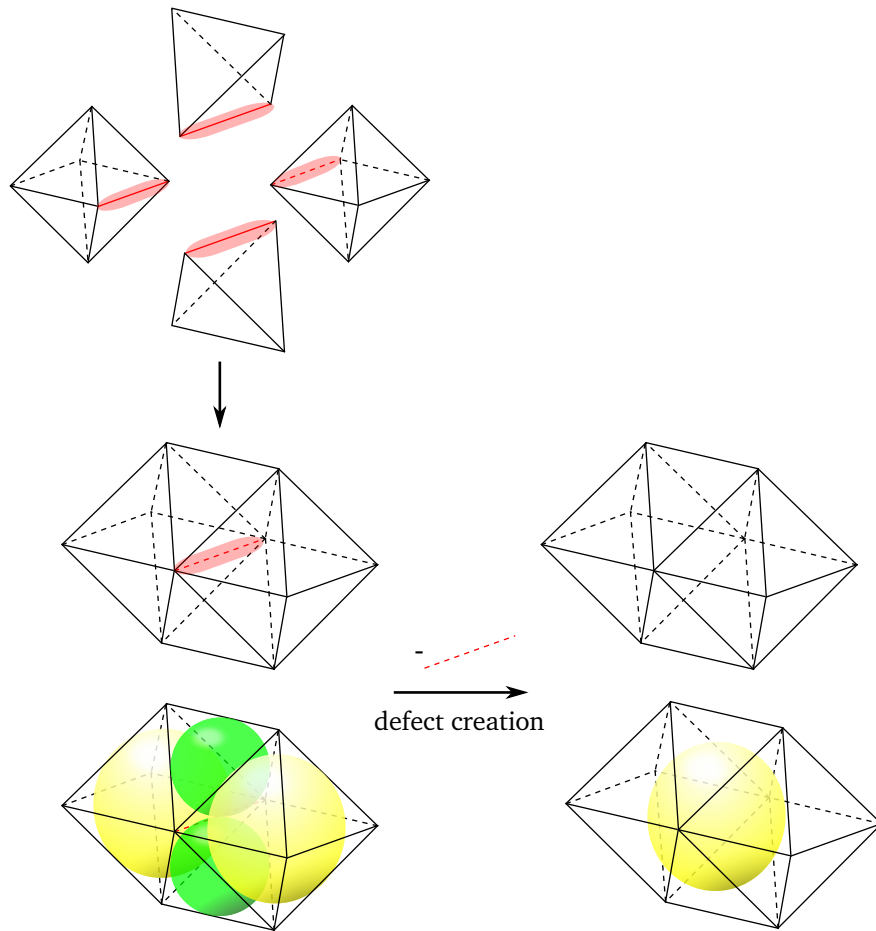


Figure S6: **Left:** Representation of the two octahedral and two tetrahedral pores sharing one linker (red) in the UiO–66 family, with inorganic bricks and linkers reduced to points and lines, respectively. Also indicated are the largest included spheres in both the octahedral (yellow) and tetrahedral (green) pores. **Right:** By removing one linker (red), an 11.5 coordinated structure is obtained, where the four pores are merged. While the shape and volume of this pore is altered, the largest included sphere (yellow) has the same diameter as in the defect-free material.

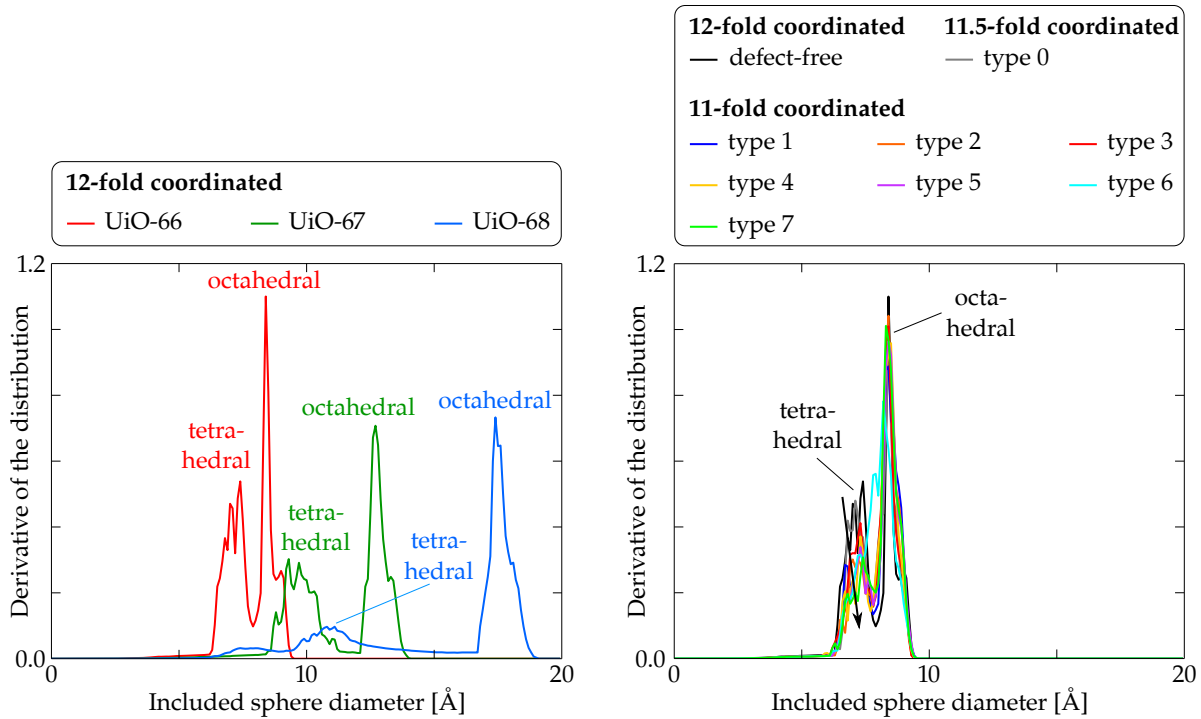


Figure S7: Pore size distributions for the defect-free UIO-66 to -68 (left), as well as for the different defect structures (right), calculated with a 0.5 Å probe radius.

S7, increasing the linker length also increases the diameter of the included spheres. For the octahedral cages, the size of the included sphere increases from 8.5 Å over 12.5 Å to 17.5 Å when going from UIO-66 to -68, in line with the original findings of Cavka *et al.*¹⁵ Note that the decrease of the tetrahedral peak height in this series is due to the increased size of the trigonal windows between tetrahedral and octahedral cages, so that adjacent pores can be effectively treated as one pore for small molecules. When creating linker vacancies in UIO-66, shown in the right pane of Figure S6, tetrahedral and octahedral pores merge. In this larger pore, the largest included sphere still has a diameter similar to the largest included sphere in the octahedral pore. In the pore size distribution, creating a linker defect hence results in a decrease of the peak heights, which is more pronounced for the tetrahedral peak.

4 Pressure and free energy profiles

In Figure 4 and Figure 8 of the main text, the pressure profiles as a function of the constrained unit cell volume are shown for the defect-free UiO–66 to –68, as well as for the defect UiO–66 structures. To allow for an accurate determination of the equilibrium volume, loss-of-crystallinity pressure and bulk modulus, the $\langle P_i(V) \rangle$ data as obtained from $(N, V, \sigma_a = 0, T)$ data at $T = 300$ K were fitted to a polynomial curve. To avoid overfitting issues while still capturing sufficient detail of the profile, the degree of this polynomial was varied. A seventh-order polynomial was found to be the maximum degree to avoid that the corresponding Vandermonde matrix becomes rank-deficient. In the next subsection, the coefficients of these fits are provided for the different materials. In the second subsection, thermodynamic integration is applied to determine the free energy curves for these materials. Finally, the results for UiO–66 are compared with the finite-pressure approach of Ortiz *et al.*,¹⁶ and the soft mode causing mechanical instability is identified.

4.1 Coefficients of the polynomial fit

To reduce the noise in the results obtained from the different $(N, V, \sigma_a = 0, T)$ simulations, the average internal pressure $\langle P_i \rangle$ as a function of the volume V for each material is fitted to a seventh-order polynomial, following:

$$\langle P_i(V) \rangle = \sum_{i=0}^7 c_i \left(\frac{V}{\bar{V}} \right)^i \quad (\text{S4.1})$$

Table S24: Expansion coefficients c_i and average volume \bar{V} of Eq. (S4.1) for the seventh-order polynomial $\langle P_i(V) \rangle$ fitted to the different UiO–66-type materials.

Material	c_0 [a.u.]	c_1 [a.u.]	c_2 [a.u.]	c_3 [a.u.]	c_4 [a.u.]	c_5 [a.u.]	c_6 [a.u.]	c_7 [a.u.]	\bar{V} [\AA^3]
UiO–66	−442	3 117	−9 407	15 757	−15 818	9 518	−3 178	454	8 850
UiO–67	130	−916	2 775	−4 660	4 690	−2 828	946	−135	19 250
UiO–68	187	−1 320	3 979	−6 660	6 681	−4 017	1 341	−192	35 500
type 0	−215	1 515	−4 570	7 647	−7 669	4 609	−1 537	219	8 850
type 1	−424	2 984	−8 994	15 045	−15 085	9 066	−3 024	432	8 850
type 2	−443	3 113	−9 362	15 624	−15 630	9 373	−3 119	445	8 850
type 3	−318	2 256	−6 855	11 555	−11 671	7 065	−2 373	341	8 850
type 4	−295	2 083	−6 288	10 534	−10 576	6 364	−2 125	304	8 850
type 5	21	−146	435	−721	717	−427	141	−20	8 850
type 6	−299	2 107	−6 351	10 626	−10 655	6 404	−2 136	305	8 850
type 7	−222	1 574	−4 772	8 030	−8 097	4 893	−1 641	236	8 850

Here, \bar{V} indicates the average of the volume range over which the fit is carried out and c_i are the expansion coefficients. The volume grid points were spaced apart by $\Delta V = 10 \text{ \AA}^3$ for UiO-66 and the defect structures, by $\Delta V = 20 \text{ \AA}^3$ for UiO-67, and by $\Delta V = 40 \text{ \AA}^3$ for UiO-68. While the inclusion of the scaling factor \bar{V} is optional, it results in coefficients c_i which share the same dimension. In Table S24, these coefficients and the average volume are reported for the materials investigated in the main text.

4.2 Free energy profiles

Thermodynamic integration can be applied to integrate the pressure profiles to free energy profiles as a function of the unit cell volume, according to

$$F(V) - F(V_{\text{ref}}) = \int_{V_{\text{ref}}}^V \frac{\partial F(V')}{\partial V'} dV' = - \int_{V_{\text{ref}}}^V \langle P_i(V') \rangle dV'. \quad (\text{S4.2})$$

Here, $V_{\text{ref}} = V_0$, e.g., the free energy profile will be zero at the equilibrium volume.

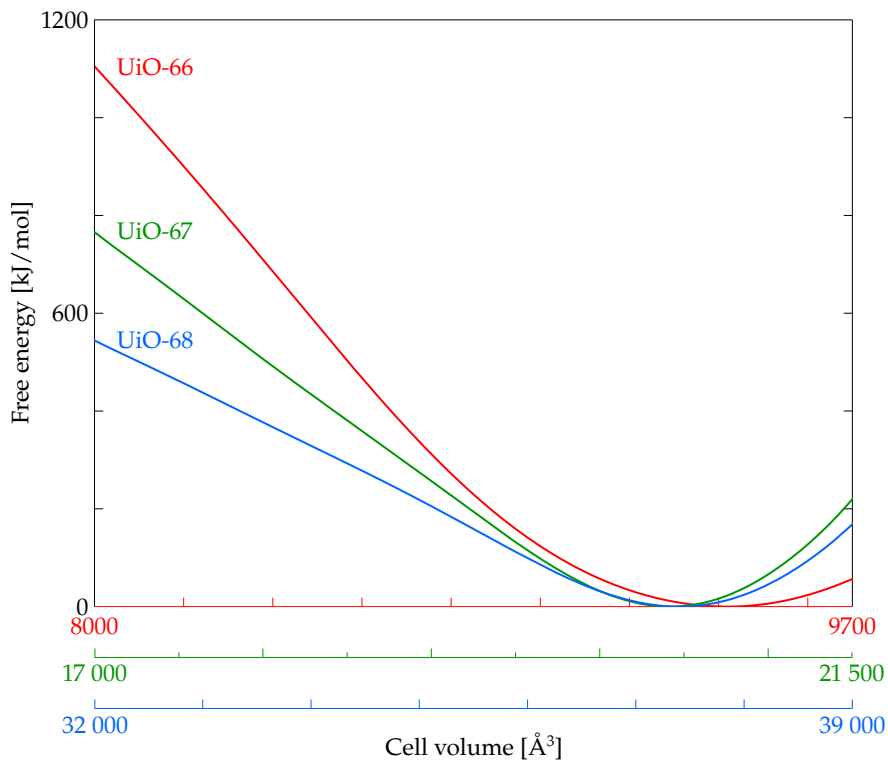


Figure S8: Free energy F as a function of the constrained unit cell volume V for the defect-free UiO-66 to -68, obtained by thermodynamic integration of the pressure profiles of Figure 4.

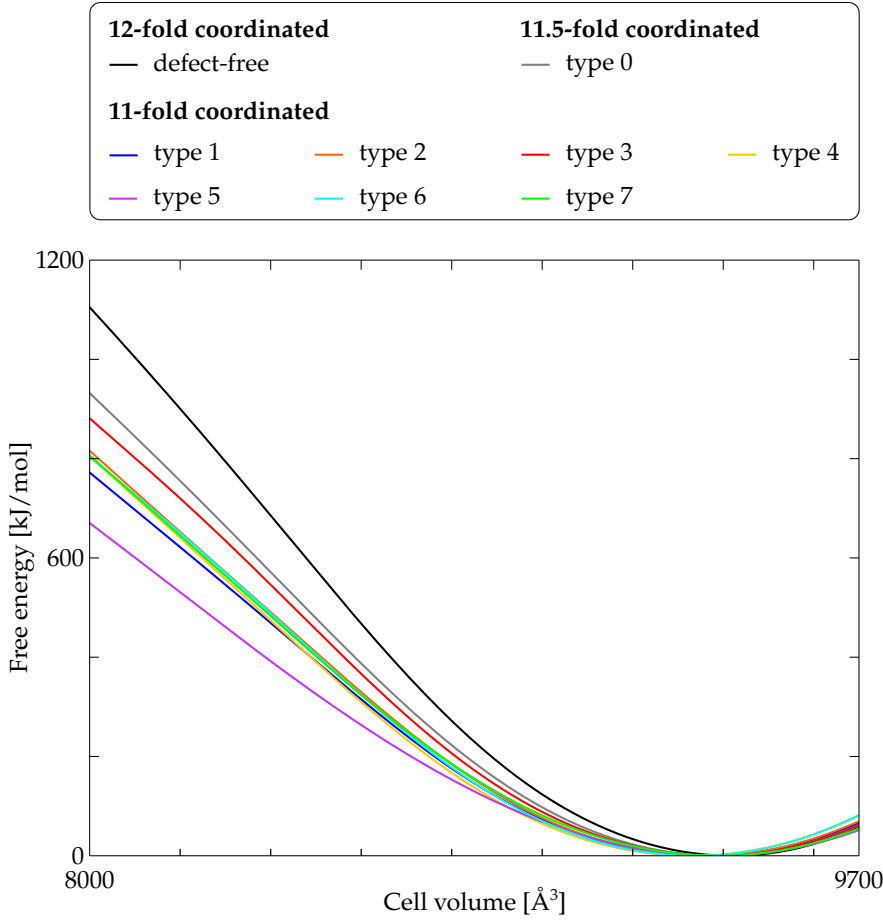


Figure S9: Free energy F as a function of the constrained unit cell volume V for the defect-free UiO-66 and the different defect-containing materials, obtained by thermodynamic integration of the pressure profiles of Figure 8.

By applying this procedure on the pressure profiles of Figure 4 and Figure 8 of the main text, the free energy profiles of Figures S8 and S9 are obtained, where the polynomial fits to the simulation data are integrated. Based on the curvature of the free energy profiles of Figure S9, it is clear that the bulk modulus decreases with increasing number of linker vacancies. Moreover, by comparing the free energy at the volume for which a loss-of-crystallinity is observed with the free energy at equilibrium, an estimate can be made of the free energy needed to induce the loss of crystallinity.

4.3 Identification of the soft mode

As outlined in Section 4.2 of the main manuscript, the constant-pressure approach of Ortiz *et al.* was employed to identify the soft mode(s) responsible for the mechanical instability of the pristine UiO–66.¹⁶ In this procedure, the elastic stiffness tensor \mathbf{C} of the defect-free UiO–66 is calculated based on the variance of the elastic tensor $\boldsymbol{\varepsilon}$ through the following thermodynamic relation:

$$[\mathbf{C}^{-1}]_{ijkl} = \frac{V}{k_B T} (\langle \varepsilon_{ij}\varepsilon_{kl} \rangle - \langle \varepsilon_{ij} \rangle \langle \varepsilon_{kl} \rangle), \quad (\text{S4.3})$$

where k_B is Boltzmann's constant, V is the system's volume, and T is the temperature at which the simulation is carried out. To study the effect of an elevated pressure on this elastic tensor, 21 ($N, P, \sigma_a = \mathbf{0}, T$) simulations were carried out on the conventional UiO–66 unit cell with a fixed pressure between 0 and 2000 MPa, using a step of 100 MPa. These simulations were run for a simulation time of 6 ns, of which the first 1 ns was discarded as equilibration time. This extended simulation time allows to reduce the uncertainty in the elastic constants to less than 1 GPa. From these simulations, the Born stability criteria as shown in Figure 5 of the main manuscript are obtained, and compression is identified as the soft mode causing the mechanical instability of UiO–66.

Furthermore, to further investigate the chemical nature of the mechanical instability, the vibrational density of states (VDOS) was calculated for the defect-free UiO–66, at three different volumes:

- (i) At 9400 Å³, near the mechanical equilibrium at ambient conditions;
- (ii) At 8400 Å³, near the point of mechanical instability as determined from the $P(V)$ curve shown in Figure 4;
- (iii) At 8000 Å³, in the low-symmetry region.

The three 550 ps ($N, V, \sigma_a = \mathbf{0}, T$) simulations were carried out at 300 K on the conventional unit cell, and the first 50 ps were discarded as equilibration time. For each of these simulations, we calculated the vibrational density of states, which is given by the velocity power spectrum (VPS):

$$D(\omega) = \int_0^\infty \exp(-i\omega t) \langle \mathbf{v}(\tau) \cdot \mathbf{v}(\tau + t) \rangle dt. \quad (\text{S4.4})$$

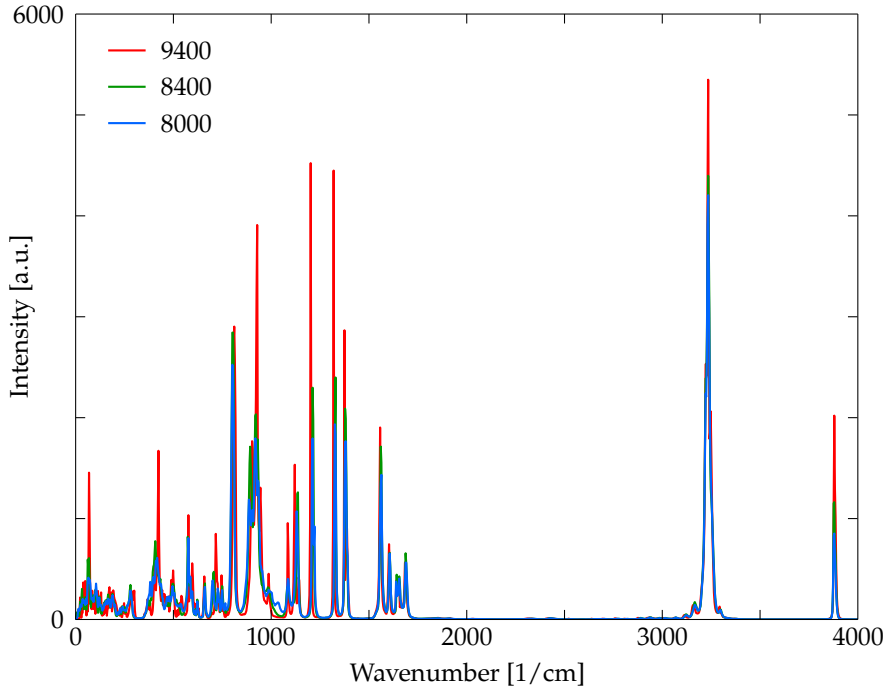


Figure S10: Vibrational density of states stemming from 550 ps ($N, V, \sigma_a = \mathbf{0}, T$) simulations at 300 K for the defect-free UiO-66 at three volumes: 9400 \AA^3 , 8400 \AA^3 and 8000 \AA^3 .

The resulting three VDOS are shown in Figure S10. It is clear that, besides the peak intensities, only small discrepancies appear between the three curves, except for a narrow frequency region near 1000 cm^{-1} , which is moreover not highly activated. Hence, the mechanical instability seems not to be related to one specific vibrational mode, but is rather characteristic of the material as a whole.

5 Study of finite-size effects

Throughout the manuscript, a UiO–66 unit cell containing 456 atoms was consistently used. To study the possible effect of the finite size of the unit cell on the structural and mechanical properties, this $1 \times 1 \times 1$ conventional unit cell was doubled along each of the three axes, obtaining a $2 \times 2 \times 2$ supercell containing 3648 atoms, which preserves the equivalency of the three crystal axes in the pristine UiO–66.

First, the pressure-versus-volume curves were constructed using this larger unit cell. For this, 550 ps ($N, V, \sigma_a = 0, T$) simulations were run at 300 K, from which the first 50 ps were discarded as equilibration time. For the conventional unit cell, a volume step $\Delta V = 10 \text{ \AA}^3$ was employed, which was increased to $\Delta V = 400 \text{ \AA}^3$ for the supercell. To increase the computational efficiency, the long-range (electrostatic and van der Waals) interactions were calculated using the LAMMPS software code,¹⁷ while the covalent interactions were, as for the case of the conventional unit cell, calculated via Yaff.¹⁸ To account for the possible minor differences between the two software codes, the conventional unit cell was also simulated, both using LAMMPS and Yaff. As shown in Figure S11, Yaff and LAMMPS yield pressure curves which almost perfectly overlap for the conventional $1 \times 1 \times 1$ unit cell. Moreover, also the pressure curve for the supercell (note that the cell volume always denotes the volume of the conventional unit cell) is in very good agreement with the pressure curve of the conventional cell. As shown in Table S25, the key mechanical properties under study remain virtually unaltered. There is only a minor effect in the region where the material becomes unstable, reflected in the volume at which the maximum in the pressure is obtained. This volume increases from 8444 \AA^3 for the conventional unit cell to 8490 \AA^3 for the supercell, an increase of only 0.6%. In conclusion, the effects of the finite unit cell on the mechanical properties of the pristine UiO–66 are very minor, and localized near the onset of

Table S25: Effect of the finite size of the simulation cell on the equilibrium volume, bulk modulus, and loss-of-crystallinity pressure of UiO–66.

	$1 \times 1 \times 1$ (Yaff)	$1 \times 1 \times 1$ (LAMMPS)	$2 \times 2 \times 2$ (LAMMPS)
Equilibrium volume [\AA^3]	9 419	9 419	9 422
Bulk modulus [GPa]	22.2	22.3	22.0
Loss-of-crystallinity pressure [GPa]	1.83	1.83	1.84

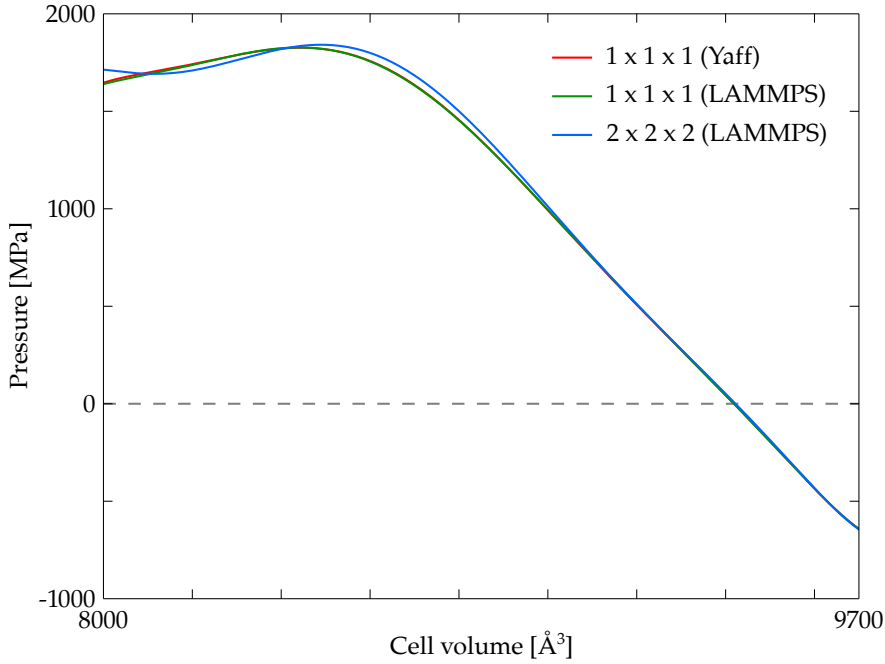


Figure S11: Internal pressure $\langle P_i \rangle$ as a function of the constrained unit cell volume V for UiO–66, resulting from $(N, V, \sigma_a = \mathbf{0}, T)$ simulations at $T = 300$ K, performed on either the conventional $1 \times 1 \times 1$ unit cell (Yaff and LAMMPS) or the $2 \times 2 \times 2$ supercell (LAMMPS).

instability. Moreover, they do not alter the loss-of-crystallinity pressure of 1.83 GPa reported in the manuscript.

Second, the radial distribution functions shown in Figure 7 of the main manuscript were recalculated using $(N, V, \sigma_a = \mathbf{0}, T)$ simulations at 300 K, using the $2 \times 2 \times 2$ supercell to assess the effect of the finite unit cell size on the structural parameters. Since the supercell parameter is about 42 Å, the radial distribution functions depicted in Figure S12 only cover distances up to half the lattice parameter of the supercell. Comparison with Figure 7 of the main manuscript shows that short-range disorder is again present in the 8000 Å³ unit cell. Moreover, this loss of crystallinity is again obtained from a distance of about 6 Å onwards. In contrast, clear peaks in the radial distribution function at 9400 Å³ can be distinguished up to 17 Å, in complete agreement with the results obtained using the conventional unit cell.

In conclusion, the calculations above show that only minor differences in the structural and mechanical properties are obtained when increasing the conventional unit cell to a $2 \times 2 \times 2$ supercell, indicating that the dispersion of phonons is already adequately described using the conventional unit cell. Since finite-size effects are expected to be the largest in this initial scale-up from

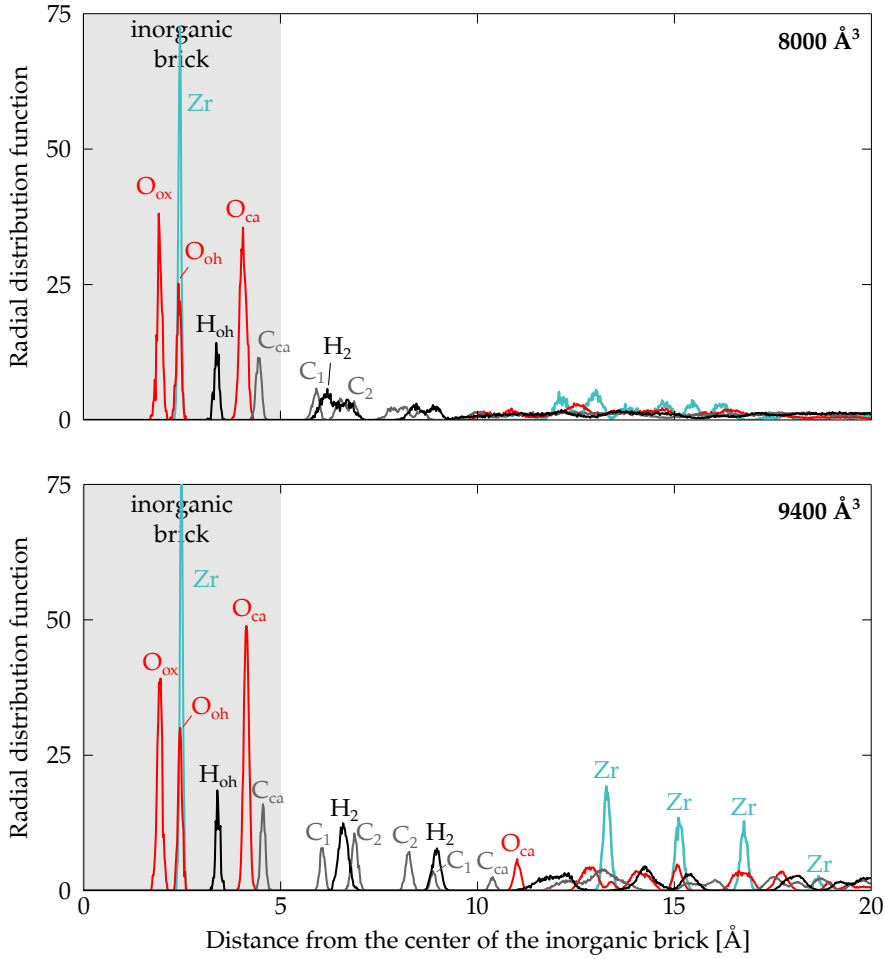


Figure S12: Radial distribution functions of UiO–66 with respect to the center of an inorganic brick, resulting from $(N, V, \sigma_a = \mathbf{0}, T)$ simulations of a $2 \times 2 \times 2$ unit cell at $T = 300$ K and $V = 8000 \text{ \AA}^3$ (top) or $V = 9400 \text{ \AA}^3$ (bottom). The same color code as in Figure 7 of the main manuscript is used.

$1 \times 1 \times 1$ to $2 \times 2 \times 2$, it can be assumed the conventional unit cell is already sufficiently large to reliably determine the structural and mechanical properties of the pristine UiO–66. By similarity, this statement is also expected to hold for the other materials studied in this manuscript.

References

- (1) Morris, W.; Doonan, C. J.; Yaghi, O. M. *Inorg. Chem.* **2011**, *50*, 6853–6855.
- (2) Verstraelen, T.; Vandenbrande, S.; Heidar-Zadeh, F.; Vanduyfhuys, L.; Van Speybroeck, V.; Waroquier, M.; Ayers, P. W. *J. Chem. Theory Comput.* **2016**, *12*, DOI: 10.1021/acs.jctc.6b00456.
- (3) Chen, J.; Martínez, T. J. *Chem. Phys. Lett.* **2007**, *438*, 315–320.
- (4) Vanduyfhuys, L.; Verstraelen, T.; Vandichel, M.; Waroquier, M.; Van Speybroeck, V. *J. Chem. Theory Comput.* **2012**, *8*, 3217–3231.
- (5) Halgren, T. A. *J. Comput. Chem.* **1996**, *17*, 520–552.
- (6) Bush, B. L.; Bayly, C. I.; Halgren, T. A. *J. Comput. Chem.* **1999**, *20*, 1495–1516.
- (7) Lii, J.; Allinger, N. *J. Am. Chem. Soc.* **1989**, *111*, 8576–8582.
- (8) Allinger, N. L.; Zhou, X.; Bergsma, J. *J. Mol. Struc.–THEOCHEM* **1994**, *312*, 69–83.
- (9) Becke, A. D. *J. Chem. Phys.* **1988**, *88*, 2547–2553.
- (10) Yang, L.-M.; Ganz, E.; Svelle, S.; Tilset, M. *J. Mater. Chem. C* **2014**, *2*, 7111–7125.
- (11) Willems, T. F.; Rycroft, C. H.; Kazi, M.; Meza, J. C.; Haranczyk, M. *Microporous Mesoporous Mater.* **2012**, *149*, 134–141.
- (12) Martin, R. L.; Smit, B.; Haranczyk, M. *J. Chem. Inf. Model.* **2012**, *52*, 308–318.
- (13) Pinheiro, M.; Martin, R. L.; Rycroft, C. H.; Jones, A.; Iglesia, E.; Haranczyk, M. *J. Mol. Graph. Model.* **2013**, *44*, 208–219.
- (14) Spek, A. L. *J. Appl. Cryst.* **2003**, *36*, 7–13.
- (15) Cavka, J. H.; Jakobsen, S.; Olsbye, U.; Guillou, N.; Lamberti, C.; Bordiga, S.; Lillerud, K. P. J. *Am. Chem. Soc.* **2008**, *130*, 13850–13851.
- (16) Ortiz, A. U.; Boutin, A.; Fuchs, A. H.; Coudert, F.-X. *J. Phys. Chem. Lett.* **2013**, *4*, 1861–1865.
- (17) Plimpton, S. *J. Comp. Phys.* **1995**, *117*, 1–19, <http://lammps.sandia.gov>.
- (18) Verstraelen, T.; Vanduyfhuys, L.; Vandenbrande, S.; Rogge, S. M. J. *Yaff, Yet Another Force Field*, <http://molmod.ugent.be/software/>.